Applications of Calcium Compounds, Bamboo Biochar and Sudanese Clay for Wastewater Treatment

Ahmed Hassan

A Thesis Submitted in Fulfilment of the Requirements for the Degree of Doctor of Philosophy in Chemical Engineering

Prince of Songkla University

2015

Thesis Title Application of Calcium Compounds, Bamboo biochar and Sudanese clay for wastewater treatment

Author Mr. Ahmed Hassan Alamin Ebrahim

Major Program Chemical Engineering

Major Advisor

……...

(Assoc. Prof. Dr. Lupong Kaewsichan)

Examining Committee:

…….Chairperson

(Assoc. Prof. Dr. Chayanoot Sangwichien)

…….

(Assoc. Prof. Dr. Lupong Kaewsichan)

…….

(Assoc. Prof. Dr. Nurak Grisdanurak)

……..……

(Assoc. Prof. Dr. Pakamas Chetpattananondh)

The Graduate School, Prince of Songkla University, has approved this thesis as fulfilment of the requirements for the Doctor of Engineering Degree in Chemical Engineering.

……

(Assoc. Prof. Dr. Teerapol Srichana)

Dean of Graduate School

This is to certify that the work here submitted is the result of the candidate's own investigations. Due acknowledgement has been made of any assistance received.

…….. Signature

(Assoc. Prof. Dr. Lupong Kaewsichan)
Major Advisor

…… Signature

(Mr. Ahmed Hassan Alamin Ebrahim)
Candidate

I hereby certify that this work has not been accepted in substance for any other degree, and is not being currently submitted in candidature for any degree.

……. Signature

(Mr. Ahmed Hassan Alamin Ebrahim)
Candidate

Thesis Title	Application of Calcium Compounds, Bamboo biochar and Sudanese clay for wastewater treatment
Author	Mr. Ahmed Hassan Alamin Ebrahim
Major Program	Chemical Engineering
Academic Year	2015

ABSTRACT

The aim of this research is to enhance the adsorption of Pb, Zn, Cd, and 2,4-Dichlorophenol (2,4-DCP) by many types of adsorbent mixtures from aqueous solutions. The first case of sorption characteristics of Pb(II), Zn(II) and Cd(II) from aqueous solutions through a low-cost adsorbent mixture comprising of bamboo biochar (BB) and calcium sulphate (CS), and a more expensive mixture of hydroxyapatite (HAP) and calcium sulphate (CS), were investigated. The effects of equilibrium contact time and adsorbate concentration conducted in batch experiments were studied. Adsorption equilibrium was established in 40 (min). The adsorption mechanism of Pb(II), Zn(II) and Cd(II) from these two adsorbent mixtures carried out through a kinetic rate order. A pseudo second-order kinetic model was applied for the adsorption processes. The model yielded good correlation (R^2 >0.92) of the experimental data. Adsorption of Pb(II), Zn(II) and Cd(II) using (BB&CS) and (HAP&CS) correlated well (R^2 >0.86) with both Langmuir and Freundlich isotherm equations under the concentration range studied. Hence, the effectiveness of an inexpensive natural material (BB&CS) mixture in Pb(II), Zn(II) and Cd(II) removal is established, and is promising for use in other heavy metal adsorptions.

The second case investigate the removal of 2,4-DCP and Pb(II) from aqueous solution in a circulation fluidized-bed column by two types of adsorbent mixtures: BC (bamboo char plus calcium sulphate), and HBC (hydroxyapatite plus bamboo char plus calcium sulphate); both manufactured in ball shape. The main material bamboo char was characterized by Fourier transforms infrared spectroscopies (FTIR), Differential thermal analysis (DTA) and scanning electron microscope image (SEM). The adsorption experiments were conducted in a fluidized bed circulation column. Adsorption isotherms and kinetic studies were established under 180-min operating process time at different initial concentration of 2,4-DCP and Pb(II) solutions ranging from 5-10 mg/L and 30-70 mg/L respectively, and at different flow rates ranging from 0.25-0.75 L/min. The obtained data were fitted well with both the Langmuir and Freundlich isotherm models indicating favorable condition of monolayer adsorption. The kinetics of both adsorbents complies with the pseudo second-order model. BC was proven a new effective composite and low cost adsorbent which can be applied in the field of wastewater treatment, and it could also play an important role in industrial water treatment.

The third case in this research concerned fixed bed column adsorption, the experiments were carried out to procedure was adsorption possibility of ground-mixed adsorbent containing clay taken from Sudan (SC) and bamboo biochar (BB) made in Thailand to form CB new adsorbent using for the removal of Lead ion from aqueous

solution. Description of SC properties was performed employing XRD, XRF and FTIR techniques; and for BB, were applied SEM and FTIR. The effects of flow rate solution in range 10 to 20 ml/min, the bed height in range 10 to 40 mm and the initial concentration of Lead ion between 5 to 30 mg/L, on the breakthrough curves characteristics of the column adsorption process were studied. The fixed bed column adsorption process was detected to be better performed at low solution flow rate, high Lead ion initial concentration and low adsorbent CB bed height. The Bed depth service time (BDST) model was applied in the fixed bed column performance experimental results and the variables of model were estimated. Also more three other models were applied for fitting the adsorption results: Adams-Bohart, Thomas, and Yoon-Nelson. All this models are valid but the correlation coefficient R^2 of determination for the (BDST) and the Thomas and Yoon-Nelson models were found better fitted than the Adams-Bohart model and hence these were applied to expect the adsorption of Lead ion in the column. The CB adsorbent mixture was displayed to be appropriate adsorbent mixture for adsorption, of Lead ion.

The second step of fixed column mode experiments was carried out for adsorption equilibrium and determined the adsorbent capacity by using ratio 1:1 of adsorbent mixture (CB) as powder. It's used for adsorptive removal of inorganic compound (especially heavy metal ions). The main objective of this step is to investigate the adsorption of Pb(II) from aqueous solution by this adsorbent with application of Response Surface Methodology (RSM) for optimum condition as mentioned earlier of that three variables, flowrate, concentration and adsorbent bed height on the adsorbent capacity yield. The results showed that the maximum adsorbent capacity yield was about 18.64 mg/g obtained by using 15 ml/min flowrate, 17.5 mg/L inlet Pb(II) concentration and 10 mm of bed height. From the analysis of variance (ANOVA), the most influential factor for each experimental design response was identified. The optimum conditions of adsorption Pb(II) on CB adsorbent capacity 26 mg/g, from aqueous solution in fixed bed column were found of 10 ml/min of flowrate, 14.53 mg/L solution concentration and 10 mm bed height.

ACKNOWLEDGMENT

First and foremost, I would like to express my profound sense of obligations, unending appreciation, heartfelt thanks and praise to the ‘‘Almighty Allah’’ for showering immense blessing and mercy upon me in every phase of my life.

I would like to express my warm, deepest and sincere of gratitude, veneration and earnest thanks to my esteemed advisor, Prof. Dr. Lupong Kaewsichan of the Department of Chemical engineering, Faculty of Engineering, Prince of Songkla University, for his affectionate encouragement, sincere co-operation kindness, active guidance, scholar supervision and constructive criticism during my study since the first day of being his student.

Besides my advisor I deem it a great privilege to express sincere and heartfelt thanks regard to chairperson and members of my examining committee, Assoc. Prof. Dr. Chayanoot Sangwichien, Assoc. Prof. Dr. Pakamas Chetpattananondh, of the Department of Chemical engineering, Faculty of Engineering, Prince of Songkla University, and Assoc. Prof. Dr. Nurak Grisdanurak of the Department of Chemical Engineering, Faculty of Engineering, Thammasat University.

I would like to thanks all Department of Chemical Engineering members, staff, students, Discipline of Excellence in Chemical Engineering (DOE), Faculty of Engineering, and Graduate School of Prince of Songkla University are highly appreciated for their kind co-operation during my study. This study could not be succeeded in that the financial support from DOE and the Graduate School of Prince of Songkla University, under the international graduate scholarship program, I am great full acknowledge this financial support.

Finally, I would like to thank our small family (my wife, my son and my daughter), my big family and my parents for their love encouragement, support throughout my study and spiritually throughout my life.

Contents

	Page
Abstract	v
Acknowledgments	vii
Contents	vii
List of Figures	x
List of Tables	xi
List of Abbreviations and Symbols	xiii
List of Publications	xv
1. Introduction	
1.1 Research Background.	1
1.1.1 Wastewater.	1
1.1.2 Heavy metal in industrial wastewater.	1
1.1.3 Phenolic compound in wastewater.	2
1.1.4 Wastewater treatment by decreasing of heavy metal content and phenolic compound.	2
1.2 Bamboo biochar.	3
1.3 Hydroxyapatite.	4
1.4 Calcium Sulphate.	4
1.5 Clay.	5
2. Objectives.	5
3. Experimental model, parameter and apparatus.	6
3.1 Experimental models.	6
Pseudo first-order Kinetic model.	6
Pseudo second-order kinetic model.	6
Langmuir isotherm model.	6
Frendluch isotherm model.	7
Bed-depth service-time (BDST) model.	7
Adam-Bohart model.	7
Thomas model.	8

Yoon-Nelson model. 8
3.2 Experimental setup. 8
4. Method. 10
4.1 Batch adsorption. 10
4.2 Circulation column adsorption. 11
4.3 Fixed bed column adsorption. 12
5. Results and discussion. 12
5.1 Batch Adsorption. 12
5.1.1 Batch adsorption of Pb(II). 12
5.1.2 Batch adsorption of Zn(II) and Cd(II). 16
5.2 Circulation column adsorption. 22
5.2.1 Circulation column adsorption of 2,4 DCP. 22
5.2.2 Circulation column adsorption of Pb(II). 27
5.3. Fixed bed column adsorption. 33
6. Conclusion remarks. 41
References 43
Appendix
Appendix A
Appendix B
Appendix C

List of Tables

Table		Page
1.	Adsorption kinetic model rate constants for Pb(II) removal.	14
2.	Isotherm parameters for sorption of Pb(II) by different adsorbent.	15
3.	Adsorption kinetic model rate constants for Zn (II) and Cd (II) removal.	18
4.	Isotherms parameters for sorption of Zn(II) and Cd(II) by different adsorbents.	21
5.	Adsorption kinetic model rate constants for 2, 4-DCP removal by different adsorbents.	26
6.	Isotherm parameters for sorption of 2, 4-DCP by different adsorbent.	27
7.	Adsorption kinetic model rate constants for Pb(II) removal by different adsorbents.	31
8.	Isotherm parameters for sorption of Pb(II) by different adsorbent.	33
9.	Adams-Bohart model result from linear regression analysis.	36
10.	Thomas model result from linear regression analysis.	37
11.	Yoon–Nelson model result from linear regression analysis.	37
12.	Experimental design matrix and results.	38
13.	Analysis of variance (ANOVA) summarized	39
14.	Continue analysis of variance (ANOVA) summarized	40

List of Figures

Figure		Page
1.	Process Diagram.	9
2.	The fixed bed experimental setup.	10
3.	Pb(II) removal efficiency vs. contact time for the (BB&CS) and the (HAP&CS) adsorbent mixtures.	13
4.	Effect of initial Pb(II) concentration C_e on the equilibrium capacity q_e for the (BB&CS) and the (HAP&CS) adsorbent mixtures.	13
5.	Removal capacity of Pb(II), pseudo second-order model fit, for (BB&CS) and (HAP&CS) mixtures.	14
6.	Langmuir isotherm $1/C_e$ vs. Pb(II) adsorption q_e for (BB&CS) and (HAP&CS) mixtures.	15
7.	Freundlich isotherm Log C_e vs. Pb(II) adsorption Logq_e for (BB&CS) and (HAP&CS) mixtures.	15
8(a).	Effect of initial metal ion concentration in HAP&CS.	16
8(b).	Effect of initial metal ion concentration of Zn and Cd in BB&CS.	16
9(a).	Effect of contact time in removal metal ion concentration in HAP&CS.	17
9(b).	Effect of contact time in removal metal ion concentration in BB&CS.	17
10(a).	Kinetic model for removal of Zn and Cd ions in adsorbent (HAP&CS) in a pseudo-second model.	18
10(b).	Kinetic model for removal of Zn and Cd ions in adsorbent (BB&CS) in pseudo-second order model.	19
11(a).	Langmuir isotherm for the adsorption of Zn and Cd in adsorbent (HAP&CS).	19
11(b).	Langmuir isotherm for the adsorption of Zn and Cd in adsorbent (BB&CS).	20
12(a).	Freundlich isotherm for the adsorption of Zn and Cd ions in adsorbent (HAP&CS).	21
12(b).	Freundlich isotherm for the Adsorption of Zn and Cd ions in adsorbent (BB&CS).	21
13.	Initial pH solution of 2, 4-DCP adsorption vs. Percentage of removal.	22
14.	Contact time of circulation fluidization vs. Percentage of removal.	23
15.	Flow rate of 2, 4-DCP solution vs. Percentage removal.	24
16.	Initial concentration of 2, 4-DCP solutions vs. Percentage of removal.	24
17.	Results from pseudo-first order kinetic model for the removal of 2, 4-DCP.	25
18.	Results from pseudo-second order kinetic model for the removal of 2, 4-DCP.	25
19.	Langmuir isotherms (1/qe) vs. 1/Ce for the adsorption of 2, 4-DCP.	26
20.	Freundlich isotherm ln(qe) vs. 1n(Ce) for the adsorption of 2, 4-DCP.	27
21.	Initial pH of Pb(II) vs. Percentage of removal.	28
22.	Contact time of circulation fluidization vs. Percentage of removal.	28
23.	Flow rate of Pb(II) solution vs. Percentage removal.	29

List of Figures (continue)

Figure **Page**

24. Initial concentration of Pb(II) solutions vs. Percentage of removal. 30
25. Results from Pseudo-first order kinetic model for the removal of Pb(II). 30
26. Results from Pseudo-second order kinetic model for the removal of Pb(II). 31
27. Langmuir isotherms ($1/q_e$) vs. ($1/C_e$)for the adsorption of Pb(II). 32
28. Freundlich isotherm $\ln(q_e)$ vs. $\ln(C_e)$ for the adsorption of Pb(II). 33
29. Breakthrough curves for Pb(II) adsorption on the CB at different flow rate (at constant inlet Pb(II) concentration of 17.5 (mg/L) and bed height of 25 (mm)). 34
30. Breakthrough curves for Pb(II) adsorption on the CB at different inlet Pb(II) concentrations (at constant bed height of 25 (mm) and flow rate of 15 (ml/min)). 34
31. Breakthrough curves for Pb(II) adsorption on the CB at different bed height (at constant inlet Pb(II) concentration of 17.5 (mg/L) and flowrate of 15 (ml/min)). 35
32. BDST plot for Pb(II) adsorption on CB. 35
33. Experimental results versus predicted values 40

List of Abbreviation and Symbols

BB	Bamboo biochar.
CS	Calcium Sulphate.
HAP	Hydroxyapatite.
BC	Bamboo biochar plus Calcium Sulphate.
HBC	Hydroxyapatite plus Bamboo biochar plus Calcium Sulphate.
SC	Sudanese Clay.
CB	Clay (Sudan) plus Bamboo biochar.
FTIR	Fourier Transform Infrared.
SEM	Scanning electron microscope.
XRD	X-ray Diffraction.
XRF	X-ray Fluorescence.
AR	Analytical Reagents.
AAS	Atomic Absorption Spectroscopy.
BDST	Bed Depth Service Time.
2, 4-DCP	2,4- dichlorophenol.
q_e	Amounts in of Pb(II) adsorbed at equilibrium time (mg/g).
q_t	Amounts of Pb(II) adsorbed at time t (mg/g).
k_1	The pseudo-first order reaction rate constant (g/mg min).
k_2	The pseudo-second order reaction rate constant (g/mg min).
t	Time (min).
q_{max}	The maximum monolayer adsorption capacity of the adsorbent (mg/g).
C_e	The equilibrium concentration of Pb(II) in the solution (mg/L).
b	The equilibrium constant (L/mg).
R_L	The degree of suitability.
K_L	The Langmuir isotherm constant (L/mg).
K_F	The Freundlich adsorption isotherm constant (L/mg).
n	Coefficient related to the sorption intensity.
Q	Volumetric flow rate (ml/min).
C_{ad}	Adsorbed concentration in (mg/L).
q_{total}	The total adsorbed metal quantity in the column in (mg).
M_{total}	Total amount of metal ions dispatched to the column (mg).
N	Adsorption capacity of the bed (mg/L).
Z	Depth of the column bed (cm).
v	Linear flow velocity of lead solution through the bed (ml/cm^2 h).
K_α	The rate constant (L/mg h).
k_{AB}	Kinetic constant (L/mg min).
F	Linear velocity calculated by dividing the flow rate by the column section area (mm/min).
N_0	Saturation concentration (mg/L).
k_{Th}	Thomas rate constant (ml/min mg).
q_0	The equilibrium Pb(II) uptake per g of the adsorbent (mg/g).
C_o	Inlet Pb(II) concentration (mg/L).

C_t	Outlet concentration at time t (mg/L).
W	Mass of adsorbent (g).
k_{YN}	The Yoon–Nelson proportionality constant (min^{-1}).
τ	The time required for retaining 50% of the initial sorbate (min).

List of Publications

The list of publications was sorted in order of the study. The publications of the batch adsorption of Pb(II), Zn(II), and Cd(II) metals ions, fluidized bed column adsorption of Pb(II) and 2,4-Dichlorophenol, and fixed bed column adsorption of Pb(II), were attached in Appendix A, Appendix B and Appendix C, respectively.

1. Publications of batch adsorption

1.1 Conference Paper

A. Hassan and L. Kaewsichan, ‘‘Removal of Pb(II) from Aqueous Solutions Using Mixtures of Bamboo Biochar and Calcium Sulphate, and Hydroxyapatite and Calcium Sulphate’’, The 3rd EnvironmentAsia International Conference on “Towards International Collaboration for an Environmentally Sustainable World” Thai Society of Higher Education Institutes on Environment June 17-19, 2015, Montien Riverside Hotel, Bangkok, Thailand.

1.2 Journal Paper

A. Hassan, L. Kaewsichan, ‘‘Removal of Pb(II) from Aqueous Solutions Using Mixtures of Bamboo Biochar and Calcium Sulphate, and Hydroxyapatite and Calcium Sulphate’’, EnvironmentAsia, vol.9, No.1, pp 37-44, 2016.

1.3 Journal Paper

A. H. Alamin, L. Kaewsichan, ‘‘Adsorption of Zn(II) and Cd(II) ions from aqueous solutions by Bamboo biochar cooperation with Hydroxyapatite and Calcium Sulphate’’, International Journal of ChemTech Research, vol.7, No.5, pp 2159-2170, 2014-2015.

2. Publications of fluidized bed column adsorption

2.1 Journal paper

A. H. Alamin, L. Kaewsichan, ‘‘Sorption of 2, 4-Dichlorophenol onto 2 mixtures: Bamboo biochar plus Calcium sulphate (BC) and Hydroxyapatite plus Bamboo biochar plus Calcium sulphate (HBC), in fluidized bed circulation column’’, **this manuscript had been Accepted to publish in Polish Journal of Chemical Technology.**

2.2 Journal Paper

A. H. Alamin, L. Kaewsichan, ‘‘Sorption of Pb(II) onto 2 mixtures: Bamboo biochar plus Calcium sulphate (BC) and Hydroxyapatite plus Bamboo biochar plus Calcium sulphate (HBC), in fluidized bed circulation column’’, **This manuscript have been submitted to international journal of chemical engineering.**

3. Publications of fixed bed column adsorption

3.1 Journal Paper

A. H. Alamin, L. Kaewsichan, ‘‘Adsorption of Pb(II) Ions from Aqueous Solution in Fixed Bed Column by Mixture of Clay plus Bamboo Biochar’’, **This manuscript had been accepted to publish in Walailak Journal of Science and technology.**

3.2 Journal Paper

A. H. Alamin, L. Kaewsichan, ‘‘Adsorption of Lead (II) from Aqueous Solution on Fixed-bed Column by Mixture of Clay and Biochar Using a Response Surface Method’’, **this manuscript is draft.**

List of Permissions

1. Journal Paper

A. Hassan, L. Kaewsichan, ‘‘Removal of Pb(II) from Aqueous Solutions Using Mixtures of Bamboo Biochar and Calcium Sulphate, and Hydroxyapatite and Calcium Sulphate’’, EnvironmentAsia, vol.9, No.1, pp 37-44, 2016.

EnvironmentAsia

The International journal published by the Thai Society of Higher Education Institutues on Environment

Date : October 14, 2015

Ahmed Hassan Alamin
Department of Chemical Engineering,
Faculty of Engineering,
Prince of Songkla University,
Hat Yai, Songkhla 90112
Thailand
Email: ahmed.10000@yahoo.com

Dear Ahmed Hassan Alamin,

Thank you very much for submitting the manuscript entitled "**Removal of Pb(II) from Aqueous Solutions Using Mixtures of Bamboo Biochar and Calcium Sulphate, and Hydroxyapatite and Calcium Sulphate "** by **Ahmed Hassan and Lupong Kaewsichan** for publication in the ***EnvironmentAsia.***

I am pleased to inform you that the manuscript has been accepted to be published in the ***EnvironmentAsia*** Vol. 9 No.1 (January 2016) by two independent referees.

Thank you for considering ***EnvironmentAsia*** for the publication of your research.

Your sincerely,

Associate Professor Dr. Voravit Cheevaporn
Editor-in-chief
EnvironmentAsia

This journal is now covered by

refine your research SCOPUS™ DOAJ DIRECTORY OF OPEN ACCESS JOURNALS EBSCO HOST THOMSON REUTERS

EDITORIAL OFFICE: Associate Professor Dr. Voravit Cheevaporn, Faculty of Science , Burapha University, Chonburi 20130 Email : voravit@buu.ac.th

1. Introduction

1.1. Research Background

Water is an important requirement in most of industrial processes system such as, heating, cooling, production, cleaning and rinsing. An unregulated, industrial wastewater has the possibility to be a highly toxic source of pollution [1]. For examples of the impacts that may happen when industrial wastes are discharged include petroleum hydrocarbons, heavy metals, surfactants, toxins and/or salts, which may pollute receiving waters rendering them unsuitable as a water supply or pose a threat to aquatic life. The addition of industrial waste to sewers can increase the cost and risk to the community of treating sewage. Industrial pollutants such as oxygen scavengers may corrode pipes and equipment in the sewerage collection system and in treatment plants. Greases and suspended matter can cause pipe blockages and odours [2]. Industry has a corporate responsibility to take action to ensure discharged water is of an acceptable standard, and accept costs of any required clean up. The most cost-effective solutions usually focus on preventing contaminants from ever entering the wastewater stream or developing a closed system of water use.

1.1.1. Wastewater

Wastewater is defined as a combination of the liquid or water-carried wastes removed from residences, institutions, commercial and industrial establishments, together with such groundwater, surface water, and storm water as may be present. Wastewater contains nutrients, which can stimulate the growth of aquatic plants, and may contain toxic compounds or compounds that potentially may be mutagenic or carcinogenic.

1.1.2. Heavy metals in industrial wastewater

Heavy metals are elements which have atomic weights between 63.5 and 200.6, and specific gravities greater than 5.0. Most of the point sources of heavy metal pollutants are industrial wastewater from mining, metal processing, tanneries, pharmaceuticals, pesticides, organic chemicals, rubber and plastics, lumber and wood products, etc. Due to the discharge of large amounts of metal contaminated wastewater, industries bearing heavy metals, such as Cd, Cr, Cu, Ni, As, Pb, and Zn,

are the most hazardous among the chemical intensive industries [3]. Heavy metals are transported by runoff water and contaminate water sources downstream from the industrial site [4]. Because of their high solubility in the aquatic environments, heavy metals can be absorbed by living organisms. It cause serious health effects, including reduced growth and development, cancer, organ damage, nervous system damage, and in extreme cases, death. This can lead to joint diseases such as rheumatoid arthritis, and diseases of the kidneys, circulatory system, nervous system, and damaging of the fatal brain [3].

1.1.3. Phenolic compound in wastewater

Phenolic compounds pose a major worldwide environmental health problem concerning industrial handling of phenol and metal process. Chlorophenol is a group of chemical, of which chlorines (between one and five) have been added to phenol [5]. Main pollution sources containing chlorophenols are wastewaters from pesticide, paint, solvent, pharmaceutics, wood, paper and pulp industries, as well as water disinfecting process [6]. In addition, phenolic derivatives are largely used as intermediates in productions of plastics, colors, pesticides, insecticides, etc. [7]. However, phenol containing water - when chlorinated during disinfection of water - results in formation of chlorophenol [8].

Chlorophenols and related compounds are toxic to humans and aquatic lives, which are carcinogenic, mutagenic, and resistant to biodegradation. Results of phenolic compound discharging into the environment, affected to the contamination the environment and living organisms [9]. Phenols are considered as priority pollutants since they are harmful to organisms at low concentrations and many of them have been classified as hazardous pollutants because of their potential to harm human health. The United States Environmental Protection Agency (USEPA) and the European Union (EU) have designated phenols as priority pollutants [10]. Thus, removal of phenol from drinking water is of great importance, and has been receiving particular concerns in the last few decades [11].

1.1.4. Wastewater treatment from heavy metal and phenolic compound

The removal of heavy metals from industrial effluents has several traditional and advanced techniques to decrease their impact on the environment such as physicochemical, biological and thermal processes. A physicochemical technique includes adsorption, coagulation, chemical precipitation, ultra-filtration, etc. most of these methods has advantages and disadvantages. Among of these methods, adsorption is the most effective and economical because of their relative low cost and have other advantages [12]. There are many type of adsorbents such as salt of phosphates, activated carbons are considered an efficient treatment for the removal of organic compounds and metals from both liquid and gas phases but expensive [13]. Alternatively, low cost and unconventional adsorbents such as Bamboo biochar, rice husk, fly ash, peat, lignite, saw dust etc. are used to removal of toxic metals which is effective and economical.

Treatment technologies, of phenol depending on the load of phenolic compound in wastewater, are either physiochemical or biological [14]. Some conventional methods used to remove phenol from aqueous solutions are: adsorption, precipitation and coagulation, ion exchange, filtration, membrane separation, chemical oxidation, sedimentation, and reverse osmosis [15].

1.2 Bamboo biochar

Biochar is a charcoal produced from biomass materials. In many cases, the term is used specifically to mean charcoal produced by pyrolysis process. Bamboo is one of outstanding renewable biomass resource due to its fast growing speed and short growth cycle [16, 17]; an inexpensive and environmentally friendly adsorbent. Bamboo char has been commercially used in water purification, dehumidification, odour adsorbents and health products, at low prices as $400–600 per ton in 2012 China [17]. A year ago is using biochar as adsorbent for heavy metal such as Pb, Zn, Cd, etc. Biochar, which is a by-product of bio refineries, has attracted much attention recently due to its proven role in environmental management issues [18]. Bamboo biochar is one of good natural adsorbent. Bamboo charcoal may be an ideal amendment for nutrient conservation and heavy metal stabilization due to its excellent adsorption capability [19]. Because of it has high porosity more than many biomass wood materials.

In case of phenol could be removed effectively through adsorption process using a variety of adsorbents [20], but without mentioning the use of Bamboo biochar. Preservative of various functional groups on Bamboo biochar surface can contribute a unique and specific preferential for different molecules uptake by active carbons [21]. Furthermore, it is well known that nano-size adsorbents, possess excellent surface properties, such as large accessible internal and external surface [22].

1.3 Hydroxyapatite

The term "apatite" applies to a group of compounds with a general formula in the form $M_{10}(XO_4)_6Z_2$, where $M^{2+}$is a metal and species XO_4^{3-} and Z^- are anions. Hydroxyapatite (HAP), also called hydroxyl appetite's a naturally occurring mineral form of calcium apatite with the formula $Ca_5(PO_4)_3(OH)$, but is usually written $Ca_{10}(PO_4)_6(OH)_2$ to denote that the crystal unit cell comprises two entities. As apatite's are important materials with applications in medical prostheses, environmental remediation and catalysis, it is of basic interest to understand the crystal formation, dissolution processes and interfacial interactions between the crystalline and amorphous phases [23]. HAP can be synthesized in the laboratory by a variety of methods including the sol-gel process, hydrothermal synthesis, microwave synthesis, ultrasonic spray pyrolysis; wet precipitation; emulsion system synthesis, and sono-chemical synthesis. And can be produced from coral, seashell, and eggshell and also from body fluids [24]. Many research works have found that (HAP) can effectively remove lead ion in aqueous solution under different experimental conditions and show potential removal capacities, with removal percentage trending to 100% [25]. Synthetic hydroxyapatite (HAP) has been extensively studied for its kinetics and chemical reaction with a wide variety of metals e.g., Pb, Cu, Cd, Zn, Sb and U [26, 27, 28, 29, 30].

1.4 Calcium Sulphate

Calcium salts (chlorides, sulphates, and carbonates) are better lead precipitators than the corresponding sodium salts [31]. Moreover such composites have been described for use as resorbable biomaterials in bone surgery [32], but have never been used for the retention of heavy metals from polluted water [33].

1.5 Clay

Clays are one of the constituents of the nature, also can be utilized as adsorbents through their surface area, mechanical and chemical constancy and their structural characteristics [34]. Many case and type of soil adsorbents have been investigated for the removal and adsorption of heavy metals, such as Chinese loess [35], clay [36] and bentonite [37]. In common way the capability of clays is in its predisposition to expand and effectively increase in the surface area to accommodate more heavy metal ions [38]. The Pb(II) was found to be more easily adsorbed onto montmorillonite, for both case, as raw form and as its acid activated derivatives [39]. The removal of Pb(II) by Sudan clay is particularly extractive because it is come from natural as mentioned earlier; local product; therefor, no cost it means cheap and easily available source aluminosilicate [40]. Moreover the adsorption capacity of clay can be amended via mix with other adsorbent for example Bamboo biochar.

2. Objectives

2.1 Study the treatment of heavy metal (Pb(II), Zn(II), and Cd(II)) in water by using two mixtures of adsorbents, BB&CS and HAP&CS and investigate the adsorption isotherms and adsorption kinetic through Langmuir and Freundlich models and pseudo second-order kinetic model, respectively .

2.2 Investigate adsorption of 2, 4-dichlorophenol (2, 4-DCP) and Pb(II) in aqueous solution onto two types of ball-shape adsorbents: Bamboo biochar plus Calcium sulphate (BC) and Hydroxyapatite plus Bamboo biochar plus Calcium sulphate (HBC) in a circulation fluidized-bed column. Adsorption isotherm of Langmuir and Freundlich will be investigated. Moreover, adsorption kinetics pseudo-first order and pseudo-second order will be simulated for comparison.

2.3 Adsorption efficiency of Lead ion from aqueous solution using fixed bed column by employing a mixture of Sudanese clay (SC) plus bamboo biochar (BB) will investigated. Principal design variables: solution feed flow rate, fixed column bed height and initial inlet concentration of Lead ion solution, and evaluate by using a laboratory scale and the effect of running operation conditions on the removal percentage and adsorption of Pb(II) will studied.

2.4 The effect of operating conditions on the adsorbent capacity will be conducted for the optimum operating conditions, flowrate of Pb(II) solution, initial concentration of metal solution and the bed height of adsorbent in the column. The conditions are analysed using design of experiments (DOE) and response surface methodology (RSM).

3. Experimental model, parameter and apparatus

3.1. Experimental models

The experimental models are categorized with three parts; the kinetics models (pseudo first-order and pseudo second-order), the isotherm model (Langmuir and Freundlich), and fixed bed column breakthrough curve models (Bed-depth service-time (BDST), Adams-Bohart, Thomas, and Yoon-Nelson).

3.1.1. Pseudo first-order kinetic model

The pseudo-first order equation can be explained using Lagergren equation (1):

$$\log(q_e - q_t) = \log(q_e) - \frac{k_1}{2.303}\ t \qquad (1)$$

Where q_e and q_t are the amounts of metal Pb or 2, 4 DCP, adsorbed at equilibrium and at time t in (mg/g), respectively, and k_1 is the pseudo-first order rate constant in (g/mg h).

3.1.2. Pseudo second-order kinetic model

The pseudo-second order kinetic model equation, based on equilibrium adsorption is equation (2):

$$\frac{t}{q_t} = \frac{t}{q_e} + \frac{1}{k_2 q_e^2} \qquad (2)$$

Where q_e and q_t are as described in Equation (1); and k_2 is the rate constant of second-order adsorption in (g/mg h).

3.1.3. Langmuir isotherm model

The Langmuir isotherm assumes monolayer adsorption onto a surface with a finite number of identical sites, and its linear form is expressed in equation (3):

$$\frac{C_e}{q_e} = \frac{1}{b\, q_{max}} + \frac{C_e}{q_{max}} \quad (3)$$

Where q_e and q_{max} are the observed and the maximum uptake capacities (mg/g); C_e the equilibrium concentration (mg/L); and b the equilibrium constant (L/mg).

3.1.4. Freundlich isotherm model

The Freundlich equation proposes an empirical model based on the sorption on heterogeneous surface, and is in the form of equation (4):

$$\log q_e = \log K_f + \frac{1}{n} \log C_e \quad (4)$$

Where K_f (L/g) and n are the Freundlich isotherm constants and intensity of adsorption, respectively; q_e and C_e are as described for equation (3).

3.1.5. Bed-depth service-time (BDST) model

The breakthrough curves using the BDST model is based on measuring the bed capacity at different percentage of breakthrough values. The model is based on an assumption that the rate of adsorption is controlled by the surface reaction between the adsorbate and the unused capacity of the adsorbent. Constants from the model can be easily scaled up for different concentration and flowrate without conducting more experiments. Moreover, it can be used to predict the fixed bed column performance at any bed height. The linear relationship between bed depth and service time is given by Eq. (5) [41]:

$$t = \frac{NZ}{C_0 v} - \frac{1}{K_\alpha C_0} \ln\left[\left(\frac{C_0}{C}\right) - 1\right] \quad (5)$$

Where C is the breakthrough Pb(II) concentration (mg/L); N the adsorption capacity of the bed (mg/L); Z the depth of the column bed (cm); v the linear flow velocity of lead solution through the bed (ml/cm^2 h); and K_α the rate constant (L/mg h).

3.1.6. Adam-Bohart model

Adams-Bohart model [42] is commonly used for description of the initial part of the breakthrough curve [43], and the model equation is expressed as Eq. (6):

$$\ln \frac{C_t}{C_0} = k_{AB} C_0 t - k_{AB} N_0 \frac{Z}{F} \quad (6)$$

Where C_0 and C_t (mg/L) are the inlet and effluent Pb(II) concentration; k_{AB} (L/mg min) the kinetic constant; F (mm/min) the linear velocity calculated by dividing the flowrate by the column section area; Z (mm) the bed depth of column; and N_0 (mg/L) the saturation concentration.

3.1.7. Thomas model

One of the most popular and widely used models for describing the process theory of adsorption in a fixed bed column is the Thomas model [44]. This model assumes plug flow behavior in the bed, and uses Langmuir isotherm for equilibrium and second-order reversible reaction kinetics. The model equation is expressed as Eq. (7):

$$\ln\left(\frac{C_0}{C_t} - 1\right) = \frac{k_{Th}\, q_0\, W}{Q} - k_{Th}\, C_0\, t \qquad (7)$$

Where k_{Th} (ml/min mg) is the Thomas rate constant; q_0 (mg/g) the equilibrium Pb(II) uptake per g of the adsorbent; C_o (mg/L) the inlet Pb(II) concentration; C_t (mg/L) the outlet concentration at time t; W (g) the mass of adsorbent; Q (ml/min) the flowrate; and t (min) the flow time.

3.1.8. Yoon-Nelson model

The Yoon and Nelson [45] had developed a model based on the assumption that the sorption rate of decrease in the probability adsorption of adsorbate molecule (solution) is proportional to the probability of the adsorbate adsorption and the adsorbate breakthrough on the adsorbent. The linear form of the equation as Eq. (8):

$$\ln\left(\frac{C_t}{C_0 - C_t}\right) = k_{YN}t - \tau\, k_{YN} \qquad (8)$$

Where k_{YN} (min^{-1}) is the Yoon–Nelson proportionality constant; and τ (min) the time required for retaining 50% of the initial sorbate.

3.2. Experimental setup

For batch adsorption studies, a series of six glass conical flask 250 ml were utilized for each batch experiment. Each of the sex vessels was initially filled

with known amount of adsorbents and filled with 50 ml of different heavy metal solutions concentration. All these conical flasks were put in mechanical end shaker to obtained agitation of adsorbents with the adsorbate, by different time interval, after that were filtrated every flask and measured the residual metal remaining in solution. Adsorption experiments were investigated in different batches for the adsorbents and different heavy metals solution with varies concentration.

Study of Pb(II) adsorption was carried out at laboratory scale; fluidized bed reactor was used as the adsorption system to improve mixing and homogeneity. The experiment setup consisted of a fluidized column, a water reservoir, a peristaltic pump, as shown in Figure 1. The 5 cm outside-diameter and 24 cm height reactor with an effective volume of 470 ml was made from transparent acrylic. A mesh screen was fit at the top of the circulation fluidized column in order to capture the solid coming out of the column. One conical distributor was placed at the bottom to ensure proper distribution of the fluid. Aqueous solution of Pb(II) was continuously fed upward to the reactor at different flow rates, starting from 250 to 750 ml/min. The liquid effluent stream was recycled to the hold-up tank.

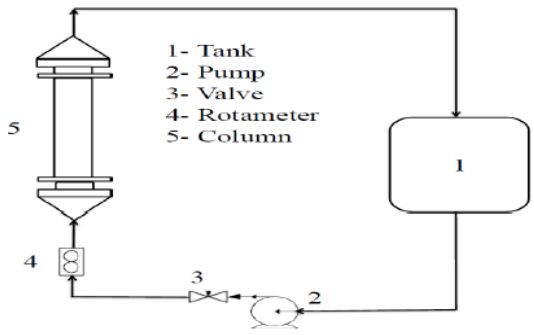

Figure 1. Process Diagram of fluidized bed circulation

Schematic diagram for the fixed bed column system is shown in Figure 2. The column was made of glass tube having 35 mm inside diameter and 240 mm in height. At the bottom of the column, a stainless steel sieve was attached, followed by a layer of glass wool.

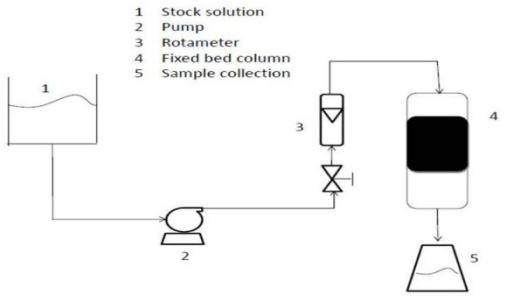

Figure 2. The fixed bed experimental setup

4. Method

4.1. Batch adsorption

All metal solutions were prepared from their nitrate salts (Analytical Reagents; AR) and distilled water. The synthetic solutions were all prepared by diluting Pb(II), Zn(II) and Cd(II) standard stock solutions (concentration 1000 ± 2 mg/L) obtained by dissolving appropriate amounts of metal salt in double distilled water. Four dilutions: 100, 200, 300 and 400 mg/L, were used form Pb(II) in each set of the experiment, and more four dilutions: 50, 75, 100 and 150 mg/L, were used from Zn(II) and Cd(II).

Batch adsorption experiments were conducted on the three adsorbent materials, for which 0.08 g, 0.05 g, and 0.05 g for (BB), (CS) and (HAP), respectively, were used to produce the two mixtures. Each mixture of (BB&CS) and (HAP&CS) was put into a 250 mL conical flask containing 50 mL of Pb(II) ions at the pre-set concentrations mentioned earlier of 100, 200, 300 and 400 mg/L, shaken, filtered and subjected to Pb(II) analysis to determine the optimum Pb(II) adsorptions. Same steps were done for Zn(II) and Cd(II) ions at the pre-set concentrations mentioned earlier of 50, 75, 100 and 150 mg/L. The effect of contact time was studied in the time range of 0-40 min. At the end of the adsorption process the suspensions were filtered through 0.45 µm syringe membrane filters and the corresponding supernatant was analysed employing a Perkin Elmer Thermos Scientific S-series model (AAnalyst100) Flam atomic absorption spectrophotometer (AAS) for residual Pb(II), Zn(II) and Cd(II) concentrations. Three replicates were conducted for each Pb(II) bio sorption experiment set, and the average values determined. The adsorbent

capacity of (BB&CS) and (HAP&CS) mixtures were calculated using general equation (9):

$$q_e = (C_e - C_t)\frac{V}{M} \quad (9)$$

Where q_e is the amount of Pb(II), Zn(II), and Cd(II) adsorbed on the adsorbent (mg/g); C_0 and C_t are the Pb(II) concentrations in the solution before and after adsorption (mg/L); V is the volume of the solution (L); and M is the amount of the adsorbents used in the reaction mixture (g).

4.2. Circulation column adsorption

Bamboo biochar (BB), used in this work as the main material, was obtained by pyrolysis process at 500°C in nitrogen atmosphere. Hydroxyapatite (HAP) and 2,4-DCP were purchased from Sigma-Aldrich Co. LLC, while calcium sulphate (CS) was from Aldrich Chemicals. BB was grinded, sieved, and mixed with CS to form an adsorbent composite BC or mixed with HAP and CS to form another adsorbent composite HBC. The weight ratio of BB:CS is 0.62:0.38, and that of BB:HAP:CS is 0.46:0.27:0.27. A glue, prepared from polyvinyl alcohol (PVA) having a molecular weight MW of 22,000, was added to the mixtures to manufacture ball-shape adsorbents. The concentration of residual phenol was determined using a double beam UV–Vis spectrophotometer (Shimadzu UV-1601 Spectrophotometer, Japan) at wave length 765 nm, and for residual of Pb(II) as mentioned earlier. Study of 2,4-DCP and Pb(II) adsorption were carried out in laboratory scale; circulation fluidized-bed reactor was used as the adsorption system to improve mixing and homogeneity. The experimental system consisted of a reactor column, a water reservoir and a peristaltic pump. Aqueous solutions of phenol, lead were continuously fed upward to the reactor at different flow rates, starting from 250 to 750 ml/min. The liquid effluent stream was recycled to the hold-up tank. Three liters of the Phenolic or lead aqueous solution was treated with adsorbent of 3 g for each adsorbent. Adsorptions of the 2,4-DCP and Pb(II) onto adsorbent BC and adsorbent HBC were compared. The suspensions in all studies were filtered through 0.45µm syringe membrane filters. All the experiments were conducted in triplicates for statistical analysis.

4.3. Fixed bed column adsorption

A known quantity of the prepared mixture of CS and BB, to form CB, was put in the circular rubber foam ring and was packed in the column to obtain the desired bed height of the adsorbent at ranges of 10-40 mm, equivalent to 0.8 to 3.2 g of CB, to study the effect of bed height. The column was connected to a distributer in order to provide a uniform flow of the solution through the column. Solution of Pb(II) of known concentrations at ranges of 5-30 mg/L was pumped downward through the column at varied flow rate at ranges of 10-20 ml/min controlled by a peristaltic pump to investigate the effects of initial concentration and the effects of flow rate. Samples of the outlet solution were collected at the exit of the column at time intervals and their concentrations were determined using a flame atomic adsorption spectrophotometer (AAS). In order to ensure the accuracy and reproducibility of all the data, all column adsorption experiments were conducted in triplicate, and mean values were used in the analysis.

5. Results and discussion

5.1. Batch Adsorption

In the beginning of this section batch adsorption characteristic for the adsorption of Pb(II) by two mixtures of (BB&CS) and (HAP&CS) from aqueous solution will be explained, and adsorption of Zn(II) and Cd(II) by both mixtures mentioned earlier will be discussed. More details of this part have been written in publications attached in **Appendix A**.

5.1.1. Batch adsorption of Pb(II)

Batch adsorption features can be explained by many ways, one of these is the effect of contact time. Figure 3 depicted the contact time effect between the aqueous solution of Pb(II) and adsorbents mixture from two combinations of (HAP&CS) and (BB&CS) that were mixing together in the shaken conical flask. The concentrations applied were of 100, 200, 300 and 400 mg/L and the contact times of adsorption were running until 40 min. It can be observed from this Figure, the percentage removal rate of Pb(II) from the aqueous solution increased rapidly and

attained up to 99% at 40 min. The equilibrium time for all adsorbents was reached before 40 min, which that means both adsorbents had similar behaviour.

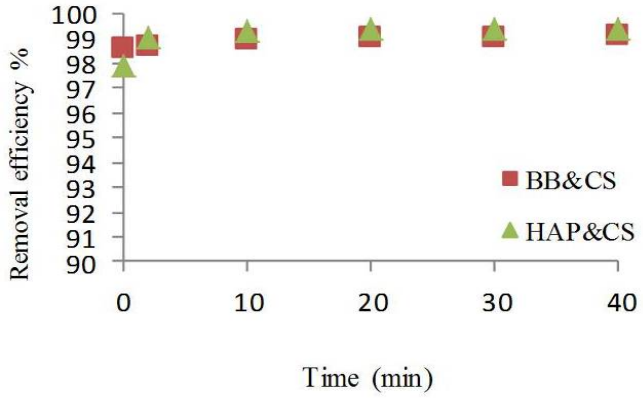

Figure 3. Pb(II) removal efficiency vs. contact time for the (BB&CS) and the (HAP&CS) adsorbent mixtures at 400 mg/L initial concentration and different time from 0 to 40 min.

As mentioned earlier, the experiments were conducted for four separate concentrations of Lead ion aqueous solution (100, 200, 300 and 400 mg/L). The effect of these concentrations was studied and described in Figure 4. The adsorption capacity of Pb(II) by both adsorbents mixtures, increased when the initial concentration of metal ion increasing for both mixtures. In Figure 4 the maximum equilibrium uptake of Lead ion removal were found to be 200 mg/g for the (HAP&CS) mixture, and 152.4 mg/g for the (BB&CS) mixture.

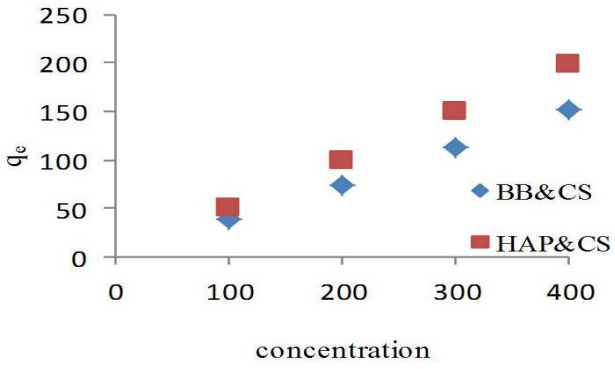

Figure 4. Effect of initial Pb(II) concentration C_e on the equilibrium capacity q_e for the (BB&CS) and the (HAP&CS) adsorbent mixtures at different concentration of 100, 200, 300 and 400 mg/L, and 40 min time

From that data of adsorption kinetics, plotting the time T versus the reaction rate t/q_t, as displayed in Figure 5, was carried out at initial Pb(II) concentration of 400 mg/L at 28 °C (room temperatures). The pseudo second-order adsorption rate constant (K_2) and (q_e) were calculated from the slope and the intercept of this plots. It can be clearly seen from Table 1 that linearity of correlation coefficients (R^2) of the pseudo second-order kinetic model are well. Based on the comparison between the values of q_e theoretically and experimental calculated, moreover it was also found that the model fitted good for removal of Pb(II) by both adsorbent mixtures.

Table 1. Adsorption kinetic model rate constants for Pb(II) removal

Adsorbents	$q_{e\ Exp}$ mg/g_{ad}	Pseudo second-order		
		$q_{e\ (Cal)}$ mg/g	K_2	R^2
BB&CS	152	151.5	0.73	0.9900
HAP&CS	199	200.0	0.50	0.9900

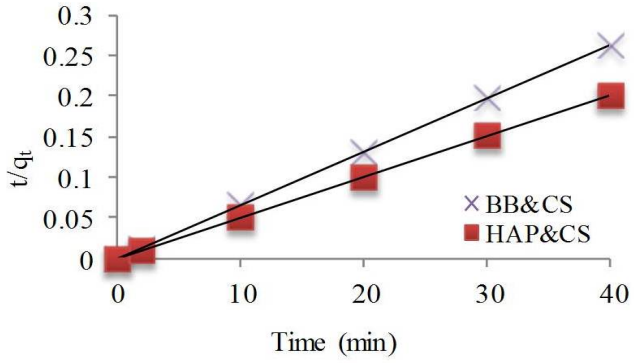

Figure 5. Removal capacity of Pb(II), pseudo second-order model fit, for (BB&CS) and (HAP&CS) mixtures at 400 mg/L initial concentration with different time from 0 to 40 min.

In the isotherms studies Figure 6, employing Langmuir model, and Figure 7, employing Freundlich model, display the intercept and slope for the lines applied in the calculations of the isotherm constants tabulated in Table 2.

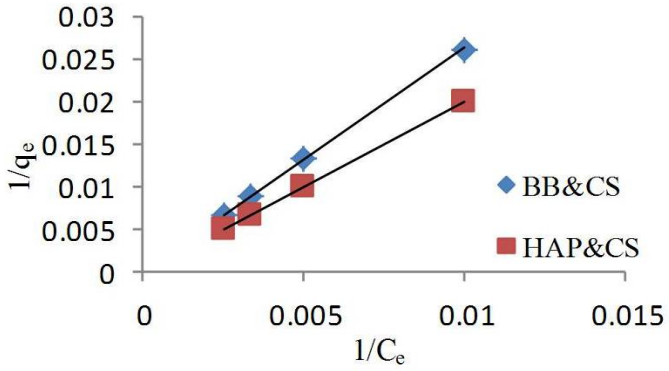

Figure 6. Langmuir isotherm $1/C_e$ vs. Pb(II) adsorption q_e for (BB&CS) and (HAP&CS) mixtures at different initial concentration of 100, 200, 300 and 400 mg/L and 40 min time of equilibrium.

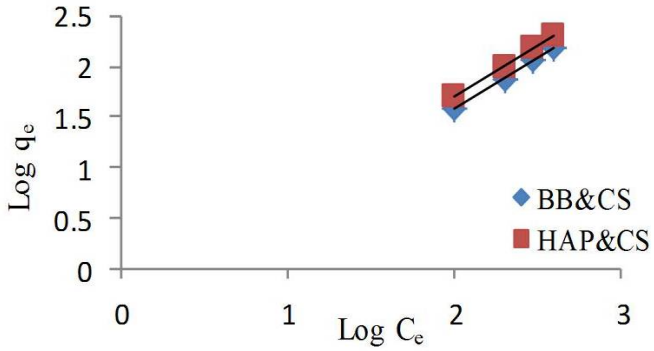

Figure 7. Freundlich isotherm Log C_e vs. Pb(II) adsorption Logq_e for (BB&CS) and (HAP&CS) mixtures at different initial concentration of 100, 200, 300 and 400 mg/L and 40 min time of equilibrium.

Table 2. Isotherm parameters for sorption of Pb(II) by different adsorbent

Adsorbents	Langmuir			Freundlich		
	q_{max}	b	R^2	K_F	n	R^2
BB&CS	152.4	0.0025	0.9998	0.387	1	0.9980
HAP&CS	200	0.0025	0.9900	0.51	1	0.9900

From Table 2 the correlation coefficient (R^2) calculated for the Langmuir isotherm is slightly better than that gained from the Freundlich isotherm, and hence the first model (Langmuir) is a little more favourable. Moreover the smaller values of constant 1/n equal the unity, that means the adsorption bond is too strong between Pb(II) and the surface of both adsorbent.

5.1.2. Batch adsorption of Zn(II) and Cd(II)

Adsorption of Zn(II) and Cd(II) by both adsorbent mixtures from aqueous solution were used diverse initial concentrations in range 50 to 150 mg/L. For all state of initial concentration for both metal ions, the sorption capacities were rise straight from the beginning at the initial state, which that depending on the saturation of the porous space and empty site in the adsorbents. From Figure 8(a), and Figure 8(b), blow describe the effect of different initial concentration on sorption capacity rate of adsorbents HAP&CS mixture and BB&CS mixture respectively.

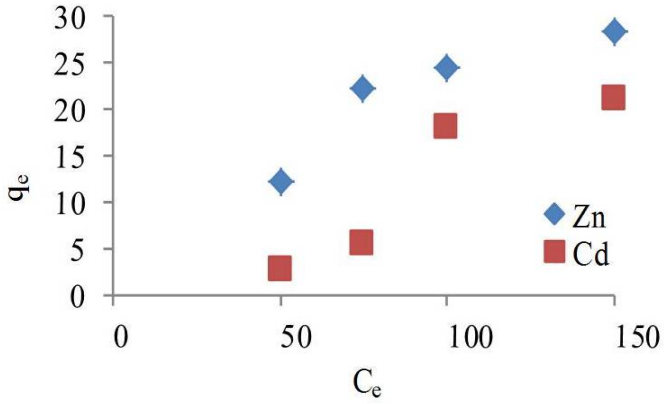

Figure 8(a). Effect of initial metal ion concentration of Zn(II) and Cd(II) in HAP&CS capacity at different concentration of 50, 75, 100 and 150 mg/L, and 40 min equilibrium time.

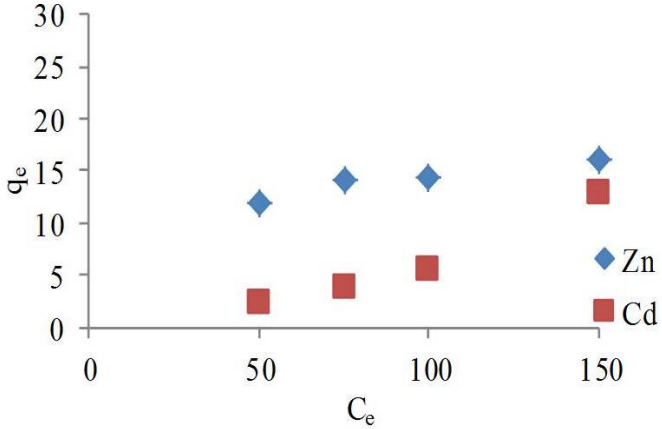

Figure 8(b). Effect of initial metal ion concentration of Zn(II) and Cd(II) in BB&CS capacity at different concentration of 50, 75, 100 and 150 mg/L, and 40 min equilibrium time

The contact time effect between the adsorbent mixtures and metal ion solutions were studied at different time interval in range from 0 to 40 min. The plots presented in Figure 9(a) and Figure 9(b) shows the percentage removal of Zn(II) and Cd(II) onto adsorbents (HAP&CS) and (BB&CS) mixtures versus time, at initial concentration 100 mg/L for both metals ion. In Figure 9(a) the maximum of Zinc ion and Cadmium ion removal percent were found to be approx. 50% of and 40% within time 30 min for adsorbent (HAP&CS) respectively. And for adsorbent (BB&CS) were found to be approx. 30% of Zn and more than 20% of Cd.

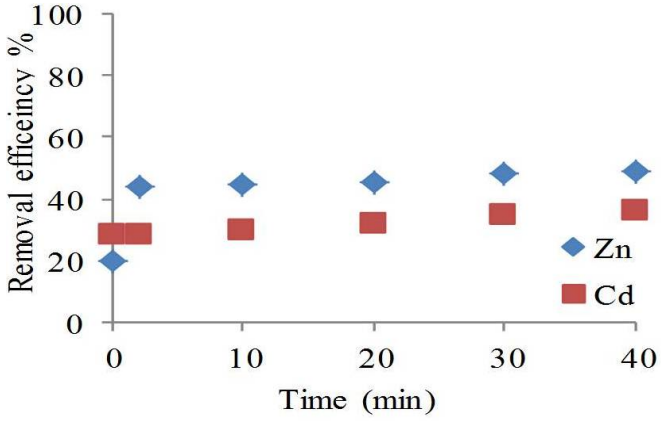

Figure 9(a). Effect of contact time in removal metal ion concentration by HAP& CS at 100 mg/L initial concentration with different time from 0 to 40 min.

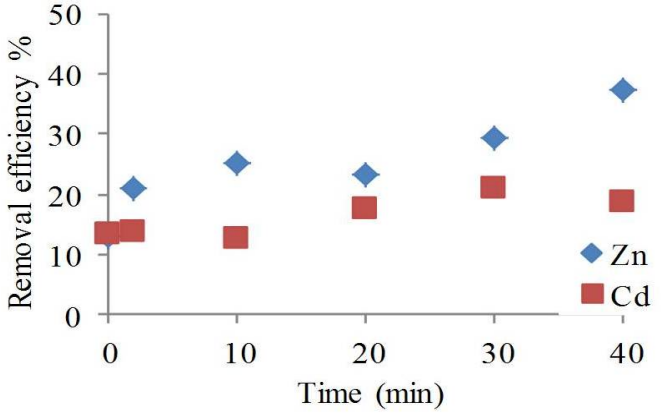

Figure 9(b). Effect of contact time in removal metal ion concentration by BB&CS at 400 mg/L initial concentration with different time from 0 to 40 min.

For the kinetic investigation was employed pseudo-second order equation. The kinetic adsorption of Zn(II) and Cd(II) onto adsorbents

(HAP&CS) and (BB&CS) mixtures were described by plots of the reaction rate t/q_t against the contact time T, as shown in Figure 10(a) and Figure 10(b) respectively. The rate constants K_2 and the theoretical $q_{e(Cal)}$ of pseudo-second order kinetic model were determined from the slope and intercept of the linear plots as mentioned in Figure 10(a) and 10(b). It can be clearly seen in Table 3 the (R^2) linear correlation coefficients of this kinetic model were good, based on the comparison between the q_e values from experiments and theoretically calculated.

Table 3. Adsorption kinetic model rate constants for Zn (II) and Cd (II) removal

Adsorbent	Metal ions	q_{eExp} mg/g_{ad}	Pseudo second order		
			$q_{e(Cal)}$ mg/g	K_2	R^2
HAP&CS	Zn	24.47	24.51	0.073	0.99
	Cd	18.05	18.018	0.0502	0.994
BB&CS	Zn	14.423	13.51	0.023	0.923
	Cd	8.0423	7.6452	0.0729	0.975

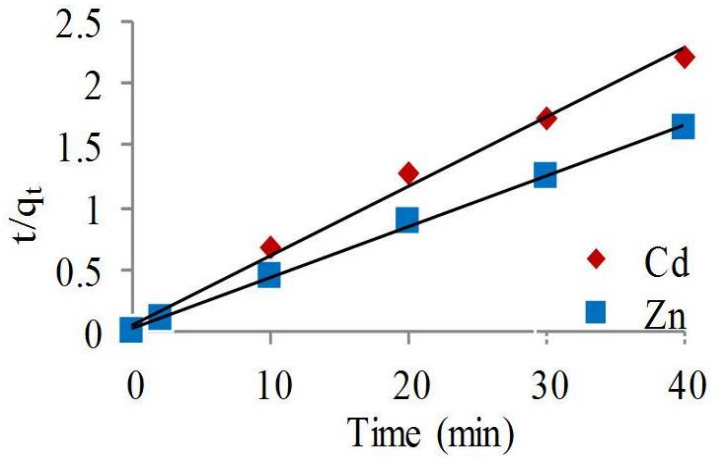

Figure 10(a). Kinetic model for removal of Zn(II) and Cd(II) ions by adsorbent HAP&CS in a pseudo-second model at 100 mg/L initial concentration with different time from 0 to 40 min.

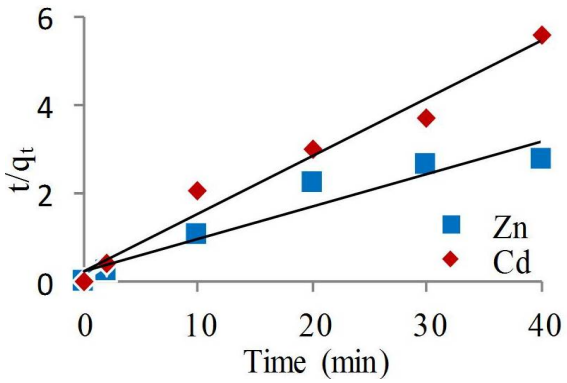

Figure 10(b). Kinetic model for removal of Zn(II) and Cd(II) by adsorbents BB&CS in a pseudo-second order at 400 mg/L initial concentration with different time from 0 to 40 min.

For the isotherms adsorption, were used Langmuir and Freundlich isotherm models. The constants b and q_m in Langmuir equation were calculated from the slope and intercept of the linear plots of $1/q_e$ against $1/C_e$ in Figure 11(a), and Figure 11(b) for adsorbents (HAP&CS) and (BB&CS) mixtures respectively. From Table 4 the q_m values for adsorbent (HAP&CS) were found to be 28.57 mg Zn(II)/g and 21.28 mg Cd(II)/g, and for adsorbent (BB&CS) mixture, were found to be 16.13mg Zn(II)/g and 12.82 mg Cd(II)/g. From the same Table depicted values (R^2) correlation coefficient of the adsorption of Zn(II) and Cd(II) by both adsorbents mixtures of 0.9096, 0.9510 and 0.9595, 0.9972 respectively, which demonstrated that fitted well of experimental results data.

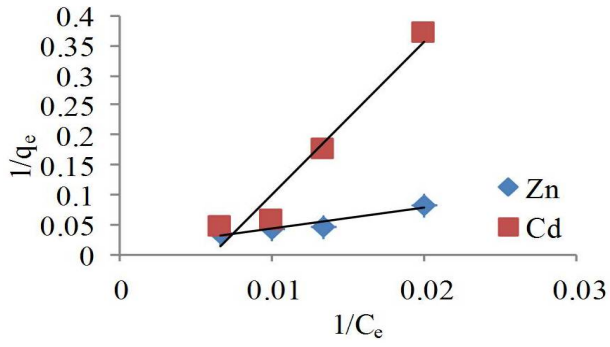

Figure 11(a). Langmuir isotherm for the adsorption of Zn(II) and Cd(II) by adsorbent HAP&CS at different initial concentration of 50, 75, 100 and 150 mg/L initial concentration and 40 min time of equilibrium.

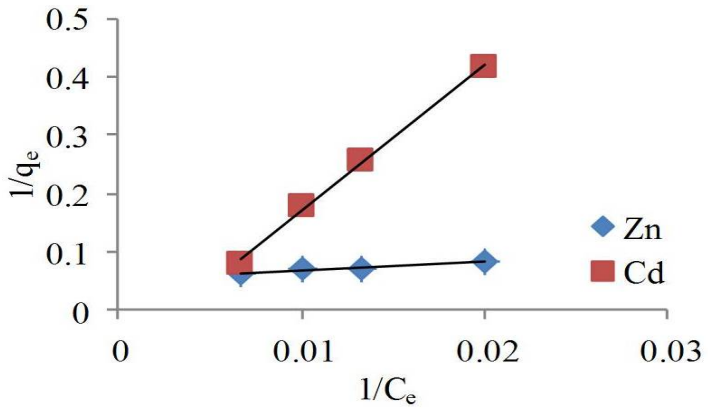

Figure 11(b). Langmuir isotherm for the adsorption of Zn(II) and Cd(II) by adsorbent BB&CS at different initial concentration of 100, 200, 300 and 400 mg/L initial concentration and 40 min time of equilibrium.

In the Freundlich isotherms model, the values of constants n and K_f were determined from the slope and intercept of the liner plots of log q_e against log C_e. The constants values of 1/n were found to be (2.5, 2.016) for Zn and Cd onto (HAP&CS) adsorbent mixture and (0.27, 1.54) for (BB&CS) adsorbent mixture respectively. All the higher values of this constant 1/n suggest that the bond of adsorption is weak. In this case 1/n >1 for adsorbent (HAP&CS) and Cd in (BB&CS), that means the sorption constant increases when the increasing solution concentration, probably reflecting an increase hydrophobic characteristic in the surface after a layer one molecule thick. In that case of adsorption of Zn by (BB&CS) adsorbent, the value of 1/n is less than unity, indicating that significant adsorption takes place in the low concentration of Zn and the opposite is true. As described in the Figure 12(a) for (HAP&CS), and Figure 12(b) for (BB&CS). While the comparison between two models, Langmuir was fitting well more than Freundlich model. However, all the calculated results were shown in Table 4.

Table 4. Isotherms parameters for sorption of Zn(II) and Cd(II) by different adsorbents.

Adsorbent	Metal ions	Langmuir			Freundlich		
		b	K	R^2	K_f	n	R^2
HAP&CS	Zn	28.57	0.010	0.9096	0.820	0.400	0.8616
	Cd	21.28	0.002	0.9510	0.001	0.496	0.9096
BB&CS	Zn	6.13	0.040	0.9595	4.230	3.700	0.9310
	Cd	12.82	0.003	0.9972	0.006	0.650	0.9782

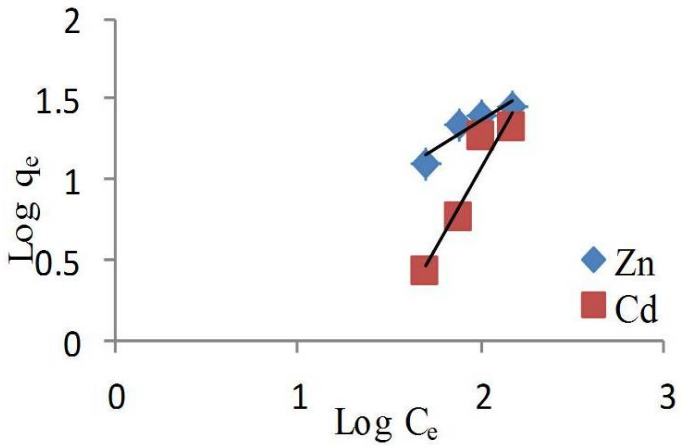

Figure 12(a). Freundlich isotherm for the adsorption of Zn(II) and Cd(II) ions by adsorbent HAP&CS at different initial concentration of 100, 200, 300 and 400 mg/L initial concentration and 40 min time of equilibrium.

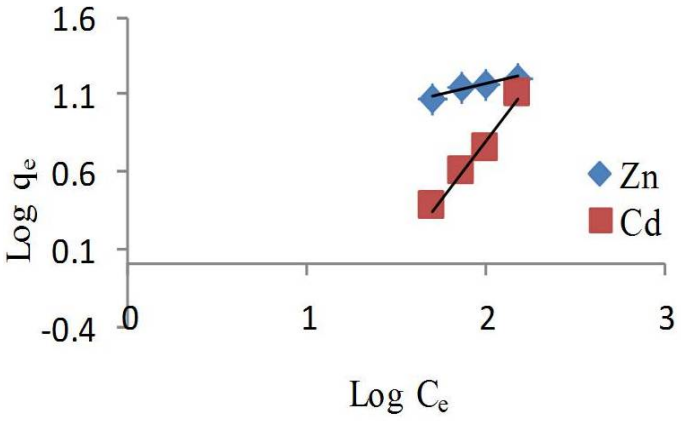

Figure 12(b). Freundlich isotherm for the Adsorption of Zn(II) and Cd(II) ions by adsorbent BB&CS at different initial concentration of 100, 200, 300 and 400 mg/L initial concentration and 40 min time of equilibrium.

5.2. Circulation column adsorption

In this section circulation column adsorption characteristic for adsorption of 2, 4-DCP and Pb(II) by two different adsorbents ball shape of BC and HBC from aqueous solution will be investigated. More details of this part have been written in publications attached in **Appendix B**.

5.2.1. Circulation column adsorption of 2,4 DCP

Adsorbent behaviour of adsorbents BC and HBC on the adsorption of 2,4-DCP were investigated from adjustment effect of the initial pH of solution in range from 3 to 10 at 28°C (room temperature) while the initial concentration of 2,4-DCP solution of 10 mg/L was permanently maintained for both adsorbents. As shown in Figure 13, the removal percentage rates of the 2,4-DCP was lower on the two ends of the pH region. Different behavior trends were noted for the both different adsorbents. For HBC adsorbent, the maximum 2,4-DCP removal percent of 60% was at pH 6, and it's percent rates dropped to 45-50% on either side. For BC adsorbent, the maximum removal percent rates of nearly 40% was at pH 8, but was rather steady between pH 6-10, though with a sharp decline at pH 4. The decline in adsorption percent rates was sharper for HBC in the alkaline range while the descent was a little sharper for BC in the acidic range. The surface charge of both adsorbents, were negative in the pH-zone between 3-10, see Figure 13. The slow rates removal of 2,4-DCP percent at highest pH range could had been resulted of strong competition between the ionic species for 2,4-DCP and the ions of OH^-, hence reducing the 2,4-DCP removal.

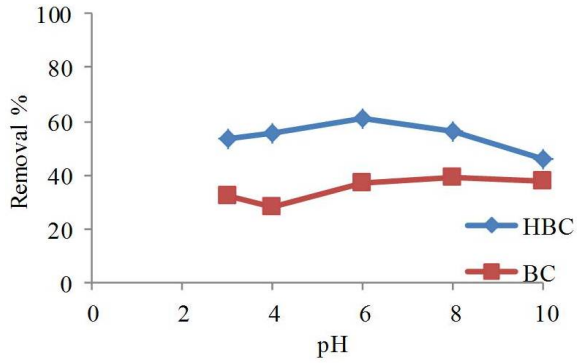

Figure 13. Initial pH solution of 2,4-DCP adsorption vs. Percentage of removal at initial pH between 3 to 10 at room temperature of 28°C and initial concentration 10 mg/L.

The efficiency of percentage removal of 2,4-DCP by adsorption onto adsorbents BC and HBC was investigated on the effect of contact time at different time intervals between 0 to 180 min at 28 °C. The adsorption rates gradually increases depending on the accumulation of 2,4-DCP on the both adsorbents surface during this time. Figure 14 describe the effect of contact time on the percentage removal and the result was that the time of equilibrium for either adsorbent was attained at approximately 180 min.

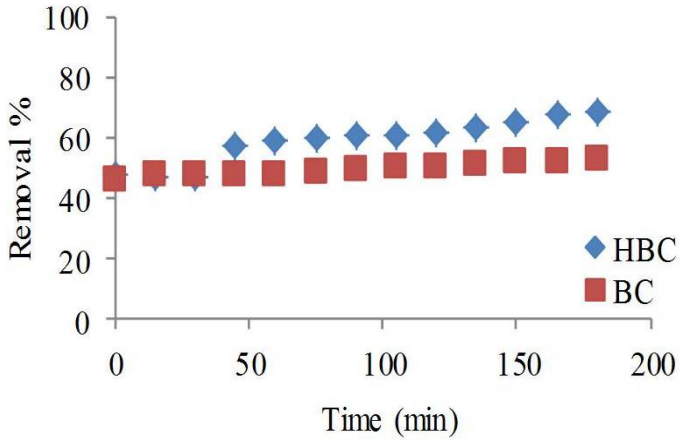

Figure 14. Contact time of circulation fluidization vs. Percentage of removal at contact time of fluidization between 0 to 180 min, flow rate of 500 ml/min, solute pH of 6.5, 3g of adsorbent, 7.5 mg/L of the 2,4-DCP initial concentration.

The effect of different flowrate was studied for adsorption of 2,4-DCP from aqueous solution using the BC and HBC adsorbents. Experiments were conducted at 28°C with flow rate between 250-750 ml/min while other parameters were kept constant (3g of adsorbent, 7.5 mg/L of the 2, 4-DCP initial concentration and solute pH of 6.5). From Figure 15, the percentage removal rates of the 2,4-DCP solution employing BC adsorbent dropped when the flow rate of the solution increasing, whereas for HBC it was the reverse. In case of HBC, the removal capacity of 2,4-DCP increased imperceptibly beneath flow rate of 500 ml/min, except at range 250 to 300 ml/min.

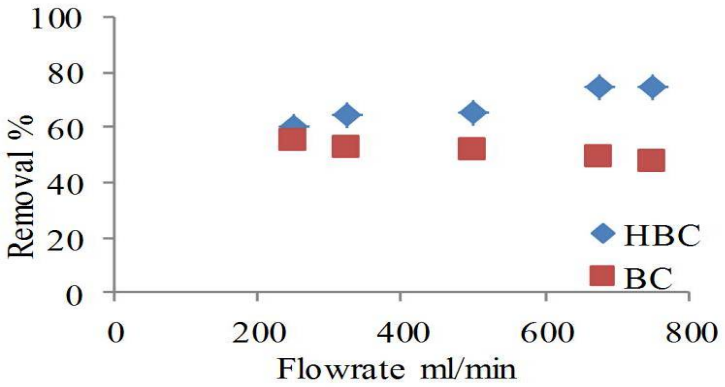

Figure 15. Flow rates of 2,4-DCP solution vs. Percentage removal at flow rate in range of 250–750 ml/min, solute pH of 6.5, 3g of adsorbent and 7.5 mg/L.

Studies were conducted at 28°C (room temperature) to study the initial concentrations effect, in range from 5-10 mg/L of 2,4-DCP, on adsorption at fixed variables: adsorbent weight of 3g, flow rate of 500 ml/min, pH of 6.5. It can be observed from Figure 16 that at lower initial concentration the sorption capacities for BC and HBC adsorbents increased with increasing initial concentration, then ascend slowly (for the BC adsorbent) or plateau off (for the HBC adsorbent). From the experiment data, the highest removal percentage for HBC was approximately 75% at 7.5 mg/L initial concentration. For the BC adsorbent, the maximum removal percentage was at 56% at 10 mg/L.

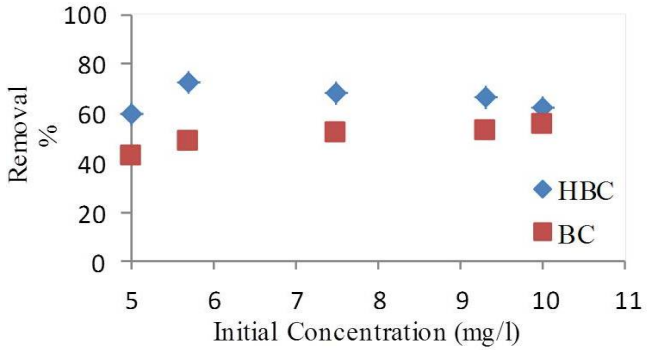

Figure 16. Initial concentration of 2, 4-DCP solutions vs. Percentage of removal at initial concentrations, from 5 to 10 mg/L, pH of 6.5, adsorbent weight of 3g and flow rate of 500 ml/min.

In the first order kinetic model equation, the values of $\log(q_e - q_t)$ for 2,4-DCP were determined and plotted against time T, as depicted in Figure 17,

while the calculated results of the pseudo-first order model are depicted in Table 5. If the plotted line is linear with good (R^2) correlation coefficient, then Lagergren equation is suitable; and it can be seen that the BC did not fare well.

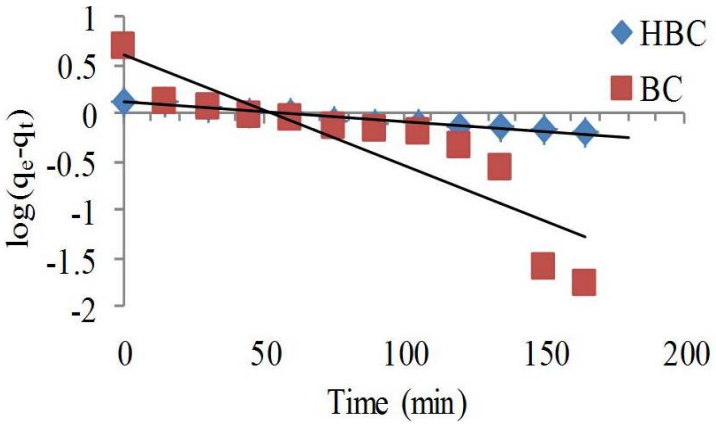

Figure 17. Results from pseudo-first order kinetic model for the removal of 2,4-DCP at initial concentrations 10 mg/L, pH of 6.5, adsorbent weight of 3g and flow rate of 500 ml/min.

From the equation of pseudo-second order kinetic model was found to be simply to expect the kinetics behaviour of adsorption over the whole zone; the linear plot of t/q_t against time T, described in Figure 18 and in Table 5 as well as, was employed to find the slope of $(1/q_e)$, and the intercept of $(1/k_2\ q_e^2)$. From Table 5, agreements between determined values of q_e and experimental values was clear; 5.68 against 5.56 for the BC, and 5.90 and 6.25 for the HBC. Thus, the second-order kinetics model is assured well than the first-order kinetics model to expect and depict the adsorption process of 2,4-DCP onto BC and HBC adsorbents.

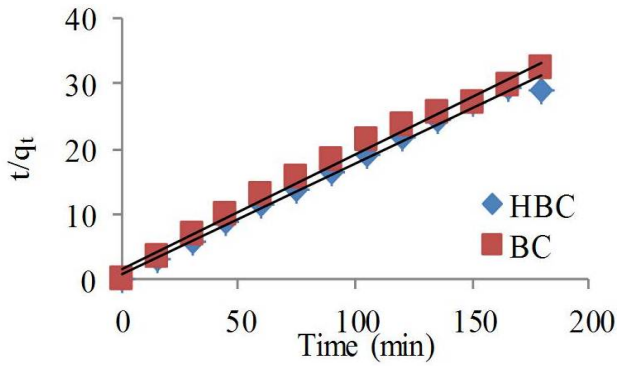

Figure 18. Results from pseudo-second order kinetic model for the removal of 2,4-DCP at initial concentrations 10 mg/L, pH of 6.5, adsorbent weight of 3g and flow rate of 500 ml/min.

Table 5. Adsorption kinetic model rate constants for 2, 4-DCP removal by different adsorbents

Adsorbent	q_{eExp} mg/g_{ad}	Pseudo-first order			Pseudo-second order		
		$q_{e(cal)}$ mg/g	k_1	R^2	$q_{e(cal)}$ mg/g	k_2	R^2
BC	5.56	4.140	0.0260	0.7810	5.68	0.0190	0.9925
HBC	6.25	1.317	0.0046	0.9421	5.90	0.0311	0.9916

For the adsorption isotherm, the plots of ($1/q_e$) against ($1/C_e$) are described in Figure 19, and the calculated data in Table 6. It can be clearly seen from the Table that the (R^2) correlation coefficients were good for two adsorbents; with HBC slightly better. And hence the Langmuir isotherm model is agreeable.

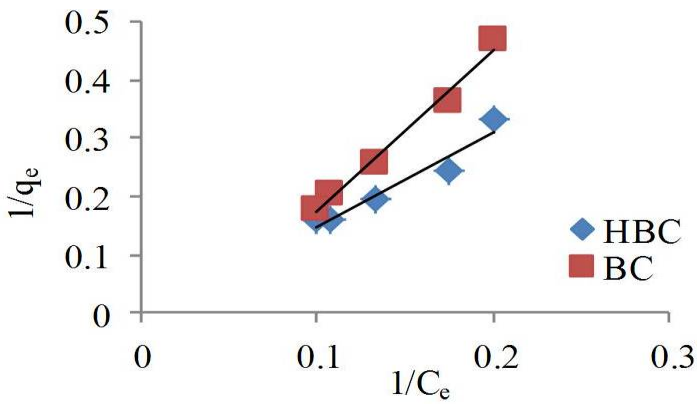

Figure 19. Langmuir isotherms ($1/q_e$) vs. $1/C_e$ for the adsorption of 2, 4-DCP (at different initial concentration in range 5-10 mg/L, contact time of fluidization 180 min, flow rate of 500 ml/min, pH of 6.5 and 3g of adsorbent).

Form the Freundlich isotherm model equation the values of K_f and n were gained from the intercept and the slope of the plots between $\ln(q_e)$ against $\ln(C_e)$ in Figure 20 and depicted in Table 6 together with other variables from the Langmuir model equation. The Freundlich model, however, obtained a better fitting for performing the adsorption of 2,4-DCP onto both adsorbents since the R^2 correlation coefficient yielded were relatively higher and the n (computed coefficient) values were less than unity. Also the value of constant 1/n were calculated, 1.26 for BC and 1.25 for HBC. In this case the values of 1/n higher than unity, that means the constant of adsorption increases when the concentration of 2,4-DCP increase.

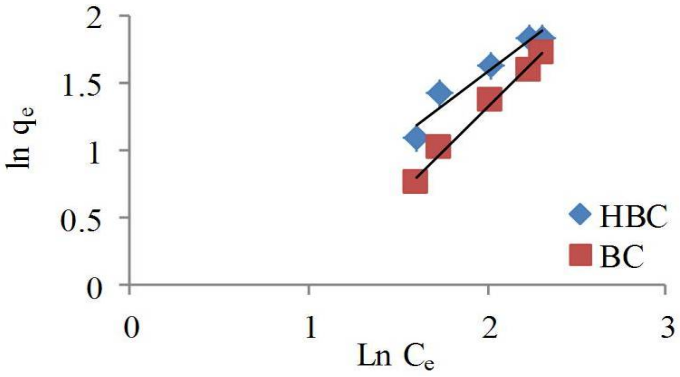

Figure 20. Freundlich isotherm ln(qe) vs. 1n(Ce) for the adsorption of 2,4-DCP at different initial concentration in range 5-10 mg/L, contact time of fluidization 180 min, flow rate of 500 ml/min, pH of 6.5 and 3g of adsorbent.

Table 6. Isotherm parameters for sorption of 2, 4-DCP by different adsorbent

Adsorbent	Langmuir			Freundlich		
	q_{max}	b	R^2	K_F	n	R^2
BC	10.69	0.0350	0.9461	0.302	0.79	0.9650
HBC	16.37	0.0315	0.9699	0.410	0.80	0.9827

5.2.2. Circulation column adsorption of Pb

A factor indicating removal percent efficiency of Pb(II) from aqueous solution is the pH. For the adsorption of Pb(II) from aqueous solution onto two adsorbents balls BC and HBC, this effects were investigated from adjustment of initial pH in range from 3 to 10 at 28 °C (room temperature) while the initial of Pb(II) concentration solution of 70 mg/L was permanently maintained. Various behaviour paths were observed for the both adsorbents as described in Figure 21. For the BC adsorbent ball, the maximum metal ions removal percentage of 94% happened at pH 10, and its rates of removal decreased dramatically to be 15% at the low acidic pH zone of 6. For the HBC adsorbent ball in the experimental data the Pb(II) removal percentage rates increased from solely above 60% at pH 3 to above 90% at pH 4. In our HBC realization, a maximum Pb(II) removal percentage rates of nearly 95% occurred at pH 10, and was rather steady between pH 8-10, though with a sharp steep at pH 6

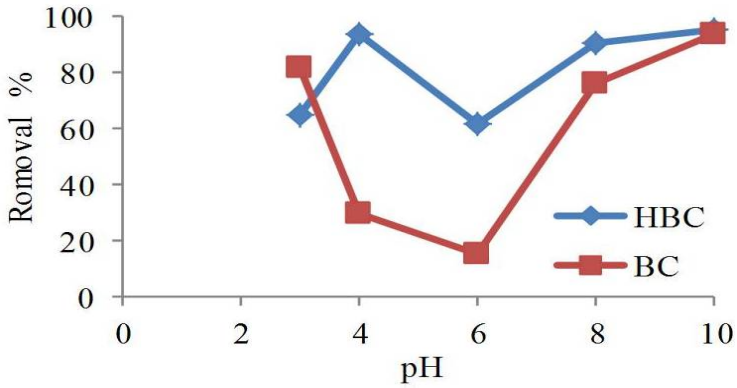

Figure 21. Initial pH of Pb(II) vs. Percentage of removal at initial pH between 3 to 10 at room temperature of 28°C and initial concentration 70 mg/L.

The percentage removal of Pb(II) by adsorption onto both adsorbents BC and HBC was studied on the effect of contact time of fluidization in the column at varied time intervals start from 0 to 180 minutes. Experiments were carried out at 28 °C (room temperature) while other parameters were kept constant (3g of adsorbents ball, pH of 6.5, initial concentration of the Pb(II) of 50 mg/L and 250 ml/min flow rate). Figure 22 observes the effect of contact time of fluidization on the Pb(II) percentage removal, and the equilibrium time for two adsorbents was patently 180 minutes. The removal percentage rates were approximately 57% for the BC adsorbent, and 69% for the HBC adsorbent at equilibrium.

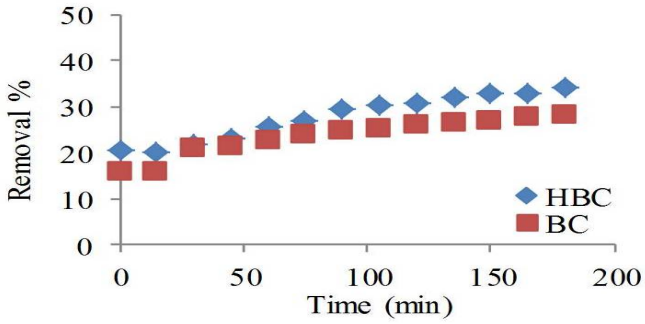

Figure 22. Contact time of circulation fluidization vs. Percentage of removal (at contact time of fluidization between 0 to 180 min, flow rate of 500 ml/min, solute pH of 6.5, 3g of adsorbent, 50 mg/L of the Pb(II) initial concentration).

The effect of different flow rate was investigated for adsorption of Lead ion from aqueous solution employing the BC and the HBC

adsorbents ball. Experiments were conducted at flow rate between 250 to 750 ml/min at 28 °C (room temperature) while the other variables were kept constant (pH of 6.5, initial concentration of the Pb (II) of 50 mg/L and 3g of adsorbents ball). Figure 23 describe the effect of different flow rate on the percentage removal rate; that for one of the adsorbent, an increase in the previous decreases the latter. From the experiments results, the highest percentages of removal rates were about 57% for the BC adsorbent, and 69% for the HBC adsorbent, at 250 ml/min flow rate. In this case of a lower flow rate, the contact or residence time was increased in the fluidization column, and the opposite happened at a higher flow rate.

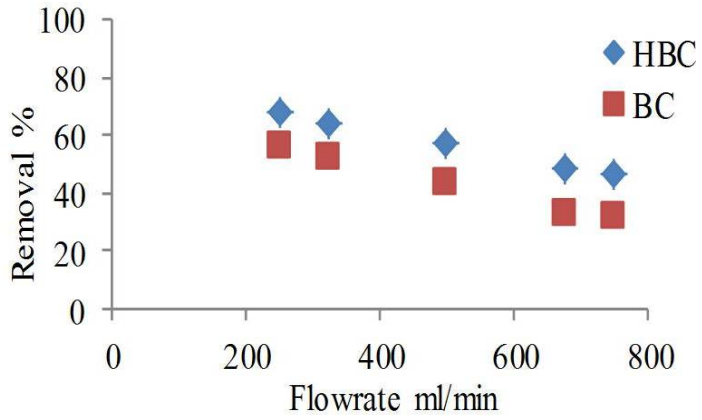

Figure 23. Flow rate of Pb(II) solution vs. Percentage removal (at flow rate in range of 250–750 ml/min, solute pH of 6.5, 3g of adsorbent and 50 mg/L).

Experiments were carried out at 28 °C (room temperature) to study this effect between 30 to 70 mg/L of Lead ion solution, whilst other parameters were kept constant (3g of adsorbent ball weight, flow rate of solution of 500 ml/min and pH of 6.5). Figure 24 depicts the effect of different initial concentration on the removal percentage rate of metal ion. The capacities of sorption for the BC adsorbent and the HBC adsorbent behave identically. For this effect, rise in initial Lead concentration was followed by an rise in capacity rate of Pb(II). Though the pore girth and shape of the BC and the HBC adsorbents vary, these are constants, concept that at low initial Lead concentration, the diffusion is greater. From the experiment result, the highest percentages of removal rates were 53% for the BC adsorbent, and 77% for the HBC adsorbent, at 30 mg/L initial concentration.

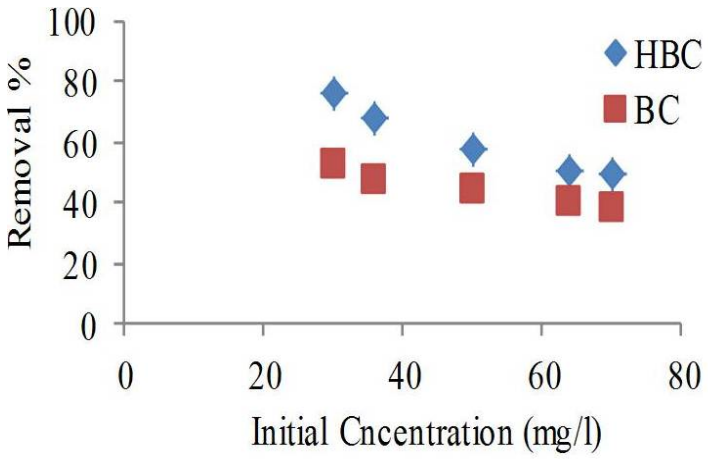

Figure 24. Initial concentration of Pb(II) solutions vs. Percentage of removal (at initial concentrations, from 30 to 70 mg/L, pH of 6.5, adsorbent weight of 3g and flow rate of 500 ml/min).

The both kinetic models, pseudo-first order and pseudo-second order, were employed to study the Pb(II), adsorption kinetics onto adsorbents balls BC and HBC. From the equation of the first order, the values of constant k_1 and q_e were determined from the slope and the intercept of the plot of $\log(q_e-q_t)$ against time, described in Figure 25, while the calculated results of the pseudo-first order model are depicted in Table 7. It can be seen this model is not quite appropriate because of the value of q_e calculated (7.98 for the BC, and 20.77 for the HBC) differed frequently from q_e got from experimental (40.29 for the BC, and 41.20 for the HBC).

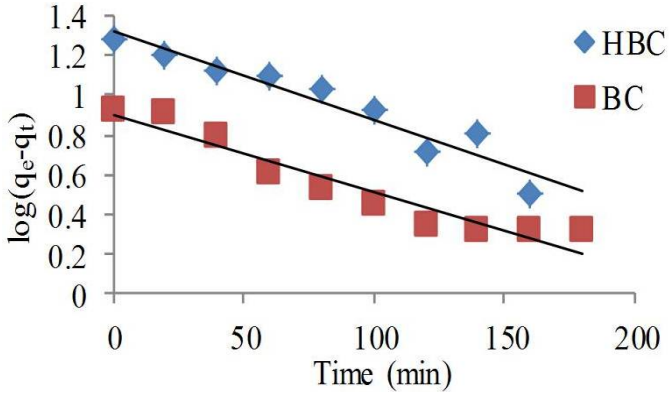

Figure 25. Results from Pseudo-first order kinetic model for the removal of Pb(II) (at initial concentrations 70 mg/L, pH of 6.5, adsorbent weight of 3g and flow rate of 250 ml/min).

For Lead ion adsorption by the BC and the HBC, the k_2 constant of pseudo-second order kinetic model, and q_e cal, values were calculated from the slope and the intercept, $(1/q_e)$ and $(1/k_2\ q_e^2)$ respectively of the linear plot of (t/q_t) against time, described in Figure 26, and in the Table 7 as well. The (R^2) correlation coefficients yielded from the second order model for the BC and the HBC adsorbents were higher than those derived from the first order model. Furthermore, the agreement between the values of q_e got from experimental and that result from the calculation was clearly very close; 40.29 against 40.98 for the BC adsorbent, and 41.20 against 40.98 for the HBC adsorbent.

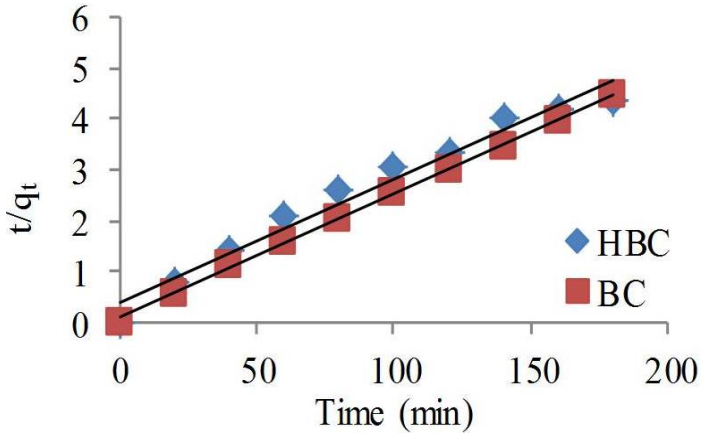

Figure 26. Results from Pseudo-second order kinetic model for the removal of Pb(II), (at initial concentrations 70 mg/L, pH of 6.5, adsorbent weight of 3g and flow rate of 250 ml/min).

Table 7. Adsorption kinetic model rate constants for Pb(II) removal by different adsorbents.

Adsorbent	q_{eExp} mg/g_{ad}	Pseudo-first order			Pseudo-second order		
		$q_{e(cal)}$ mg/g	k_1	R^2	$q_{e(cal)}$ mg/g	k_2	R^2
BC	40.29	7.98	0.009	0.9116	40.98	0.0075	0.9994
HBC	41.20	20.77	0.01	0.9209	40.98	0.0015	0.9719

Both isotherm models, Langmuir and Freundlich, were used here in the studying of the BC and HBC adsorbents ball. The liner plot of $(1/q_e)$ against $(1/C_e)$ of first model (Langmuir) is depicted in Figure 27, and the calculated

results described in Table 8. The values of q_{max} and K_L from the Table are estimated from the liner plot by the slope and the intercept of. The (R^2) correlation coefficients gained were good for two, the BC and the HBC adsorbents; meaning that the Langmuir model is suitable.

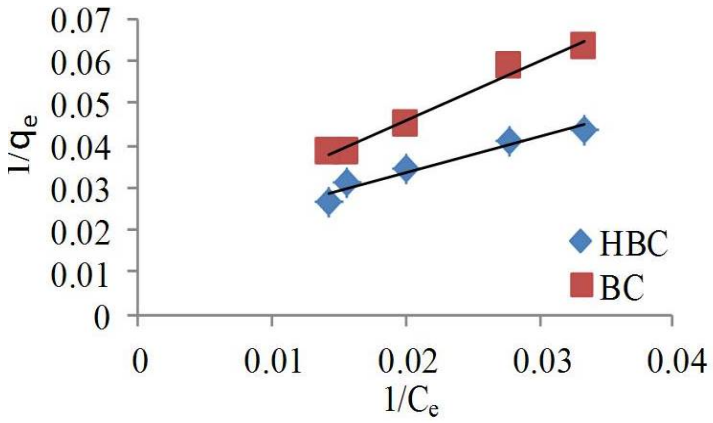

Figure 27. Langmuir isotherms ($1/q_e$) vs. ($1/C_e$)for the adsorption of Pb(II), (at different initial concentration in range 30-70 mg/L, contact time of fluidization 180 min, flow rate of 500 ml/min, pH of 6.5 and 3g of adsorbent).

The K_F and n values, for Freundlich model were gained from the plots of $\ln(q_e)$ against $\ln(C_e)$ by the slope and the intercept, in Figure 28 and depicted in Table 8, two of them with parameters from the Langmuir model. Furthermore, the highest value of K_F indicates that the Lead ion adsorption capacity of the HBC is high; and the low value of 1/n (0.64 for the BC and 0.55 for the HBC) suggests that, if any large change in the concentration of Pb(II) ions at equilibrium would not be result in a change in the value of metal adsorbed by the HBC adsorbent. The (R^2) for the Freundlich models were found to be close to those obtained from the Langmuir model. These two models gave (R^2) of more than 0.94 and thus the experimental data are fitted well.

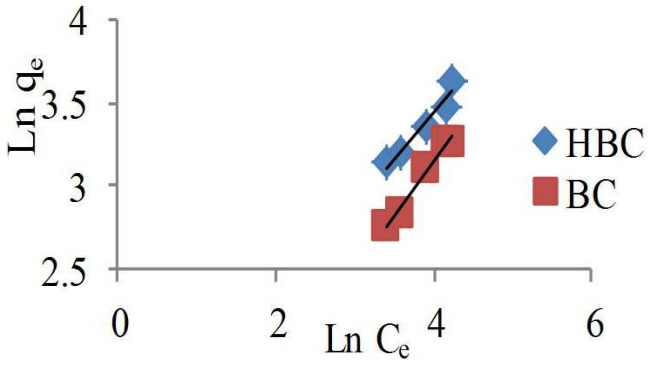

Figure 28. Freundlich isotherm $\ln(q_e)$ vs. $\ln(C_e)$ for the adsorption of Pb(II) (at different initial concentration in range 30-70 mg/L, contact time of fluidization 180 min, flow rate of 500 ml/min, pH of 6.5 and 3g of adsorbent).

Table 8. Isotherm parameters for sorption of Pb(II) by different adsorbent

Adsorbent	Langmuir			Freundlich		
	q_{max}	K_L	R^2	K_F	n	R^2
BC	57.47	0.012	0.9857	1.77	1.56	0.9853
HBC	59.52	0.020	0.9466	3.49	1.83	0.9517

5.3. Fixed bed column adsorption

In this section fixed bed column adsorption characteristic for adsorption of Pb(II) by adsorbent mixture (CB), contained from Sudanese Clay (SC) and Bamboo biochar (BB) from aqueous solution will be investigated. More details of this part have been written in publications attached in **Appendix C.**

The effect of different flow rate on fixed bed column adsorption of Lead ion using the CB adsorbent was studied under several flow rate between 10 to 20 ml/min, whilst other parameters were kept constant (bed height of the CB adsorbent 25 mm and an initial concentration of Lead ion of 17.5 mg/L). The breakthrough curves gained are depicted in Figure 29. In general the breakthrough occurred very slowly with weak flow rate. Similarly, the breakthrough time to attain saturation decreased significantly when the flow rate increasing.

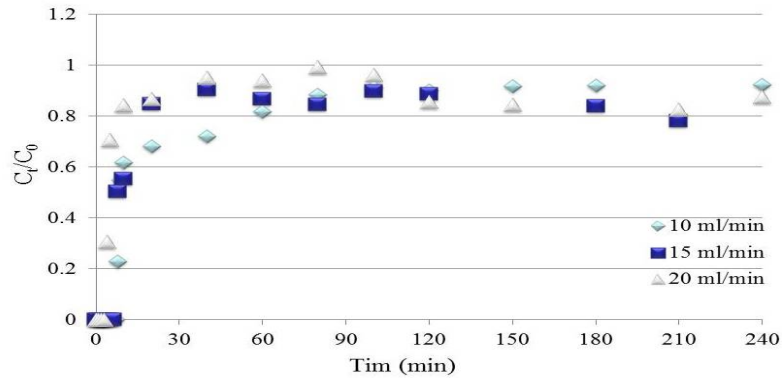

Figure 29. Breakthrough curves for Pb(II) adsorption on the CB at different flow rate 10, 15 and 20 ml/min, (at constant inlet Pb(II) concentration of 17.5 mg/L and bed height of 25 mm)

The effect of various initial metal concentration on adsorption of Lead ion by the CB adsorbent were studied employing different inlet Pb(II) concentration between 5 to 30 mg/L while other variables were fixed (bed height of adsorbent 25 mm and Pb(II) solution flow rate of 15 ml/min). Figure 30 describe the breakthrough curves gained from different concentration of Pb(II). From the adsorption results, the breakthrough time, the removal percent efficiency and the saturation time reduced when the initial concentration of the Pb(II) ions increase. The Lead ions adsorbed by the CB adsorbent mixture increased from 306 to 887 and 905 mg, in sequent when the initial concentration of 5, 17.5 and 30 mg/L.

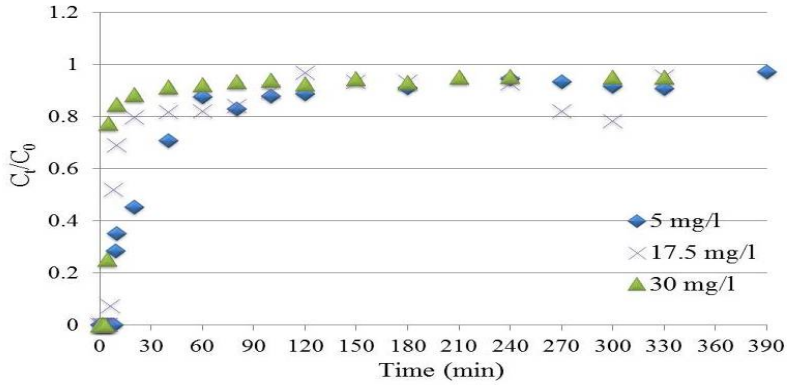

Figure 30. The breakthrough curves for Pb(II) adsorption on the CB at different inlet Pb(II) concentrations 5, 17.5 and 30 mg/L, (at constant bed height of 25 mm and flowrate of 15 ml/min)

Removal of metal ion in the adsorption process employing the CB adsorbent mixture was investigated under the effect different of bed height while the flow rate and inlet of Pb(II) solution concentration were fixed, in sequent at 15 ml/min and 17.5 mg/L. Breakthrough curves for the bed height of 10, 25 and 40 mm are depicted in Figure 31. The breakthrough curves gained were dropped with lower bed height.

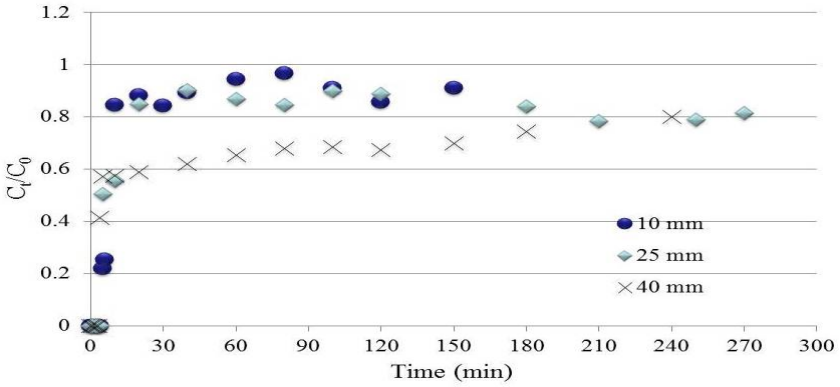

Figure 31. Breakthrough curves for Pb(II) adsorption on the CB at different bed height 10, 25 and 40 mm, (at constant inlet Pb(II) concentration of 17.5 mg/L and flow rate of 15 ml/min)

The parameters from the breakthrough curves can be applied to predict the column efficiency in design. The BDST model plot of time against bed depth at 15 ml/min flow rate was linear, as depicted in Figure 32. The value of (R^2) correlation coefficient of 0.9959 is high, meaning that, good validity of this model. The obtained values of the model variables (N) and (K_α) are 393.75 mg/L and 0.037 L/mg h, respectively.

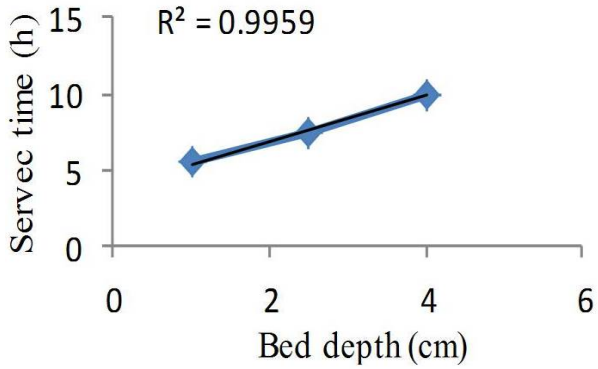

Figure 32. BDST plot for Pb(II) adsorption on CB

Adams-Bohart model was used for the experimental result and the value of adsorbent capacity (N_0) and the (k_{AB}) constant of the model were determined and presented in Table 9, with the (R^2) correlation coefficients (gained between 0.9182 to 0.9788). On the bed height variable, (N_0) increased when increasing bed height while (k_{AB}) decreased.

Table 9. Adams-Bohart model result from linear regression analysis

Initial concentration (mg/L)	Flow rate (ml/min)	Bed height (mm)	k_{AB} (L/mg min)	N_0 (mg/L)	R^2
5	15	25	0.0024	298.26	0.9267
17.5	15	25	0.000262857	939.68	0.9263
30	15	25	0.0002	1090.66	0.9544
17.5	10	25	0.000297143	891.63	0.9788
17.5	15	25	0.0002	1090.66	0.9544
17.5	20	25	0.000182857	1283.8	0.9506
17.5	15	10	0.000411429	478.81	0.9182
17.5	15	25	0.000262857	939.68	0.9263
17.5	15	40	6.28571E-05	2827.58	0.9501

The experimental results were fitted well to the Thomas model. The calculated (k_{Th}) rate constant, the maximum adsorbent capacity (q_0), and the (R^2) correlation (gained in range of 0.8839 to 0.9838) are recorded in Table 10. From the Table, (k_{Th}) rate constant decreased when the inlet concentration of Pb(II) increasing due to the rise in mass transport resistance while the (q_0) values were increasing. The maximum adsorbent capacity (q_0) decreases with increasing the bed height and flow rate. The (k_{Th}) rate constant of Thomas model reduce with increasing the bed height.

The fourth one, and final model used for the experimental results is the Yoon-Nelson model. The Yoon–Nelson suitability constant (k_{YN}) and the time wanted for retaining 50% (τ) determined for all results of the breakthrough curves with conformable (R^2) correlation coefficient are depicted in Table 11. The R^2

in range of 0.9287 and 0.9904 gained from this model. The 50% (τ) time retention was found to be significantly decreasing when the inlet Pb(II) concentration increase and the solution flow rate.

Table 10. Thomas model result from linear regression analysis

Inlet concentration (mg/L)	Flow rate (ml/min)	Bed height (mm)	k_{Th} (L/mg min)	q_0 (mg/g)	R^2
5	15	25	0.003780000	7352.58	0.8839
17.5	15	25	0.000542857	9319.21	0.9763
30	15	25	0.000610000	12313.52	0.9795
17.5	10	25	0.000577143	18018.94	0.9552
17.5	15	25	0.002834286	9852.22	0.8841
17.5	20	25	0.000542857	9319.21	0.9763
17.5	15	10	0.000942857	25444.60	0.9832
17.5	15	25	0.000577143	18018.94	0.9552
17.5	15	40	0.000377143	2682.20	0.9586

Table 11. Yoon–Nelson model result from linear regression analysis

Inlet concentration (mg/L)	Flow rate (ml/min)	Bed height (mm)	k_{YN} (L/mg min)	τ (min)	R^2
5	15	25	0.0196	221.62	0.9670
17.5	15	25	0.0124	197.84	0.9849
30	15	25	0.0183	54.73	0.9795
17.5	10	25	0.0101	205.93	0.9552
17.5	15	25	0.0124	197.84	0.9849
17.5	20	25	0.0101	67.73	0.9904
17.5	15	10	0.0165	77.55	0.9832
17.5	15	25	0.0124	197.84	0.9849
17.5	15	40	0.0028	123.11	0.9900

5.3.1 Fixed bed column adsorption optimizing

The CB adsorbent mixture ability for adsorption Lead ion in this work was calculated by capacity gained. Results data of examination are reported for the effects of three parameters on a capacity gained of CB adsorbent mixture. RSM was applied to predict the optimum values of these parameters. A mathematical model was advanced based on the experimental design performed firstly by the essential regression software, as reported in Table 15. The experimental result was applied to develop a quadratic regression model to expect the CB gained as a function of the variables including the (F, ml/min) flow rate, the (C, mg/L) initial concentration of solution Pb(II), and the (H, mm) bed height of adsorbent CB mixture, which was given by:

(CB adsorbent capacity) $Resp\_1 = 82.03 - 5.487*F + 0.368*C - 24.37H + 0.08984*F^2 - 0.02582*C^2 + 1.885*H^2 + 0.03208*FC + 0.704*FH + 0.06167*CH$ (10)

Table 12. Experimental design matrix and results

Run	Flowrate ml/min	Concentration mg/l	Bed height mm	Resp_1	Predicted Resp_1	Residuals
1	15	17.5	25	6.55	6.84	-0.293
2	17.9	24.9	34	5.7	7.09	-1.390
3	12	10	16	13.3	14.30	-1.000
4	20	17.5	25	9.3	6.74	2.563
5	15	17.5	4	6.91	6.13	0.783
6	15	17.5	25	6.65	6.84	-0.190
7	12	10	34	4	3.86	0.145
8	15	17.5	10	18.64	16.04	2.597
9	12	24.9	16	12.13	13.55	-1.419
10	17.9	10	16	5	6.35	-1.352
11	15	17.5	25	6.75	6.84	-0.09363
12	12	24.9	34	3.7	4.74	-1.038

13	17.9	10	34	2.4	3.37	-0.972
14	17.9	24.9	16	5.9	8.44	-2.535
15	10	17.5	25	12.26	11.44	0.816
16	15	30	25	6.7	4.06	2.642
17	15	5	25	2.3	1.56	0.737

The analysis of variance (ANOVA) summarized in Table 13 and 14, demonstrated that the models were highly significant at 95% confidence level, with high F-Value and low F-significance. The P-values and regression coefficients were shown in same table; these were used for check the significance of each coefficient. From that test, it was found that flowrate (F) and bed height (H) were the most significant factors (p-values <0.05) affecting the CB capacity yield and the removal percentage of Pb(II) in CB. Additionally, as can be seen in Figure 33, the values predicted for CB capacity response by the mathematical model were in good agreement with the experimental results, confirming the fitness of the model.

The good quality of the model developed was estimated based on the (R^2) correlation coefficient. From the Figure 33, the model data fit good with the experimental data, as indicated by the calculation coefficients (R^2) of 0.875 for the model expectation of CB gained, as will show the points of results were well distributed near to a straight forward line, while proposed a good relation between expected and the experimental data of the response. This specified that 87.5% of the total difference in the Lead ion uptake in CB adsorbent mixture. The R^2 correlation coefficient from Eq.10 was reflect as mild to validate the fit validate, while may be lead to large difference in CB adsorbent capacity gained expected from the model.

Table 13. Analysis of variance (ANOVA) summarized

ANOVA						
Source	SS	SS%	MS	F	F Signif	df
Regression	262.51	88	29.17	5.446	0.01802	9
Residual	37.49	12	5.356			7
LOF Error	37.47	12 (100)	7.494	750.7820	0.00133	5
Pure Error	0.01996	0 (0)	0.00998			2
Total	300.00	100				16

Table 14. Continue analysis of variance (ANOVA) summarized

		P value	Std Error	-95%	95%	t Stat	VIF
b_0	82.03	0.01664	26.22	20.03	144.02	3.129	
b_1	-5.487	0.06895	2.556	-11.53	0.557	-2.147	Significant
b_2	0.368	0.650	0.776	-1.466	2.202	0.474	
b_3	-24.37	0.0085	6.735	-40.30	-8.442	-3.618	significant
b_4	0.0898	0.287	0.07799	-0.09458	0.274	1.152	
b_5	-0.0258	0.07732	0.01248	-0.05532	0.00369	-2.069	
b_6	1.885	0.06611	0.867	-0.164	3.934	2.175	
b_7	0.0321	0.415	0.03704	-0.05550	0.120	0.866	
b_8	0.704	0.05656	0.309	-0.02584	1.434	2.281	
b_9	0.06167	0.633	0.123	-0.230	0.354	0.500	

In the statistical data were shown that the model appropriate for predict the adsorbent capacity gained within the range of variables investigated. In Figure 33 describe the expected values against the experimental values for Lead ion uptake by CB adsorbent, as predicted the errors values between expected and experimental were bigger. For this case the possible reason for the lower notability and higher error of assessment were given by the model, might be there are other variables affecting in the adsorbent capacity gained, not only these three parameter. More studies were needed to verify this. Essential regression software was used to optimize the conditions, and the results showed that the maximum value of capacity yield was about 26 mg/g for a flowrate of 10 ml/min, a bed height of 10 mm, and an initial concentration of 14.5 mg/L

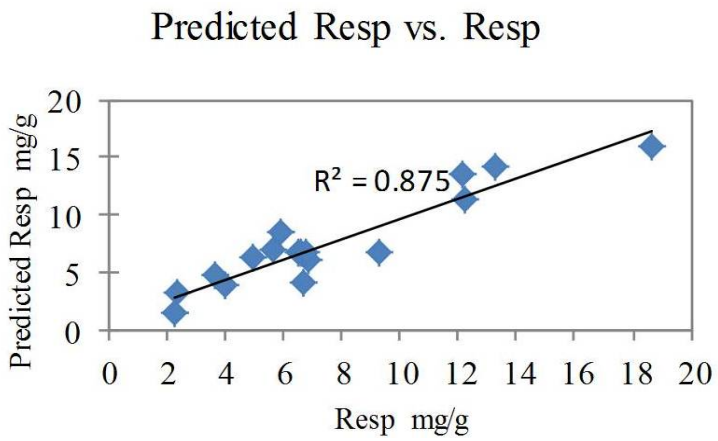

Figure 33. Experimental results versus predicted values

6. Conclusion remarks

Bamboo biochar (BB) and Hydroxyapatite (HAP) are capable of removing Pb(II) from aqueous solutions, particularly when they are mixed with Calcium sulphate (CS). In this study, the adsorption capacities of the mix-adsorbents for a 400 (mg/L) Pb(II) contamination were found to be able to remove 152.4 (mg Pb(II)/g) when using (BB&CS), and 200 (mg Pb(II)/g) when using (HAP&CS). Though at three-fourths efficiency, this work has shown that low-cost (BB&CS) adsorbent can play an important role in adsorption of lead from water and/or wastewater, compared to the use of higher-price (HAP&CS). The combination of (BB) and (CS) to remove lead ions from aqueous solutions is found to be promising.

The adsorbents mixtures (HAP&CS) and (BB&CS) were able to substantially remove Zn(II) and Cd(II) from aqueous solutions. The adsorbent capacity were found to be 24.47 mg Zn(II)/g, and 18.05 mg Cd(II)/g for adsorbent mixture (HAP&CS), and 14.423mg Zn(II)/g, and 8.0423 mg Cd(II)/g for adsorbent mixture (BB&CS). Clearly from this results both adsorbents mixture had ability to adsorb zinc more than cadmium, that due to difference in the size of atoms between Zn(II) and Cd(II). However, the comparison between Pb(II), Zn(II) and Cd(II), both adsorbents mixture had very high ability to adsorb lead more than other metals in this study.

Bamboo biochar plus Calcium sulphate (BC), and Hydroxyapatite plus BC were studied for their capacity in the removal of 2,4-dichlorophenol (2,4-DCP) in aqueous solution. The time of fluidization, adsorption kinetics and isotherms, among others, were studied. HBC and BC adsorbents are thus suitable and acceptable for the removal of 2,4-DCP from aqueous solutions at parameters it depended like the pH, the initial concentration of 2,4-DCP, the flow rate of the solution and the time of fluidization. Both adsorbents were compared for the removal of phenol via adsorption with many others, and HBC was found to be of good standing, while BC, though in the lower rank, fared acceptably based on its adsorbent capacity and isotherms and kinetics study. Taken its low cost into consideration, BC could be regarded as a new, moderately effective adsorbent that can be applied in the field of wastewater treatment and industries.

The BC and BC plus Hydroxyapatite (HBC) were investigated for their capacity in the removal of Pb(II) in aqueous solution. The initial pH of the solution, the time of circulation in the column, the flow rate, initial concentration, adsorption kinetics and isotherms, were studied. The suitable time of circulation in the column was found to be 180 min. Both adsorbents are thus suitable for the removal of Pb(II) from aqueous solution at variables they depended such as the initial concentration of Pb(II), the pH, the time of circulation in the column and the flow rate of the solution. Hence it can be concluded that BC offers a new effective and low cost adsorbent.

The CB, adsorbent mixture of Sudanese clay plus Bamboo biochar, was used for removal of Lead ions from aqueous solution in the fixed bed column. Different parameters studied were: initial concentration Lead ion, solution flow rate, and adsorbent bed height. The process system was detected to perform better at low solution flow rate, high Lead ions initial concentration and low adsorbent mixture bed height. The Bed depth service time (BDST) model was applied in the fixed bed column performance experimental results and the parameters of this model were determined. The column results gained fitted well with also three other mathematical models: the Adams–Bohart, the Thomas and the Yoon-Nelson models. All these models can be suitable, but the (BDST) and Thomas and the Yoon-Nelson models, were found to better expect the breakthrough curves than the Adams-Bohart model. This study described that the adsorbent mixture CB can employ an important role in adsorption of Lead ion from aqueous solution in the fixed bed column.

It was demonstrated that adsorption process were generated by using mixed of clay and Bamboo biochar with ratio 1:1 in the column for adsorption Pb(II) from aqueous solution. Flowrate and bed height were identified as the most significant factors affecting the adsorbent (CB) capacity yield. The model was adequate for predicting the CB capacity yield at less than 5% error. From RSM, a maximum value of 29 mg/g of the CB capacity yield was obtained at 10 ml/min of flowrate, 15 mg/L of solution concentration, and bed height of 10 mm. Experiments were conducted at the optimum conditions in order to verify the accuracy of the simulated optimum conditions. The CB capacity yield was 25 mg/g as compared to simulated value of 26 mg/g (4 % error).

References

1) E. Corcoran, C. Nellemann, E. Baker, R. Bos, D. Osborn, H. Savelli (eds), Sick Water, The central role of wastewater management in sustainable development. A Rapid Response Assessment, UNEP, UN-HABITAT, GRID-Arendal, (2010) 1-82. www.grida.no.

2) Government of Australia, Water Quality Protection Note, Industrial wastewater management and disposal, WQPN51, October (2009) 1-28.

3) M. A. Barakat. New trends in removing heavy metals from industrial wastewater, J. Arab. J. Chem. 4 (2011) 361–377.

4) N. K. Srivastava, C.B. Majumder, Novel biofiltration methods for the treatment of heavy metals from industrial wastewater, J. Hazard. Mater. 151 (2008) 1-8.

5) I. A. W. Tan, A. L. Ahmad, B. H. Hameed, Adsorption isotherms, kinetics, thermodynamics and desorption studies of 2, 4, 6-trichlorophenol on oil palm empty fruit bunch-based activated carbon, J. Hazard. Mater. 164 (2009) 473-482.

6) R. Gao, J. Wang, Effects of pH and temperature on isotherm parameters of chlorophenols biosorption to anaerobic granular sludge, J. Hazard. Mater. 145 (2007) 398-403.

7) B. H. Hameed, L. H. Chin., S. Rengaraj, Adsorption of 4-chlorophenol onto activated carbon prepared from rattan sawdust, Desalination 225 (2008) 185-198.

8) Z. Aksu, D. Akpınar, Modelling of simultaneous biosorption of phenol and nickel(II) onto dried aerobic activated sludge, Sep. Purif. Technol. 21 (2000) 87-99.

9) Z. Xuequan, W. Xiankai, S. Huixiang, W. Dahui, Adsorption of 2,4-dichlorophenol from aqueous solution onto microwave modified activated carbon: Kinetics and equilibrium, Transactions of Tianjin University. J. 15 (2009) 408-414.

10) O. Hamdaoui, E. Naffrechoux, J. Suptil, C. Fachinger, Ultrasonic desorption of p-chlorophenol from granular activated carbon, Chem. Eng. J. 106 (2005) 153-161.

11) M. Yan, G. Naiyun, C. Wenhai, L. Cong, Removal of phenol by powdered activated carbon adsorption, Frontiers Environ. Sci. Eng. 7 (2013) 158-165.

12) S. V. Yadla, V. Sridevi1, and M. V. V. C. Lakshmi1, A Review on Adsorption of Heavy Metals from Aqueous Solution, J. Chem. Bio. Phy. Sci. 2 (2012) 1585-1593.

13) S. B. Chen, Y. B. Ma, L. Chen and K. Xian, Adsorption of aqueousCd^{2+},Pb^{2+}, Cu^{2+} ions by nano-hydroxyapatite: Single- and multi-metal competitive adsorption study. Geochem. J. 44 (2010) 233-239.

14) M. Sarkar, P. K. Acharya, Use of fly ash for the removal of phenol and its analogues from contaminated water, J. Waste Manage. 26 (2006) 559-570.

15) N. T. Abdel-Ghani, G. A. El-Chaghaby, S. Farag, F. S. Helal, Individual and competitive adsorption of phenol and nickel onto multiwalled carbon nanotubes. J. Advanced Res. 6 (2014) 405-415.

16) N. Siddiqui, J. Don, K. Mondal, and A. Mahajan, Development of bamboo-derived sorbents for mercury removal in gas phase, Environ. Technol. J. 32 (2011) 383-394.

17) Z. Tan, J. Xiang, S. Su, H. Zeng, C. Zhou, L. Sun, S. Hu, J. Qiu, Enhanced capture of elemental mercury by bamboo-based sorbents, J. Hazard. Mater. 239 (2012) 160-166.

18) S. Kumar, V. A. Loganathan, R. B. Gupta, M. O. Barnett, An Assessment of U (VI) removal from groundwater using biochar produced from hydrothermal carbonization, J. Environ. Manage. 92 (2011) 2504-2512.

19) L. Hua, W. Wu, Y. Liu, M. B. McBride, Y. Chen, Reduction of nitrogen loss and Cu and Zn mobility during sludge composting with bamboo charcoal amendment, J. Environ. Sci. Poll. Res. 16 (2009) 1-9.

20) J. P. Wang, H. M. Feng, H. Q. Yu, Analysis of adsorption characteristics of 2,4-dichlorophenol from aqueous solutions by activated carbon fibre, J. Hazard. Mater. 144 (2007) 200-207.

21) A. T. Mohd Din, B. H. Hameed, A. L. Ahmad, Batch adsorption of phenol onto physiochemical-activated coconut shell, J. Hazard. Mater. 161(2009) 1522-1529.

22) K. Lin, J. Pan, Y. Chen, R. Cheng, X. Xu, Study the adsorption of phenol from aqueous solution on hydroxyapatite nano powders, J. Hazard. Mater. 161(2009) 231-240.

23) W. Zhu, P. Wu. Surface energetics of hydroxyapatite: a DFT study, J. Chem. Phys. Letters 396 (2004) 38-42.

24) G.Gergely, F.We´ber, I. Luka´cs , A. L.To´th, Z.E. Horva´th , J.Miha´ly, C. Bala´zsi. Preparation and characterization of hydroxyapatite from eggshell, J. Ceramics Inter. 36 (2010) 803-806.

25) H. Xu, L. Yang, P. Wang, Y. Liu, M. Peng, Removal mechanism of aqueous lead by a novel eco-material: carbonate hydroxyapatite, J. Mater. Sci & Technol. 23 (2007) 417-422.

26) D. Liao, W. Zheng, X. Li, Q. Yang, X. Yue, L. Guo, G. Zen, Removal of lead(II) from aqueous solutions using carbonate hydroxyapatite extracted from eggshell waste, J. Hazard. Mater. 177 (2010) 126-130.

27) A. Corami, S. Mignardi, V. Ferrini, Copper and zinc decontamination from single and binary-metal solutions using hydroxyapatite, J. Hazard. Mater. 146 (2007) 164-170.

28) M. Peld, K. Tonsuaadu, V. Bender, Sorption and desorption of Cd^{2+} and Zn^{2+} ions in apatite–aqueous systems, Environ. Sci & Technol. 38 (2004) 5626-5631

29) A. G. Leyva, J. Marrero, P. Smichowski, D. Cicerone, Sorption of antimony onto hydroxyapatite, Environ. Sci. & Technol. 35 (2001) 3669-3675.

30) C. C. Fuller, J. R. Bargar, J. A. Davis, M. J. Piana, Mechanism of uranium interactions with hydroxyapatite: implications for groundwater remediation, Environ. Sci. & Technol. 36 (2002) 158-165.

31) L. Agwaramgbo, N. Magee, S. Nunez, K. Mitt, Biosorption and chemical precipitation of lead using biomaterials, molecular sieves, and chlorides, carbonates, and sulfates of Na & Ca, J. Environ. Protec. 4 (2013) 1251-1257.

32) N. Evaniew, V. Tan, N. Parasu, E. Jurriaans, K. Finlay, B. Deheshi, M. Ghert, Use of a calcium sulphate-calcium. phosphate synthetic bone graft composite in the surgical management of primary bone tumors, Orthopedics 36 (2013) 216–222.

33) N. Belaicha, W. Lemlikchi, M. O. Mecherri, P. Sharrock, A. Nzihou, Composite material with calcium sulfate and calcium phosphate for heavy metals retention, Procedia Eng. 83 (2014) 403-406.

34) P. Liu, Polymer modified clay minerals: A review, Appl. Clay Sci. 38 (2007) 64-76.

35) X. Tang, Z. Li, Y. Chen, Z. Wang, Removal of Zn(II) from aqueous solution with natural Chinese loess: behaviors and affecting factors, Desalination. 249 (2009) 49-57.

36) J. U. K. Oubagaranadin, and Z. V. P. Murthy, Adsorption of divalent lead on a montmorillonite- illite type of clay, Ind. Eng. Chem. Res. 48 (2009) 10627-10636.

37) A. Mellah, S. Chegrouche, The removal of Zinc from aqueous solutions by natural bentonite, Water Res. 31 (1997) 621-629.

38) M. E. I. Ahmed, Selective adsorption of cadmium species onto organic clay using experimental and geochemical speciation modeling data, Inter. J. Eng. Technol. 8 (2016) 128-131.

39) K. G. Bhattacharyya, S. S. Gupta, Pb(II) uptake by kaolinite and montmorillonite in aqueous medium: Influence of acid activation of the clays, Colloids Surf. A. 277 (2006) 191-200.

40) M. A. Ismail, M. A. Z. Eltayeb and S. A. Abdel Maged, Elimination of heavy metals from aqueous solutions using Zeolite LTA Synthesized from Sudanese clay, Res. J. Chem. Sci. 3 (2013) 93-98.

41) R. A. Hutchins. New methods simplifies design of activated carbon system. Chem. Eng. 1973; 80, 133–138.

42) G. S. Bohart, and EQ Adams. Some aspects of the behavior of charcoal with respect to chlorine. 1. J. Am. Chem. Soc. 1920; 42, 523-544.

43) A. A. Ahmad, BH Hameed. Fixed-bed adsorption of reactive azo dye onto granular activated carbon prepared from waste. J. Hazard. Mater. 2010; 175, 298-303.

44) H. C. Thomas. Heterogeneous ion exchange in a flowing system. J. Am. Chem. Soc.1944; 66, 1664–1666.

45) Y. H. Yoon, JH Nelson. Application of gas adsorption kinetics. Part 1. A theoretical model for respirator cartridge service time. Am. Ind. Hyg. Assoc. J. 1984; 45, 509–516.

Appendix

Appendix A

The publication of batch adsorption

Appendix A1

Conference Paper 1

A. Hassan and L. Kaewsichan, ‘‘Removal of Pb(II) from Aqueous Solutions Using Mixtures of Bamboo Biochar and Calcium Sulphate, and Hydroxyapatite and Calcium Sulphate’’, The 3rd EnvironmentAsia International Conference on “**Towards International Collaboration for an Environmentally Sustainable World**”Thai Society of Higher Education Institutes on Environment June 17-19, 2015, Montien Riverside Hotel, Bangkok, Thailand

I(O)_002
The 3rd EnvironmentAsia International Conference on
"Towards International Collaboration for an Environmentally Sustainable World"
Thai Society of Higher Education Institutes on Environment
June 17-19, 2015, Montien Riverside Hotel, Bangkok, Thailand

Removal of Pb(II) from Aqueous Solutions Using Mixtures of Bamboo Biochar and Calcium Sulphate, and Hydroxyapatite and Calcium Sulphate

Ahmed Hassan and Lupong Kaewsichan

Department of Chemical Engineering, Prince of Songkla University, Hat Yai, Songkhla, Thailand

Abstract

Sorption characteristics of Pb(II) from aqueous solutions through a low-cost adsorbent mixture comprising of Bamboo biochar (BB) and Calcium Sulphate (CS), and a more expensive mixture of Hydroxyapatite (HAP) and Calcium Sulphate (CS), were investigated. The effects of equilibrium contact time, and adsorbate concentration conducted in batch experiments were studied. Adsorption equilibrium was established in 40 minutes. The adsorption mechanism of Pb(II) from these two adsorbent mixtures was carried out through a kinetic rate order. A pseudo-second order kinetic model was applied for the adsorption processes. The model yielded good correlation ($R^2 > 0.999$) of the experimental data. Adsorption of Pb(II) using BB&CS and HAP&CS correlated well ($R^2>0.99$) with both the Langmuir and Freundlich isotherm equations under the concentration range studied. Hence, the effectiveness of an inexpensive natural material BB&CS mixture in Pb(II) removal is established, and is promising for use in other heavy metal adsorptions.

Keywords: Natural adsorbents; Bamboo biochar; Calcium sulphate; Hydroxyapatite; Heavy metal adsorption

1. Introduction

Heavy metals generally are recognized to be a threat toward humans and ecosystems because of their high toxicity (Ramesh et al. 2013). Contamination from them has attracted considerably global attention, according to their voluminous discharge into the environment from industrial activities (Heidari et al. 2013). Lead is a toxic element for humans and animals at some concentration and a serious public health issue worldwide (Xu et al. 2007). Lead as the form of Pb(II) is often found in textile dying, ceramic and glass industries, petroleum refining, battery manufacture and mining operations (Heidari et al. 2013). It is extremely toxic and can damage the kidney, liver, brain, nervous, and reproductive systems; among other adverse effects to humans (Ramesh et al. 2013). Therefore, it is necessary to eliminate such hazardous heavy metal ion in wastewater before discharging it into the ecosystem (Farghali et al. 2013). Subsequently, considerable efforts have been spent in treating Pb-containing wastes at their source.

Traditional techniques for the elimination of heavy metal ions include precipitation, membrane filtration, sorption, and ion exchange, etc. For all treatment methods, it is a struggle between cost-effectiveness and environmental regulations. One of these methods, the sorption technique, has been used widely because it is simple, economical, and cost-effective (Zhao et al. 2011). In this method, material like biochar has been used as adsorbent. It has shown strong sorption affinity for organic compounds and may play an important role in controlling organic pollutants in the environment (Cornelissen et al. 2005). Main benefit for the use of biochar is from its structured carbon matrix with high degree of porosity and extensive surface area that enhances its sorbent characteristics, thereby plays an important role in controlling contaminants (Chen et al. 2011). Wood biochar, especially bamboo biochar (BB), has higher carbon content and is more hydrophobic and aromatic than those produced from rice husks. Moreover, bamboo biochar is a material with the lowest level of humification (Zhang et al. 2014) suitable for removal of metal ions. Its high sorption is due to three mechanisms: electrostatic interactions; ionic exchange between ionisable protons and heavy metal cations; and sorptive interaction (Xu et al. 2013). Furthermore, the mechanism of biochar adsorption depends on functional groups and specific surface area

Hydroxyapatite [$Ca_{10}(PO_4)_6(OH)_2$; HAP] is the main mineral constituent of teeth, bones and phosphate mineral rocks (Zamani et al. 2013). Many research works have found that HAP can effectively remove lead ion in aqueous solution under different experimental conditions and show potential removal capacities, with removal percentage trending to 100% (Xu et al. 2007). Synthetic

hydroxyapatite (HAP) has been extensively studied for its kinetics and chemical reaction with a wide variety of metals e.g., Cr, Cu, Cd, Zn, Sb and U (Liao et al.2010). Many types of reaction control Pb removal by HAP and other adsorbents, including surface adsorption, cation substitution or precipitation. Using HAP, adsorption of Pb ions on the surfaces of the adsorbent will be followed by ion exchange reaction amidst the Pb(II) adsorbed and the Ca^{+2} ions in HAP (Takeuchi et al. 1990).

Preliminary investigations by the authors revealed generally higher heavy metals adsorbing efficiencies when either the low-cost bamboo char or the higher-priced HAP were deployed as mixtures together with Calcium Sulphate (CS). Furthermore Calcium salts (chlorides, sulphates, and carbonates) are better lead precipitators than the corresponding sodium salts (Agwaramgbo et al. 2013). Moreover Such composites have been described for use as resorbable biomaterials in bone surgery (Evaniew et al. 2013), but have never been used for the retention of heavy metals from polluted water (Belaicha et al. 2014). The present work aims to investigate and compare two adsorbent mixtures; BB&CS, and HAP&CS, in the study of Pb(II) ions removal from aqueous solutions which involves equilibrium contact time, adsorbate concentration, adsorbent dose, their kinetics through pseudo-second order and applicable to the two isotherm models.

2. Materials and Method

2.1. Materials

The BB used in this study was prepared in the laboratory by pyrolysis process at 500°C; HAP was a commercial type purchased from Sigma-Aldrich (Thailand) Co. LLC**;** and CS was bought from Aldrich Chemicals and was used without further purification. $Pb(NO_3)_2$ (Lead Nitrate) standard samples were acquired from Boss Official Limited Partnership in Thailand.

2.2. Method

2.2.1 Properties of Biochar

Fourier transforms infrared spectroscopies (FTIR) (Bomem, MB 100) were carried out to identify the functional groups of the biochar. Scanning electron microscopy (Hitachi JSM-6700F SEM) was implemented to observe the surface microstructures of the biochar. The pH of the BB was measured by suspending the BB with demineralized water at a mass ratio of 1:20. The solution was then hand-stirred and allowed to stand for 5 min before measurement with a pH meter (Inyan et al. 2012). The BB surface potential was determined by measuring the zeta potential (ζ) of the colloidal biochar suspension obtained through sonication according to the procedure of Johnson (Johnson et al. 1996). Charge mobility of each suspension was determined using Brookhaven Zeta Plus (Brookhaven Instruments, Holtsville, USA), and Smoluchowski's formula was used to convert the electric mobility into zeta potential.

2.2.2 Preparation of Metal Solutions

All metal solutions were prepared from their nitrate salts (Analytical Reagents; AR) and distilled water. The synthetic solutions were all prepared by diluting Pb(II) standard stock solutions (concentration 1000 ± 2mgL^{-1}) obtained by dissolving appropriate amounts of metal salt in double distilled water. Four dilutions: 100, 200, 300 and 400 mg L^{-1}, were used in each set of the experiment.

2.2.3 Sorption Studies

Batch adsorption experiments were conducted on the three adsorbent materials, for which 0.08 g, 0.05 g, and 0.05 g for BB, CS and HAP, respectively, were used to produce the two mixtures. Each mixture of BB&CS and HAP&CS was put into a 250-mL conical flask containing 50 mL of Pb(II) ions at the pre-set concentrations mentioned earlier of 100, 200, 300 and 400 mg L^{-1}, shaken, filtered and subjected to Pb(II) analysis to determine the optimum Pb(II) adsorptions. The effect of contact time was studied in the time range of 0 – 40 minutes. At the end of the adsorption process the suspensions were filtered through 0.45µm syringe membrane filters and the corresponding

supernatant was analysed employing a Perkin Elmer Thermos Scientific S-series model (AAnalyst100) Flam atomic absorption spectrophotometer (AAS) for residual Pb(II) concentrations. Three replicates were conducted for each Pb(II) bio sorption experiment set, and the average values determined. The adsorbent capacity of BB&CS and HAP&CS mixtures were calculated using general equation 1:

$$q_e = (C_0 - C_t)\frac{V}{M} \qquad (1)$$

Where q_e is the amount of Pb(II) adsorbed on the adsorbent (mg g^{-1}); C_0 and C_t are the Pb(II) concentrations in the solution before and after adsorption (mg L^{-1}); V is the volume of the solution (L); and M is the amount of the adsorbents used in the reaction mixture (g).

2.2.4 Adsorption kinetics

The mechanism of sorption can be explained by the kinetic characteristics of sorption. For this purpose, pseudo second-order kinetic model was considered and fitted with the experimental data. The pseudo-second order reaction rate equation, as shown by (Ho et al. 1999), is described in equation (2):

$$\frac{t}{q_t} = \frac{t}{q_e} + \frac{1}{k_2 q_e^2} \qquad (2)$$

Where q_t is the amount of metal ions adsorbed (mg g^{-1}) at any given time t (min); q_e the amount of metal ion adsorbed (mg^{-1}) at equilibrium; and k_2 the second order reaction rate constant for adsorption (g (mg min)$^{-1}$). Though there is a high possibility for pore diffusion to be the rate limiting step in the batch process, the adsorption rate parameter, which controls the batch process for most of the contact time, is the inter-particle diffusion [2].

2.2.5 Adsorption isotherms

Equilibrium isotherms were described by the sorption. Adsorption of Pb(II) by BB&CS and HAP&CS were studied further to understand the mechanism by fitting the experimental data to Langmuir and Freundlich adsorption isotherms.

The Langmuir isotherm assumes monolayer adsorption onto a surface with a finite number of identical sites, and its linear form is expressed in equation 3:

$$\frac{C_e}{q_e} = \frac{1}{b\,q_{max}} + \frac{C_e}{q_{max}} \qquad (3)$$

Where q_e and q_{max} are the observed and the maximum uptake capacities (mg g^{-1}); C_e the equilibrium concentration (mg L^{-1}); and b the equilibrium constant (Lmg^{-1}). The degree of suitability (R_L) was estimated from the value of separation factor, which can be obtained by equation 4:

$$R_L = \frac{1}{1+bC_o} \qquad (4)$$

The Freundlich equation proposes an empirical model based on the sorption on heterogeneous surface, and is in the form of equation 5:

$$\mathrm{Log}\,q_e = \mathrm{Log}\,K_f + \frac{1}{n}\mathrm{Log}C_e \qquad (5)$$

Where K_f (L g^{-1}) and n are the Freundlich isotherm constants and intensity of adsorption, respectively; q_e and C_e are as described for equation (3).

3. Results and Discussion

3.1 Characteristics of Biochar

FTIR analysis of the BB revealed many functional groups on the BB surfaces**:** the bands assigned to O–H stretching; aliphatic C-H stretching; C–H stretching bands associated with aliphatic functional groups; intense bands of aliphatic CH_2; intensity of aromatic C=C stretching and C=O stretching of conjugated ketones and quinones; C=C ring stretching vibration of lignin; aromatic C=C stretching (out of plane deformation by aromatic C–H groups and could have been caused by carbonates); and C–O and C–C stretching. The BB characteristics shown by SEM on morphology are large internal surface and porous structure with an approximate porous space of 38.67µm. SEM on elemental composition in the BB samples showed available C, S, K, Cl elemental percent contents of 58.61, 1.55, 30.46, and 9.38, respectively. Physicochemical properties of BB, like pH, zeta potential for surface, and surface area available, are important factors controlling their environmental applications (Inyang et al. 2010). In this study, zeta potential for surface measurements indicated that the BB had more negative surface charge, which may be related to the surface area and the pore volume. This data seemed to predict a greater potential to adsorb abundant positively charged heavy metals and confirmed the SEM results. The zeta potential data values for BB, HAP&BB&CS mixture and HAP&BB mixture, were -56, -2, and -19 mv, respectively.

3.2 Effect of Contact Time

Adsorption characteristics can be explained by the effect of contact time. Figure 1 showed the effect of contact time between the solution containing Pb(II) and mixture adsorbents from two combinations of BB&CS and HAP&CS that were contacting inside the shaken conical flask. The four concentrations used were in the range of 100 to 400 mg L^{-1} and the adsorption contact times were operated up to 40 minutes. The percentage of adsorbed Pb(II) with different contact time was shown in the figure. It can be observed that the rate of Pb(II) ions removal was higher at the incipient step through accessibility of additional energetic scenes on the surface of both adsorbents, after that it became slower at subsequent period of contact time through shorter or fewer number of energetic scenes. Clearly from the figure, the percentage of Pb(II) removal from the aqueous solution increased rapidly and reached up to 99%. at 40 minutes. Augment of impinge time had a measly impression on the percentage of removal, and 40 min. shaking time was thus adopted as an equilibrium time for maximum adsorption. The rate of Pb(II) removal that decreases with time may be due to aggregation of Pb(II) around BB and HAP particles in the adsorbent mixtures. This aggregation hinders the migration of adsorbate, as the adsorption sites become filled up, and that the resistance to diffusion of Pb(II) molecules in the adsorbents increases (Mittal et al. 2010). Equilibrium time for both adsorbents was reached in less than 40 min, meaning that both adsorbents had similar behaviour to adsorb Pb(II).

3.3 Effect of Initial Metal Ion Concentration

As stated earlier, the experiments were carried out for four discrete concentrations of Pb(II) solution (100, 200, 300 and 400 mg L^{-1}.) The effect was investigated and presented in Figure 2. The adsorption capacity of Pb(II) by the adsorbents, (BB&CS) and (HAP&CS), increased with increasing initial concentration of metal ion for both mixtures. The maximum equilibrium uptake for Pb(II) were found to be 152.4 mg Pb(II)/g for the BB&CS mixture, and 200 mg Pb(II)/g for the HAP&CS mixture. The adsorbent containing BB shown in Figure 2 yielding low q_e is ascribed to a high contact probability between the BB and the lead ions. At low concentration level, lead ions were situated at the outer surface of the BB separately, however, with increasing solution concentration lead ions entered into the interior structure, resulting in higher removal capacity.

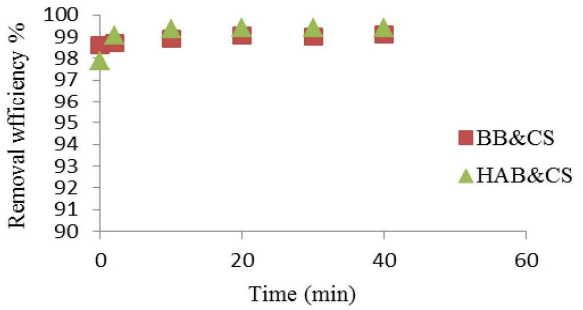

Figure 1. Pb(II) removal efficiency vs. contact time for the BB&CS and the HAP&CS adsorbent mixtures

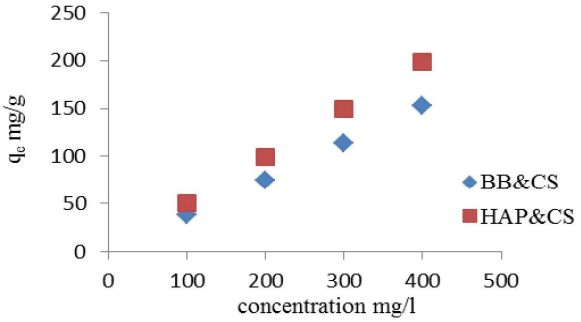

Figure 2. Effect of initial Pb(II) concentration (Ce) on the equilibrium capacity (q_e) for the BB&CS and the HAP&CS adsorbent mixtures

Experimental and theoretically calculated adsorption capacities at equilibrium (q_e), together with coefficients related to kinetic plots are listed in Table 1. Plotting the reaction rate t/q_t against time T, as shown in Figure 3, was conducted for the initial Pb(II) concentration of 400 mg/L at room temperatures. The pseudo second-order adsorption rate constant k_2 and q_e were determined from the slope and the intercept of the plots.

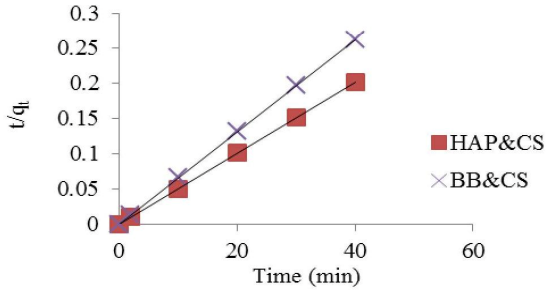

Figure 3. Removal capacity of Pb(II), pseudo second-order model fit, for BB&CS and HAP&CS mixtures

It can be seen from Table 1 that linear correlation coefficients for the pseudo second-order kinetic model are good. Based on the comparison between experimental and theoretically calculated q_e values, it was also found that the model fitted well for removal of Pb(II) by both mixtures. The calculated (cal) values of q_e from the model provide a near-perfect match between the theoretical and the experimental q_e values, together with high correlation coefficients (R^2 >0.99). The higher rate of metal adsorption for the HAP&CS mixture could be due to the presence of its more active sites, which were available in the adsorbents. The second-order reaction rate constant, k_2, for HAP&CS was found to be lower than that for BB&CS. From the above discussion, pseudo-second-order adsorption mechanism is predominant, meaning that chemical sorption takes part in the adsorption process. Once the sorptive sites are exhausted, the uptake rate is controlled by the rate of intra particle diffusion (Chaturvedi et al. 2006). This model agrees with the assumption that the rate-limiting step is chemical sorption or chemisorption involving valence forces between adsorbent and adsorbate (Taty-Costodes et al. 2003).

Table 1. Adsorption kinetic model rate constants for Pb(II) removal

Absorbent	q_{eExp} mg/g_{ad}	Pseudo second-order		
		$q_{e(cal)}$ mg/g	k_2	R^2
BB&CS	152	151.5	0.73	0.99
HAP&CS	199	200	0.5	0.99

Figure 4, using Langmuir model, and Figure 5, using Freundlich model, show the intercept and slope for the straight lines used in the calculations of isotherm constants tabulated in Table 2. Langmuir is the more important model of monolayer adsorption, based on the assumption that there are a fixed number of adsorption sites, and each site can hold only one adsorbate molecule (the adsorbed layer is one molecule in thickness).

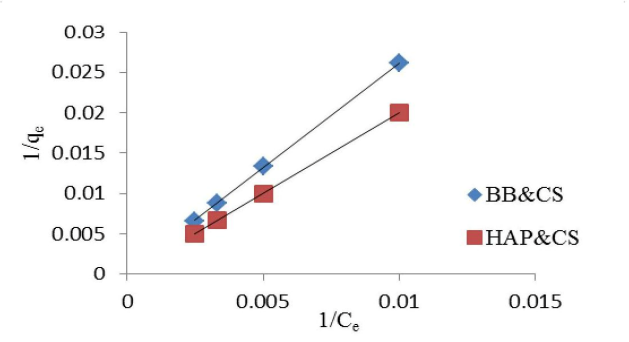

Figure 4. Langmuir isotherm ($1/C_e$) vs. Pb(II) adsorption (q_e) for BB&CS and HAP&CS mixtures

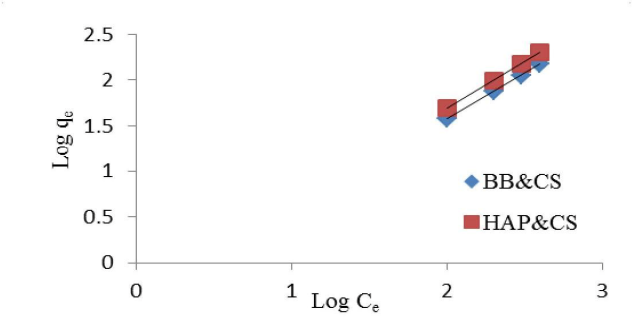

Figure 5. Freundlich isotherm (Log C_e) vs. Pb(II) adsorption (q_e) for BB&CS and HAP&CS mixtures

Table 2. Isotherm parameters for sorption of Pb(II) by different adsorbent

Absorbent	Langmuir			Freundlich		
	q_{max}	b	R^2	K_f	n	R^2
BB&CS	152.4	0.0025	0.9998	0.387	1	0.998
HAP&CS	200	0.0025	0.99	0.51	1	0.99

Table 3 shows the optimum range of the degree of suitability (R_L). The value of R_L in the Langmuir model for the initial concentration of 400mg/l was calculated to be 0.5, indicating that sorption of metal ions to BB&CS and HAP&CS adsorbents are optimum and the process is favourable.

Table 3. Ranges of R_L for type of Isotherm

Values of R_L	Type of isotherm
$R_L > 1$	Unfavorable
$R_L = 1$	Linear
$0 < R_L < 1$	Favorable
$R_L < 0$	Irreversible

The value n, equals 1 for both mixtures, also indicated that the Freundlich isotherm is acceptable. From Table 2 the coefficient of determination R^2 for the Langmuir isotherm is slightly better than that obtained from the Freundlich isotherm, and hence the Langmuir model is slightly more favourable. From the same Table, the removal capacity results (q_{max}) showed that the removal efficiency using HAP&CS was definitely higher than when BB&CS was used. However, the lower-price BB&CS is still effective for Pb(II) removal; it could remove approx. three-fourths of the heavy metal comparing to the higher-price HAP&CS, proving that adsorbent other than HAP can also yield adsorption favourable results. Moreover, the zeta potential charge of BB, as evaluated and reported earlier on the BB char characteristics, is very low (-56 mV), indicating one more reason why it is effective.

4. Conclusion

Bamboo biochar (BB) and Hydroxyapatite (HAP) are capable of removing Pb(II) from aqueous solutions, particularly when they are mixed with Calcium sulphate (CS). Pseudo second-order models yielded very high regression coefficients, indicating excellent sorption of Pb(II) onto both mixtures. Pb(II) sorption using both adsorbents were fitted to the Langmuir and the Freundlich adsorption isotherms, and the Langmuir model had been found to be slightly more favourable. In our study, the adsorption capacities of the mix-adsorbents for a 400 mg/L Pb contamination were found to be able to remove 152.4 mg Pb(II)/g when using BB&CS, and 200 mg Pb(II)/g when using HAP&CS. Though at three-fourths efficiency, this work has shown that low-cost BB&CS adsorbent can play an important role in adsorption of lead from water and/or wastewater, compared to the use of higher-price HAP&CS. The combination of BB and CS to remove lead ions from aqueous solutions is found to be promising.

Acknowledgements

The authors are grateful to the Prince of Songkla University (PSU) for her financial assistance and support to this research. We would also like to thank the PSU Department of Chemical Engineering and the Discipline of Excellence (DoE) in Chemical Engineering for assistance in the carrying out of needed chemical analyses.

References

Agwaramgbo L, Magee N, Nunez S, Mitt K. Biosorption and Chemical Precipitation of Lead Using Biomaterials, Molecular Sieves, and Chlorides, Carbonates, and Sulfates of Na & Ca. Journal of Environmental Protection. 2013; 4 (11): 1251-57.

Belaicha N, Lemlikchi W, Mecherri MO, Sharrock P, Nzihou A. Composite Material with Calcium Sulfate and Calcium Phosphate for Heavy Metals Retention. Procedia Engineering. 2014; 83: 403-06.

Chaturvedi PK, Seth CS, Misra V. Sorption Kinetics and Leachability of Heavy Metal from the Contaminated Soil Amended with Immobilizing Agent (Humus Soil and Hydroxyapatite). Chemosphere. 2006; 64 (7): 1109-14.

Chen X, Chen G, Chen L, Chen Y, Lehmann J, McBride MB, Hay AG. Adsorption of Copper and Zinc by Biochars Produced from Pyrolysis of Hardwood and Corn Straw in Aqueous Solution. Bioresource Technology. 2011; 102 (19):8877-84.

Cornelissen G, Gustafsson O, Bucheli TD, Jonker MTO, Koelmans AA, Paul CM, van Noort PCM. Extensive Sorption of Organic Compounds to Black Carbon, Coal, and Kerogen in Sediments and Soils: Mechanisms and Consequences for Distribution, Bioaccumulation, and Biodegradation. Environ Sci Technol. 2005; 39 (18):6881-95.

Evaniew N, Tan V, Parasu N, Jurriaans E, Finlay K, Deheshi B, Ghert M. Use of a Calcium Sulfate–Calcium. Phosphate Synthetic Bone Graft Composite in the Surgical Management of Primary Bone. Tumors Orthopedics. 2013; 36 (2): 216–22.

Farghali AA, Bahgat M, Enaiet AA, Khedr MH. Adsorption of Pb(II) Ions from Aqueous Solutions Using Copper Oxide Nanostructure. Beni-Suef University Journal of Basic and Applied Sciences. 2013; 2 (2): 61-71.

Heidari A, Younesi H, Mehraban Z, Heikkinen H. Selective Adsorption of Pb(II), Cd(II), and Ni(II) Ions from Aqueous Solution Using Chitosan–MAA Nanoparticles. International Journal of Biological Macromolecules. 2013; 61: 51-263.

Ho YS, McKay G. Pseudo-second Order Model for Sorption Processes. Process Biochemistry. 1999; 34 (5): 451-65.

Inyang M, Gao B, Yao Y, Xue Y, Zimmerman AR, Pullammanappallil P, Cao X. Removal of Heavy Metals from Aqueous Solution by Biochars Derived from Anaerobically Digested Biomas. Bioresource Technology. 2012; 110: 50-56.

Inyang M, Gao B, Pullammanappallil P, Ding W, Zimmerman AR. Biochar from Anaerobically Digested Sugarcane Bagasse. Bioresource Technology. 2010; 101 (22): 8868-72.

Johnson PR, Sun N, Elimelech M. Colloid Transport in Geochemically Heterogeneous Porous Media: Modelling and Measurement. Environmental Science & Technology. 1996; 30 (11): 3284-93.

Liao D, Zheng W, Li X, Yang Q, Yue X, Guo L, Zeng G. Removal of Lead(II) from Aqueous Solutions Using Carbonate Hydroxyapatite Extracted from Eggshell Waste. Journal of Hazardous Materials. 2010; 177 (1-3): 126-30.

Mittal A, Mittal J, Malviya A, Gupta VK. Removal and Recovery of Chrysoidine Y from Aqueous Solutions by Waste Materials. Journal of Colloid and Interface Science. 2010; 344 (2): 497-507.

Ramesh ST, Rameshbabu N, Gandhimathi R, Srikanth Kumar M, Nidheesh PV. Adsorptive Removal of Pb(II) from Aqueous Solution Using Nano-sized Hydroxyapatite. Journal of Applied Water Science. 2013; 3 (1): 105-13.

Takeuchi Y, Arai H. Removal of Coexisting Pb^{2+}, Cu^{2+} and Cd^{2+} Ions from Water by Addition of Hydroxyapatite Powder. Journal of Chemical Engineering of Japan. 1990; 23 (1): 75-80.

Taty-Costodes VC, Fauduet H, Porte C, Delacroix A. Removal of Cd(II) and Pb(II) Ions, from Aqueous Solutions, by Adsorption onto Sawdust of Pinus sylvestris. Journal of Hazardous Materials. 2003; 105 (1–3): 121-42.

Xu H, Yang L, Wang P, Liu Y, Peng M. Removal Mechanism of Aqueous Lead by a Novel Eco-material: Carbonate Hydroxyapatite. Journal of Materials Sciences and Technology. 2007; 23 (3): 417-22.

Xu X, Cao X, Zhao L, Wang H, Yu H, Gao B. Removal of Cu, Zn, and Cd from Aqueous Solutions by the Dairy Manure-derived Biochar. Environmental Science and Pollution Research. 2013; 20 (1): 358-68.

Zamani S, Salahi E, Mobasherpour. I. Removal of Nickel from Aqueous Solution by Nano Hydroxyapatite Originated from Persian Gulf Corals. Canadian Chemical Transactions Journal. 2013; 1 (3): 173-90.

Zhang J, Li F, Luo C, Shao L, He P. Humification Characterization of Biochar and Its Potential as a Composting Amendment. Journal of Environmental Sciences. 2014; 26 (2): 390-97.

Zhao G, Li J, Ren X, Chen C, Wang X. Few-Layered Graphene Oxide Nanosheets as Superior Sorbents for Heavy Metal Ion Pollution Management. Environ. Sci. Technol. 2011; 45 (24): 10454-62.

Appendix A2

Journal Paper 2

A. Hassan, L. Kaewsichan, ‘‘Removal of Pb(II) from Aqueous Solutions Using Mixtures of Bamboo Biochar and Calcium Sulphate, and Hydroxyapatite and Calcium Sulphate’’, EnvironmentAsia, vol.9, No.1, pp 37-44, 2016.

EnvironmentAsia
The international journal published by the Thai Society of Higher Education Institutes on Environment

Available online at www.tshe.org/ea/index.html
EnvironmentAsia 9(1) (2016) 37-44
DOI 10.14456/ea.1473.5

Removal of Pb(II) from Aqueous Solutions Using Mixtures of Bamboo Biochar and Calcium Sulphate, and Hydroxyapatite and Calcium Sulphate

Ahmed Hassan and Lupong Kaewsichan

Department of Chemical Engineering, Prince of Songkla University, Hat Yai, Songkhla, Thailand

Abstract

Sorption characteristics of Pb(II) from aqueous solutions through a low-cost adsorbent mixture comprising of Bamboo biochar (BB) and Calcium Sulphate (CS), and a more expensive mixture of Hydroxyapatite (HAP) and Calcium Sulphate (CS), were investigated. The effects of equilibrium contact time, and adsorbate concentration conducted in batch experiments were studied. Adsorption equilibrium was established in 40 (min). The adsorption mechanism of Pb(II) from these two adsorbent mixtures was carried out through a kinetic rate order. A pseudo second-order kinetic model was applied for the adsorption processes. The model yielded good correlation ($R^2 > 0.999$) of the experimental data. Adsorption of Pb(II) using (BB&CS) and (HAP&CS) correlated well ($R^2 > 0.99$) with both the Langmuir and Freundlich isotherm equations under the concentration range studied. Hence, the effectiveness of an inexpensive natural material (BB&CS) mixture in Pb(II) removal is established, and is promising for use in other heavy metal adsorptions.

Keywords: natural adsorbents; bamboo biochar; calcium sulphate; hydroxyapatite; heavy metal adsorption

1. Introduction

Heavy metals generally are recognized to be a threat toward humans and ecosystems because of their high toxicity (Ramesh *et al*., 2013). Contamination from them has attracted considerably global attention, according to their voluminous discharge into the environment from industrial activities (Heidari *et al*., 2013). Lead is a toxic element for humans and animals at some concentration and a serious public health issue worldwide (Xu *et al*., 2007). Lead as the form of Pb(II) is often found in textile dying, ceramic and glass industries, petroleum refining, battery manufacture and mining operations (Freitas *et al*., 2008). It is extremely toxic and can damage the kidney, liver, brain, nervous, and reproductive systems (Ramesh *et al*., 2013); among other adverse effects to humans (Godwin, 2001). Therefore, it is necessary to eliminate such hazardous heavy metal ion in wastewater before discharging it into the ecosystem (Farghali *et al*., 2013). Subsequently, considerable efforts have been spent in treating Pb-containing wastes at their source.

Traditional techniques for the elimination of heavy metal ions include precipitation, membrane filtration, sorption, and ion exchange, etc. (Zhao *et al*., 2011; Matlock *et al*., 2002; Yang *et al*., 2011). For all treatment methods, it is a struggle between cost-effectiveness and environmental regulations. One of these methods, the sorption technique, has been used widely because it is simple, economical, and cost-effective (Zhao *et al*., 2011). In this method, material like biochar has been used as adsorbent. It has shown strong sorption affinity for organic compounds and may play an important role in controlling organic pollutants in the environment (Cornelissen *et al*., 2005). Main benefit for the use of biochar is from its structured carbon matrix with high degree of porosity and extensive surface area that enhances its sorbent characteristics, thereby plays an important role in controlling contaminants (Chen *et al*., 2011). Wood biochar, especially bamboo biochar (BB), has higher carbon content and is more hydrophobic and aromatic than those produced from rice husks, moreover, bamboo biochar is a material with the lowest level of humification (Zhang *et al*., 2014) suitable for removal of metal ions. Its high sorption is due to three mechanisms: electrostatic interactions; ionic exchange between ionisable protons and heavy metal cations; and sorptive interaction (Xu *et al*., 2013). Furthermore, the mechanism of biochar adsorption depends on functional groups, specific surface area and many other parameters (Kołodyńska *et al*., 2012).

Hydroxyapatite [$Ca_{10}(PO_4)_6(OH)_2$; HAP] is the main mineral constituent of teeth, bones and phosphate mineral rocks (Zamani *et al*., 2013). Many research works have found that (HAP) can effectively remove lead ion in aqueous solution under different experimental conditions and show potential removal capacities, with removal percentage trending to 100% (Xu *et al*.,

2007). Synthetic hydroxyapatite (HAP) has been extensively studied for its kinetics and chemical reaction with a wide variety of metals e.g., Pb, Cu, Cd, Zn, Sb and U (Liao *et al.*, 2010; Corami *et al*., 2007; Peld *et al*., 2004; Leyva *et al*., 2001; Fuller *et al*., 2002). Many types of reaction control Pb removal by (HAP) and other adsorbents, including surface adsorption, cation substitution or precipitation. Using (HAP), adsorption of Pb ions on the surfaces of the adsorbent will be followed by ion exchange reaction amidst the Pb(II) adsorbed and the Ca^{+2} ions in (HAP) (Takeuchi and Arai, 1990).

Calcium salts (chlorides, sulphates, and carbonates) are better lead precipitators than the corresponding sodium salts (Agwaramgbo *et al*., 2013). Moreover such composites have been described for use as resorbable biomaterials in bone surgery (Evaniew *et al*., 2013), but have never been used for the retention of heavy metals from polluted water (Belaicha *et al*., 2014). The present work aims to investigate and compare two adsorbent mixtures; (BB&CS), and (HAP&CS), in the study of Pb(II) ions removal from aqueous solutions which involves equilibrium contact time, adsorbate concentration, adsorbent dose, their kinetics through pseudo second-order and applicable to the two isotherm models.

2. Materials and Methods

2.1. Materials

The (BB) used in this study was prepared in the laboratory by pyrolysis process at 500°C; (HAP) was a commercial type purchased from Sigma-Aldrich (Thailand) Co. LLC; and (CS) was bought from Aldrich Chemicals and was used without further purification. $Pb(NO_3)_2$ (Lead Nitrate) standard samples were acquired from Boss Official Limited Partnership in Thailand.

2.2. Method

2.2.1. Properties of biochar

Fourier transforms infrared spectroscopies (FTIR) (Bomem, MB 100) were carried out to identify the functional groups of the biochar. Scanning electron microscopy (Hitachi JSM-6700F SEM) was implemented to observe the surface microstructures of the biochar. The pH of the (BB) was measured by suspending the (BB) with demineralized water at a mass ratio of 1:20. The solution was then hand-stirred and allowed to stand for 5 (min) before measurement with a pH meter (Inyang *et al.*, 2012). The (BB) surface potential was determined by measuring the zeta potential (ζ) of the colloidal biochar suspension obtained through sonication according to the procedure of Johnson *et al.* (1996). Charge mobility of each suspension was determined using Brookhaven Zeta Plus (Brookhaven Instruments, Holtsville, USA), and Smoluchowski's formula was used to convert the electric mobility into zeta potential.

2.2.2. Preparation of metal solutions

All metal solutions were prepared from their nitrate salts (Analytical Reagents; AR) and distilled water. The synthetic solutions were all prepared by diluting Pb(II) standard stock solutions (concentration 1000 ± 2 (mg/L)) obtained by dissolving appropriate amounts of metal salt in double distilled water. Four dilutions: 100, 200, 300 and 400 (mg/L), were used in each set of the experiment.

2.2.3. Sorption studies

Batch adsorption experiments were conducted on the three adsorbent materials, for which 0.08 (g), 0.05 (g), and 0.05 (g) for (BB), (CS) and (HAP), respectively, were used to produce the two mixtures. Each mixture of (BB&CS) and (HAP&CS) was put into a 250 (mL) conical flask containing 50 (mL) of Pb(II) ions at the pre-set concentrations mentioned earlier of 100, 200, 300 and 400 (mg/L), shaken, filtered and subjected to Pb(II) analysis to determine the optimum Pb(II) adsorptions. The effect of contact time was studied in the time range of 0-40 (min). At the end of the adsorption process the suspensions were filtered through 0.45 (μm) syringe membrane filters and the corresponding supernatant was analysed employing a Perkin Elmer Thermos Scientific S-series model (AAnalyst100) Flame atomic absorption spectrophotometer (AAS) for residual Pb(II) concentrations. Three replicates were conducted for each Pb(II) bio sorption experiment set, and the average values determined. The adsorbent capacity of (BB&CS) and (HAP&CS) mixtures were calculated using general equation (1), (Tangjuank *et al*., 2009):

$$q_e = (C_0 - C_t)\frac{V}{M} \quad (1)$$

Where q_e is the amount of Pb(II) adsorbed on the adsorbent (mg/g); C_0 and C_t are the Pb(II) concentrations in the solution before and after adsorption (mg/L); V is the volume of the solution (L); and M is the amount of the adsorbents used in the reaction mixture (g).

2.2.4. Adsorption kinetics

The mechanism of sorption can be explained by the kinetic characteristics of sorption. For this purpose, pseudo second-order kinetic model was considered and fitted with the experimental data. The pseudo second-order reaction rate equation, as shown by (Ho *et al*., 1999), is described in equation (2):

$$\frac{t}{q_t} = \frac{t}{q_e} + \frac{1}{k_2 q_e^2} \quad (2)$$

Where q_t is the amount of metal ions adsorbed (mg/g) at any given time t (min); q_e the amount of metal ion adsorbed (mg/g) at equilibrium; and k_2 the second-order reaction rate constant for adsorption (g/mg min). Though there is a high possibility for pore diffusion to be the rate limiting step in the batch process, the adsorption rate parameter, which controls the batch process for most of the contact time, is the inter-particle diffusion (Ramesh *et al*., 2013; Weber and Morris, 1963; Allen *et al*., 1989)

2.2.5. Adsorption isotherms

Equilibrium isotherms were described by the sorption. Adsorption of Pb(II) by (BB&CS) and (HAP&CS) were studied further to understand the mechanism by fitting the experimental data to Langmuir and Freundlich adsorption isotherms. The Langmuir isotherm assumes monolayer adsorption onto a surface with a finite number of identical sites, and its linear form is expressed in equation (3), (Kołodyńska *et al*., 2012):

$$\frac{C_e}{q_e} = \frac{1}{bq_{max}} + \frac{C_e}{q_{max}} \quad (3)$$

Where q_e and q_{max} are the observed and the maximum uptake capacities (mg/g); C_e the equilibrium concentration (mg/L); and b the equilibrium constant (L/mg). The degree of suitability R_L was estimated from the value of separation factor, which can be obtained by equation (4), as shown by (Weber and Chakravorti, 1974):

$$R_L = \frac{1}{1 + bC_0} \quad (4)$$

The Freundlich equation proposes an empirical model based on the sorption on heterogeneous surface, and is in the form of equation (5), (Kołodyńska *et al*., 2012):

$$\log q_e = \log K_f + \frac{1}{n} \log C_e \quad (5)$$

Where K_f (L/g) and n are the Freundlich isotherm constants and intensity of adsorption, respectively; q_e and C_e are as described for equation (3).

3. Results and Discussion

3.1. Characteristics of biochar

FTIR analysis of the (BB) revealed many functional groups on the (BB) surfaces: the bands assigned to O-H stretching; aliphatic C-H stretching; C-H stretching bands associated with aliphatic functional groups; intense bands of aliphatic CH_2; intensity of aromatic C=C stretching and C=O stretching of conjugated ketones and quinones; C=C ring stretching vibration of lignin; aromatic C=C stretching (out of plane deformation by aromatic C-H groups and could have been caused by carbonates); and C-O and C-C stretching. The (BB) characteristics shown by SEM on morphology are large internal surface and porous structure with an approximate porous space of 38.67 (μm). SEM on elemental composition in the (BB) samples showed available C, S, K, Cl elemental percent contents of 58.61, 1.55, 30.46, and 9.38, respectively. Physicochemical properties of (BB), like pH, zeta potential for surface, and surface area available, are important factors controlling their environmental applications (Inyang *et al*., 2010). In this study, zeta potential for surface measurements indicated that the (BB) had more negative surface charge, which may be related to the surface area and the pore volume. This data seemed to predict a greater potential to adsorb abundant positively charged heavy metals and confirmed the SEM results. The zeta potential data values for (BB), (HAP&BB&CS) mixture and (HAP&BB) mixture were -56, -2, and -19 (mV), respectively.

3.2. Effect of contact time

Adsorption characteristics can be explained by the effect of contact time. Fig. 1 showed the effect of contact time between the solution containing Pb(II) and mixture adsorbents from two combinations of (BB&CS) and (HAP&CS) that were contacting inside the shaken conical flask. The four concentrations used were in the range of 100 to 400 (mg/L) and the adsorption contact times were operated up to 40 (min). The percentage of adsorbed Pb(II) with different contact time was shown in the figure. It can be observed that the rate of Pb(II) ions removal was higher at the incipient step through

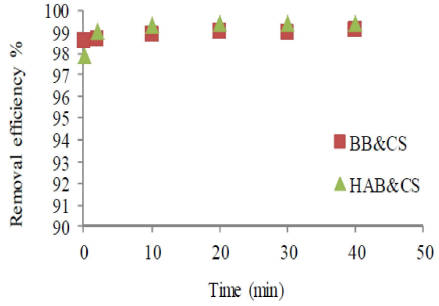

Figure 1. Pb(II) removal efficiency vs. contact time for the (BB&CS) and the (HAP&CS) adsorbent mixtures

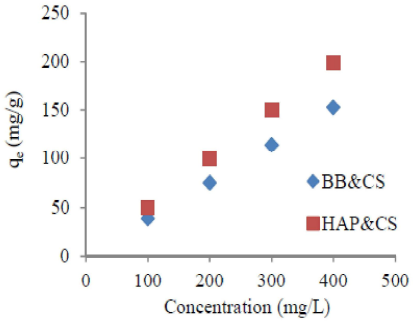

Figure 2. Effect of initial Pb(II) concentration C_e on the equilibrium capacity q_e for the (BB&CS) and the (HAP&CS) adsorbent mixtures

accessibility of additional energetic scenes on the surface of both adsorbents, after that it became slower at subsequent period of contact time through shorter or fewer number of energetic scenes. Clearly from the figure, the percentage of Pb(II) removal from the aqueous solution increased rapidly and reached up to 99% at 40 (min). Augment of impinge time had a measly impression on the percentage of removal, and 40 (min) shaking time was thus adopted as an equilibrium time for maximum adsorption. The rate of Pb(II) removal that decreases with time may be due to aggregation of Pb(II) around (BB) and (HAP) particles in the adsorbent mixtures. This aggregation hinders the migration of adsorbate, as the adsorption sites become filled up, and that the resistance to diffusion of Pb(II) molecules in the adsorbents increases (Mittal *et al*., 2010). Equilibrium time for both adsorbents was reached in less than 40 (min), meaning that both adsorbents had similar behaviour to adsorb Pb(II).

3.3. Effect of initial metal ion concentration

As stated earlier, the experiments were carried out for four discrete concentrations of Pb(II) solution (100, 200, 300 and 400 (mg/L)). The effect was investigated and presented in Fig. 2. The adsorption capacity of Pb(II) by the adsorbents, (BB&CS) and (HAP&CS), increased with increasing initial concentration of metal ion for both mixtures. The maximum equilibrium uptake for Pb(II) were found to be 152.4 (mg Pb(II)/g) for the (BB&CS) mixture, and 200 (mg Pb(II)/g) for the (HAP&CS) mixture. The adsorbent containing (BB) shown in Fig. 2, yielding low q_e is ascribed to a high contact probability between the (BB) and the lead ions. At low concentration level, lead ions were situated at the outer surface of the (BB) separately, however, with increasing solution concentration lead ions entered into the interior structure, resulting in higher removal capacity.

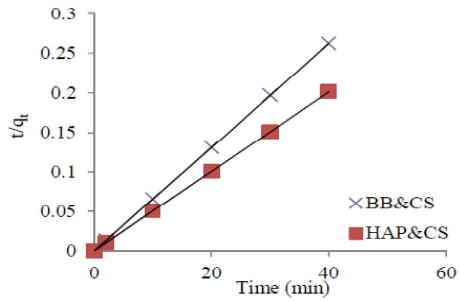

Figure 3. Removal capacity of Pb(II), pseudo second-order model fit, for (BB&CS) and (HAP&CS) mixtures

Table 1. Adsorption kinetic model rate constants for Pb(II) removal

Absorbent	q_{eExp} mg/g_{ad}	Langmuir		
		qe(cal) mg/g	k_2	R^2
BB&CS	152	151.5	0.73	0.99
HAP&CS	199	200	0.5	0.99

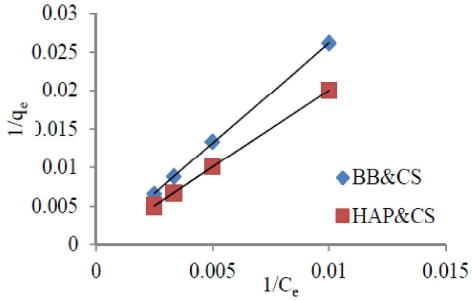

Figure 4. Langmuir isotherm $1/C_e$ vs. Pb(II) adsorption q_e for (BB&CS) and (HAP&CS) mixtures

Experimental and theoretically calculated adsorption capacities at equilibrium q_e, together with coefficients related to kinetic plots are listed in Table 1. Plotting the reaction rate t/q_t against time T, as shown in Fig. 3, was conducted for the initial Pb(II) concentration of 400 (mg/L) at room temperatures. The pseudo second-order adsorption rate constant k_2 and q_e were determined from the slope and the intercept of the plots.

It can be seen from Table 1 that linear correlation coefficients for the pseudo second-order kinetic model are good. Based on the comparison between experimental and theoretically calculated q_e values, it was also found that the model fitted well for removal of Pb(II) by both mixtures. The calculated (cal) values of q_e from the model provide a near-perfect match between the theoretical and the experimental q_e values, together with high correlation coefficients (R^2>0.99). The higher rate of metal adsorption for the (HAP&CS) mixture could be due to the presence of its more active sites, which were available in the adsorbents. The second-order reaction rate constant, k_2, for (HAP&CS) was found to be lower than that for (BB&CS). From the above discussion, pseudo second-order adsorption mechanism is predominant, meaning that chemical sorption takes part in the adsorption process. Once the sorptive sites are exhausted, the uptake rate is controlled by the rate of intra particle diffusion (Chaturvedi *et al*., 2006). This model agrees with the assumption that the rate-limiting step is chemical sorption or chemisorption involving valence forces between adsorbent and adsorbate (Taty-Costodes *et al*., 2003).

Fig. 4, using Langmuir model, and Fig. 5, using Freundlich model, show the intercept and slope for the straight lines used in the calculations of isotherm constants tabulated in Table 2. Langmuir is the more important model of monolayer adsorption, based on the assumption that there are a fixed number of adsorption sites, and each site can hold only one adsorbate molecule (the adsorbed layer is one molecule in thickness).

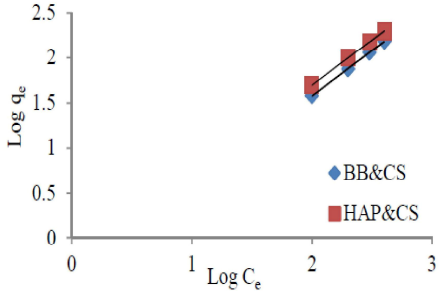

Figure 5. Freundlich isotherm Log C_e vs. Pb(II) adsorption Logq_e for (BB&CS) and (HAP&CS) mixtures

Table 2. Isotherm parameters for sorption of Pb(II) by different adsorbent

Absorbent	Langmuir			Freundlich		
	q_{max}	b	R^2	k_f	n	R^2
BB&CS	152.4	0.0025	0.9998	0.387	1	0.998
HAP&CS	200	0.0025	0.99	0.51	1	0.99

Table 3. Ranges of RL for type of Isotherm

Values of R_L	Type of Isotherm
$R_L > 1$	Unfavorable
$R_L = 1$	Linear
$0 < R_L < 1$	Favorable
$R_L < 0$	Irreversible

Table 3 shows the optimum range of the degree of suitability R_L. The value of R_L in the Langmuir model for the initial concentration of 400 (mg/L) was calculated to be 0.5, indicating that sorption of metal ions to (BB&CS) and (HAP&CS) adsorbents are optimum and the process is favourable.

The value n, equals 1 for both mixtures, also indicated that the Freundlich isotherm is acceptable (Farouq and Yousef, 2015). From Table 2 the coefficient of determination R^2 for the Langmuir isotherm is slightly better than that obtained from the Freundlich isotherm, and hence the Langmuir model is slightly more favourable. From the same Table, the removal capacity results qmax showed that the removal efficiency using (HAP&CS) was definitely higher than when (BB&CS) was used. However, the lower-price (BB&CS) is still effective for Pb(II) removal; it could remove approx. three-fourths of the heavy metal comparing to the higher-price (IIAP&CS), proving that adsorbent other than (HAP) can also yield adsorption favourable results. Moreover, the zeta potential charge of (BB), as evaluated and reported earlier on the (BB) char characteristics, is very low -56 (mV), indicating one more reason why it is effective.

4. Conclusions

Bamboo biochar (BB) and Hydroxyapatite (HAP) are capable of removing Pb(II) from aqueous solutions, particularly when they are mixed with Calcium sulphate (CS). Pseudo second-order model yielded very high regression coefficients, indicating excellent sorption of Pb(II) onto both mixtures. Pb(II) sorption using both adsorbents were fitted to the Langmuir and the Freundlich adsorption isotherms, and the Langmuir model had been found to be slightly more favourable. In our study, the adsorption capacities of the mix-adsorbents for a 400 (mg/L) Pb(II) contamination were found to be able to remove 152.4 (mg Pb(II)/g) when using (BB&CS), and 200 (mg Pb(II)/g) when using (HAP&CS). Though at three-fourths efficiency, this work has shown that low-cost (BB&CS) adsorbent can play an important role in adsorption of lead from water and/or wastewater, compared to the use of higher-price (HAP&CS). The combination of (BB) and (CS) to remove lead ions from aqueous solutions is found to be promising.

Acknowledgements

The authors are grateful to the Prince of Songkla University (PSU) for her financial assistance and support to this research. We would also like to thank the PSU Department of Chemical Engineering and the Discipline of Excellence (DoE) in Chemical Engineering for assistance in the carrying out of needed chemical analyses.

References

Agwaramgbo L, Magee N, Nunez S, Mitt K. Biosorption and chemical precipitation of lead using biomaterials, molecular sieves, and chlorides, carbonates, and sulfates of Na & Ca. Journal of Environmental Protection 2013; 4(11):1251-57.

Allen SJ, McKay G, Khader KYH. Intraparticle diffusion of a basic dye during adsorption onto sphagnum peat. Environmental Pollution 1989; 56(1): 39-50.

Belaicha N, Lemlikchi W, Mecherri MO, Sharrock P, Nzihou A. Composite material with calcium sulfate and calcium phosphate for heavy metals retention. Procedia Engineering 2014; 83:403-06.

Chaturvedi PK, Seth CS, Misra V. Sorption kinetics and leachability of heavy metal from the contaminated soil amended with immobilizing agent (humus soil and hydroxyapatite). Chemosphere 2006; 64(7):1109-14.

Chen X, Chen G, Chen L, Chen Y, Lehmann J, McBride MB, Hay AG. Adsorption of copper and zinc by biochars produced from pyrolysis of hardwood and corn straw in aqueous solution. Bioresource Technology 2011; 102(19): 8877-84.

Corami A, Mignardi S, Ferrini V. Copper and zinc decontamination from single and binary-metal solutions using hydroxyapatite. Journal of Hazardous Materials 2007; 146(1-2): 164-70.

Cornelissen G, Gustafsson O, Bucheli TD, Jonker MT, Koelmans AA, van Noort PCM. Extensive sorption of organic compounds to black carbon, coal, and kerogen in sediments and soils: mechanisms and consequences for distribution, bioaccumulation, and biodegradation. Environmental Science and Technology 2005; 39(18): 6881-95.

Evaniew N, Tan V, Parasu N, Jurriaans E, Finlay K, Deheshi B, Ghert M. Use of a calcium sulphate-calcium phosphate synthetic bone graft composite in the surgical management of primary bone tumors. Orthopedics 2013; 36(2): 216-22.

Farghali AA, Bahgat M, Enaiet Allah A, Khedr MH. Adsorption of Pb(II) ions from aqueous solutions using copper oxide nanostructures. Beni-Suef University Journal of Basic and Applied Sciences 2013; 2(2): 61-71.

Farouq R, Yousef NS. Equilibrium and kinetics studies of adsorption of Copper (II) ions on natural biosorbent. International Journal of Chemical Engineering and Applications 2015; 6(5): 319-24.

Freitas OMM, Martins RJE, Delerue-Matos CM, Boaventura RAR. Removal of Cd(II), Zn(II) and Pb(II) from aqucous solutions by brown marine macro algae: kinetic modelling. Journal of Hazardous Materials 2008; 153 (1-2): 493-501.

Fuller CC, Bargar JR, Davis JA, Piana MJ. Mechanism of uranium interactions with hydroxyapatite: implications for groundwater remediation. Environmental Science and Technology 2002; 36(2):158-65.

Godwin HA. The biological chemistry of lead. Current Opinion in Chemical Biology 2001; 5(2): 223-27.

Heidari A, Younesi H, Mehraban Z, Heikkinen H. Selective adsorption of Pb(II), Cd(II), and Ni(II) ions from aqueous solution using chitosan-MAA nanoparticles. International Journal of Biological Macromolecules 2013; 61: 251-63.

Ho YS, McKay G. Pseudo-second order model for sorption processes. Process Biochemistry 1999; 34(5): 451-65.

Inyang M, Gao B, Pullammanappallil P, Ding W, Zimmerman AR. Biochar from anaerobically digested sugarcane bagasse. Bioresource Technology 2010; 101(22): 8868-72.

Inyang M, Gao B, Yao Y, Xue Y, Zimmerman AR, Pullammanappallil P, Cao X. Removal of heavy metals from aqueous solution by biochars derived from anaerobically digested biomass. Bioresource Technology 2012; 110: 50-56.

Johnson PR, Sun N, Elimelech M. Colloid transport in geochemically heterogeneous porous media: modelling and measurements. Environmental Science and Technology 1996; 30(11): 3284-93.

Kołodyńska D, Wnętrzak R, Leahy JJ, Hayes MHB, Kwapiński W, Hubicki Z. Kinetic and adsorptive characterization of biochar in metal ions removal. Chemical Engineering Journal 2012; 197: 295-305.

Leyva AG, Marrero J, Smichowski P, Cicerone D. Sorption of antimony onto hydroxyapatite. Environmental Science and Technology 2001; 35(18): 3669-75.

Liao D, Zheng W, Li X, Yang Q, Yue X, Guo L, Zeng G. Removal of lead(II) from aqueous solutions using carbonate hydroxyapatite extracted from eggshell waste. Journal of Hazardous Materials 2010; 177 (1-3): 126-30.

Matlock MM, Howerton BS, Atwood DA. Chemical precipitation of lead from lead battery recycling plant waste water. Industrial and Engineering Chemistry Research 2002; 41(6): 1579-82.

Mittal A, Mittal J, Malviya A, Gupta VK. Removal and recovery of Chrysoidine Y from aqueous solutions by waste materials. Journal of Colloid and Interface Science 2010; 344(2): 497-507.

Peld M, Tonsuaadu K, Bender V. Sorption and desorption of Cd^{2+} and Zn^{2+} ions in apatite-aqueous systems. Environmental Science and Technology 2004; 38(21): 5626-31

Ramesh ST, Rameshbabu N, Gandhimathi R, Kumar MS, Nidheesh PV. Adsorptive removal of Pb(II) from aqueous solution using nano-sized hydroxyapatite. Journal of Applied Water Science 2013; 3(1): 105-13.

Takeuchi Y, Arai H. Removal of coexisting Pb^{2+}, Cu^{2+} and Cd^{2+} ions from water by addition of hydroxyapatite powder. Journal of Chemical Engineering of Japan 1990; 23(1): 75-80.

Tangjuank S, Insuk N, Tontrakoon J, Udeye V. Adsorption of lead(II) and cadmium(II) ions from aqueous solutions by adsorption on activated carbon prepared from cashew nut shells. Proceeding of World Academy of Science, Engineering and Technology 2009; 52:110-16.

Taty-Costodes VC, Fauduet H, Porte C, Delacroix A. Removal of Cd(II) and Pb(II) ions, from aqueous solutions, by adsorption onto sawdust of Pinus sylvestris. Journal of Hazardous Materials 2003; 105(1-3): 121-42.

Weber TW, Chakravorti RK. Pore and solid diffusion models for fixed-bed adsorbers. AIChE Journal 1974; 20(2): 228-38.

Weber WJ, Morris JC. Kinetics of adsorption on carbon from solution. Journal of the Sanitary Engineering Division 1963; 89(2): 31-60.

Xu H, Yang L, Wang P, Liu Y, Peng M. Removal mechanism of aqueous lead by a novel eco-material: carbonate hydroxyapatite. Journal of Materials Science and Technology 2007; 23(3): 417-22.

Xu X, Cao X, Zhao L, Wang H, Yu H, Gao B. Removal of Cu, Zn, and Cd from aqueous solutions by the dairy manure-derived biochar. Environmental Science and Pollution Research International 2013; 20(1): 358-68.

Yang S, Hu J, Chen C, Shao D, Wang X. Mutual effects of Pb(II) and humic acid adsorption on multiwalled carbon nanotubes/polyacrylamide composites from aqueous solutions. Environmental Science and Technology 2011; 45(8): 3621-27.

Zamani S, Salahi E, Mobasherpour I. Removal of nickel from aqueous solution by nano hydroxyapatite originated from Persian Gulf corals. Canadian Chemical Transactions 2013; 1(3): 173-90.

Zhang J, Lü F, Luo C, Shao L, He P. Humification characterization of biochar and its potential as a composting amendment. Journal of Environmental Sciences 2014; 26(2): 390-97.

Zhao G, Li J, Ren X, Chen C, Wang X. Few-layered graphene oxide nanosheets as superior sorbents for heavy metal ion pollution management. Environmental Science and Technology 2011; 45(25): 10454-62.

Received 16 June 2015
Accepted 3 July 2015

Correspondence to
Mr. Ahmed Hassan Alamin
Department of Chemical Engineering,
Faculty of Engineering,
Prince of Songkla University,
Hat Yai, Songkhla 90112
Thailand
Email: ahmed.10000@yahoo.com

Appendix A3

Journal Paper 3

A. H. Alamin, L. Kaewsichan, ‘‘Adsorption of Zn(II) and Cd(II) ions from aqueous solutions by Bamboo biochar cooperation with Hydroxyapatite and Calcium Sulphate’’, *International Journal of ChemTech Research*, vol.7, No.5, pp 2159-2170, 2014-2015.

International Journal of ChemTech Research
CODEN (USA): IJCRGG ISSN: 0974-4290
Vol.7, No.5, pp 2159-2170, 2014-2015

Adsorption of Zn(II) and Cd(II) ions from aqueous solutions by Bamboo biochar cooperation with Hydroxyapatite and Calcium Sulphate

Ahmed Hassan Alamin*[1], Lupong Kaewsichan[1]

[1]Department of Chemical Engineering, Prince of Songkla University, Songkla, Hatyai, Thailand, 90112

Abstract: Sorption characteristics of Zn(II) and Cd(II) through lower cost adsorbent materials, like Bamboo biochar adsorbents was prepared by pyrolysis process, was used with added Calcium Sulphate and Hydroxyapatite for adsorption of Zn^{+2} and Cd^{+2} from aqueous solution. For this objective was used batch adsorption process, and comparing between two mixtures of adsorbents, HAP&CS (Hydroxyapatite & Calcium Sulphate), and BB&CS (Bamboo biochar & Calcium Sulphate), for show the efficiency of those adsorbents. The properties of the biochar were characterized by scanning electron microscopy (SEM), energy dispersive analysis system by FTIR and DTA analysis. The experiments were carried out and measure response of many parameter like contact time, initial concentration of heavy metal and comparative adsorption behaviour of Zn(II) and Cd(II). The kinetics data were fit by a pseudo second –order model, and that data were analysed by Langmuir isotherm model got high correlations coefficient. From that model the maximum adsorption capacities of HAP& CS adsorbent for Zn^{+2} and Cd^{+2} ions were 24.47 mg/g, and 18.05 mg/g respectively, capacity of BB & CS adsorbent of Zn^{+2} and Cd^{+2} ions were14.423 mg/g and 8.0423 mg/g respectively. The results were shown advantage of using new material like BB can work as adsorbent such as HAP and replace it because of cheap, natural and many good environmental properties.
Keywords: Heavy metal, Adsorption, Bamboo biochar, Hydroxyapatite, Calcium Sulphate.

Introduction

The main goal for treatment of wastewater pollution in all field industrial, exploration, agricultural and waste application is to reduce the hazardous of toxicity like organic and heavy metal. Many industrial processes in the plating industry involve heavy metals for metal finishing and their effluent must be treated prior to discharge[1]. High reservation of wastewater material emerging from this kind of industries because it contains large quantity of hazardous substances. The US Environmental Protection Agency (USEPA) prepared a list of 129 organic and inorganic pollutants found in wastewater that constitute serious health hazards. This Priority Pollutants List includes thirteen elements: Sb, As, Be, Cd, Cr, Cu, Pb, Hg, Ni, Se, Ag, Tl and Zn[2]. Treatment processes for metal removal from wastewaters include precipitation, membrane filtration, ion exchange, adsorption and co-precipitation/adsorption. Therefore, a novel treatment method, which requires lower construction and operating costs and can be adopted irrespectively of the size of the industry, should be developed [3]. Cost effective alternative technologies or adsorbents for the treatment of metal-containing wastewaters are needed [4]. However, most of these techniques have some disadvantages such as complicated treatment process and high cost [5]. The good method, have more effective and economical is adsorption process for wastewater. However, for long time search for good adsorbent and without cost to reduce the cost of treatment of heavy metal like Zn and Cd. Many years ago using biochar as adsorbent heavy metal. Biochar, which is a by-product of bio refineries, has attracted much attention recently due to its proven role in environmental management issues [6].

When cheap biomass, particularly agricultural by-production is mainly associated with the machinery and heating, which is only about 4$ per gigajoule [7]. Bamboo biochar is one of good natural adsorbent. Bamboo charcoal may be an ideal amendment for nutrient conservation and heavy metal stabilization due to its excellent adsorption capability [8]. Because of it has high porosity more than many biomass wood materials.

Other material recently used in this field of disposes heavy metal from wastewater and have other environmental uses, Hydroxyapatite. It was a good member in apatite grope and has excellent behaviour to reduce contaminated heavy metal. The apatite mineral group has been shown to be effective both in sequestering dissolved metals and in transforming soil-bound metals to less soluble phases[9]. In this study we propose to use low cost adsorbent like Bamboo biochar cooperation with Calcium Sulphate and Hydroxyapatite, and comparative test the possibility of using this material as adsorbents for the removal of Cd^{2+} and Zn^{2+} from aqueous solution, effect of morphology on their adsorption efficiency. This material used with added Calcium Sulphate can be improved the efficiency; however in previous used to treatment by precipitate but here tray to find good mixture between them. This study investigate the sorption of Cd^{2+} and Zn^{2+} ions from aqueous solutions by adsorbents materials HAP&CS, and BB&CS, by equilibrium contact time, adsorbent dose and adsorbent concentration. Also objective of this study is to investigate the sorption mechanism of Cd^{2+} and Zn^{2+} on the surface of these two adsorbents through pseudo-second order.

Material and Method

Materials

Hydroxyapatite and $Zn(NO_3)_2$ and $Cd(NO_3)_2$ standard samples used in this work were purchased from Boss official limited partnership in Thailand. All metal solutions were prepared from their nitrate salts (AR) and distilled water. For the Bamboo biochar used here was prepared in lab. The concentration of residual $Zn(NO_3)_2$ and $Cd(NO_3)_2$ ions in the supernatant was determined by using an atomic absorption spectrophotometer. The suspensions in all studies were filtered through 0.45µm syringe membrane filters. All the experiments were done in triplicate and the average value was taken for analysis.

Adsorbent characterization

The shape and prose morphology of the BB was characterized by electron microanalysis- elemental mapping analysis used devise scanning electron microscope, JSM-5800 LV, JEOL Japan, attached with energy dispersive X-ray spectrometer, ISIS 300, Oxford, England. By method WI-RES-SEM-001 and WI-RES-EDX-001 and showed the content of BB sample. Analysis of functional groups in BB sample by Fourier Transform Infrared Spectrometer, EQUINOX 55, Bruker, Germany, was used method refer to WI-RES-FTIR-001 and technique pellet (KBr). It was fast and convenient method to follow the progress of pyrolysis and show the change in functional groups on the surface. For check the thermal stability of bamboo biochar used Differential Thermal Analyser, DTA7, Perkin Elmer, USA, by technique differential thermal analysis.

Production biochar from Bamboo

Bamboo wood materials collected from home gardening. The experimental design used in the laboratory pyrolysis production. Instruments used stainless steel reactor 45 cm long, and diameter of 11 with two holes, internal tray with sieve to hold, and furnace used for burning the Bamboo. The procedure used 100 grams of sample put on the sieve tray. The reactor flushed with N_2 gas for about 10 minutes at a pressure of 5 KPa to remove the air. The reactor was put inside furnace at room temp rising at an average rate of 20°C/ min until 500°C for 4 hour. The system was cooled overnight. After producing biochar, its yield was calculated.

Preparation of metal solutions

The synthetic solutions were all prepared by diluting Zn(II) and Cd(II) standard stock solutions (concentration 1000± 2mgL^{-1}) obtained by dissolving appropriate amounts of metal salt in double distilled water. Fresh dilutions were used in each experiment.

Methods

Adsorption experiments method

Metal salt of $Zn(NO_3)_2$ and $Cd(NO_3)_2$ was used to prepare metal ion (Zn(II) and Cd(II)) solution. The stock solutions concentrations (1000±2 mgL^{-1}) were prepared by dissolving appropriate amounts of metal salt in double distilled water. Fresh dilutions were used in each experiment. Use three type of adsorbent (Hydroxyapatite, Calcium Sulphate and Bamboo biochar) were used for each experiment, as (0.05:0.05:0.08) g

for HAP, CS and BB respectively, adsorbent was measured and put into a 250-mL conical flask containing 50 mL of the Zn(II) ions at the desired concentration that ranged between 50 to 150 ppm, it means 4 concentration (50, 75, 100, 150) and later on agitated, filtered and analysed by using a Perkin Elmer thermos scientific S-series model (AAnalyst100)flame atomic absorption spectrometer, and did same step for Cd(II). Kinetic study was conducted with the known dosage of HAP 0.05g, 0.05g CS and 0.08g BB for the 50 mL of metal ion solution. Samples were shaken at an agitation rate of 250 rpm. The samples were taken out at different time intervals. The sorbent solution mixtures were centrifuged for 5 min and the supernatant was analysed for the Zn(II) concentration and Cd(II). The batch sorption studies were carried out by shaking a series of bottles containing different amounts of adsorbent in 50 mL of metal ions solution prepared in the laboratory. The samples stirred at room temperature at 250 rpm for 40 minutes (equilibrium time), and their contents were centrifuged for 5 min and the supernatant liquid was analysed for Zn(II) and Cd(II) concentration. Adsorption data obtained from equilibrium studies, contact time and initiation concentration effects, were employed in the kinetic studies and the applicability of different adsorption isotherms to Zn(II) and Cd(II) ions. The percentage removal efficiency of the adsorbents (%R), which is the sorption capacity at time t min and the sorption capacity at equilibrium were calculated as follows equation (1) and (2):

$$\% \text{ (R) adsorption} = \left(\frac{C_o - C_t}{C_o}\right)100 \quad (1)$$

$$q_e = (C_0 - C_t)\frac{V}{M} \quad (2)$$

Where C_o (mg/L) and C_t (mg/L) are the liquid-phase concentrations of solute (adsorbate) at the origin and at given time t (min), respectively. C_e (mg/L) is the equilibrium concentration of Zn(II) and Cd(II) ions; V(L) is the volume of the solution while m (g) is the mass of the adsorbent.

Adsorption kinetics

From the literature, many models like pseudo- first order, pseudo- second order reaction model, for the investigated of mechanism of sorption of Zn(II) and Cd(II) in HAP+CS and BB+CS, and calculate the constant of sorption used a pseudo-second order equations model .The pseudo- second order equation model[10] can explained as:

$$\frac{t}{q_t} = \frac{t}{q_e} + \frac{1}{K_2 q_e^2} \quad (3)$$

Where q_t is the amount of metal ions adsorbed (mg g^{-1}) at any given time t (min), q_e is the amount of metal ion adsorbed (mg g^{-1}) at equilibrium and K_2 is the second order reaction rate constant for adsorption (g (mg min)$^{-1}$).

Adsorption isotherms

The mechanism responsible for the adsorption of heavy metals is a physicochemical process and may be one or a combination of many ion exchanges or surface complexation, coordination, adsorption, absorption, electrostatic interaction, chelation and micro precipitation [11].

Various isotherms model can predict and explained the relation between sorption equilibrium and remaining metal concentration. For this study applied two isotherms model, Langmuir and Freundlich. Langmuir isotherm can explain as equation (4):

$$\frac{C_e}{q_e} = \frac{1}{b\, q_{max}} + \frac{C_e}{q_{max}} \quad (4)$$

Where q_e and q_{max} are the observed and maximum uptake capacities (mg g^{-1}), C_e is the equilibrium concentration (mg L^{-1}), and b is the equilibrium constant (Lmg^{-1}). Langmuir is the most important model of monolayer adsorption, based on the assumption that there are a fixed number of adsorption sites, and each site can hold only one adsorbate molecule (the adsorbed layer is one molecule in thickness).

Freundlich isotherm can explain as equation (5):

$$\ln q_e = \ln K_f + \frac{1}{n}\ln C_e \qquad (5)$$

Where K_f (L g^{-1}) and n are Freundlich isotherm constants, q_e is the observed uptake capacities (mg g^{-1}) and C_e is the equilibrium concentration (mg L^{-1}).

Results and Discussion

Characteristics of Bamboo biochar

FTIR analysis

FTIR was a fast and convenient method to follow the progress of pyrolysis of biochar. The FTIR spectra of the biochar sample. Figure1 was shown changes of functional groups on the surfaces of the biochar produced at 500 and FRT at 5.

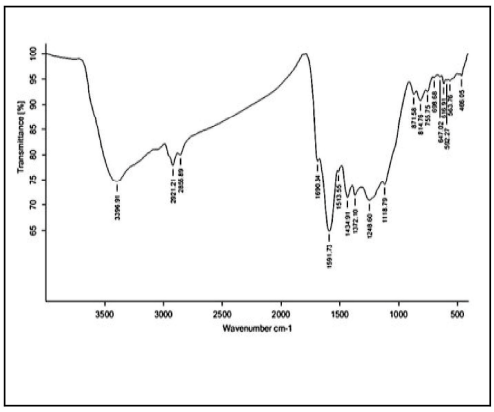

Figure 1: FTIR Analysis for progress of pyrolysis Process of characteristics the BB.

With increasing pyrolysis temperature, the bands assigned to O–H stretching vibration (near 3400 cm^{-1}) and aliphatic C-H stretching vibration (2921.21-2855cm^{-1}) decreased markedly, indicating a decrease of label aliphatic compounds in the biochar with increased pyrolysis temperature and an possible occurrence of demethoxylation, DE methylation, and dehydration of lignin. The loss of OH and aliphatic groups enhanced pore formation due to a concurrent development of fused–ring structures, especially at a high pyrolysis temperature, and this hypothesis was consistent with the results of increased surface area. The a symmetric 2921.21 cm^{-1} and symmetric 2855 cm^{-1} C–H stretching bands were associated with aliphatic functional groups. The intense bands for aliphatic CH_2 decreased with increasing temperature, indicating a decrease in the contents of nonpolar groups. The intensity of the band at 1690–1591.73 cm^{-1} (aromatic C=C stretching and C=O stretching of conjugated ketones and Quinone's) also diminished with increasing temperature. The peak at 1513.55 cm^{-1} represented the C=C ring stretching vibration of lignin, and the bands at 1434.91 cm^{-1} (aromatic C=C stretching) and 885 cm^{-1}(out–of–plane deformation by aromatic C–H groups) might be caused by carbonates. The sharp peaks at 1248.6–1000 cm^{-1} were assigned to C–O and C-C stretching, and these peaks markedly decreased probably due to the loss of polysaccharides during pyrolysis.

DTA Analysis

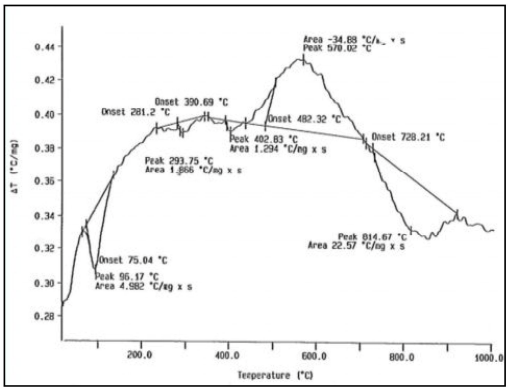

Figure 2: DTA Analysis of thermal stability for BB.

The thermal stability of Bamboo biochar described in figure 2 was checked by DTA curve can be shown clearly in that figure. These material generally showed three main peaks for loss of weight in the range 25-800 °C (see in figure). Among three peaks, the first strong peak at 75-96.17°C should be assigned to an evaporation procedure of adsorbed water molecules, the second weak peak in the range 280-294°C is likely attributed to a decomposition procedure of the surfaces, and the third broad peak appearing in the range 402-570°C may originate from the further carbonization process of this material. They have introduced new peak near 814°C. Infrared spectra 4000-400cm^{-1} was recorded using a Nicolet IR100 FTIR spectrometer that was equipped with a TGS/PE detector and a silicon beam splitter with 1 cm^{-1} resolution. The sample discs were prepared by mixing oven-dried (at 105°C) samples with spectroscopy-grade KBr in an agate mortar.

Scanning electron microscope images (SEM)

Results of characteristic Bamboo biochar by SEM had shown the morphology and elemental composition. In figure 3(a), shown the large internal surface and the porous structure**,** figure 3(b), clearly shown the approximate porous space of 38.67µm. Elemental composition of Bamboo biochar, C, S, K, and Cl were 58.61, 1.55, 30.46, and 9.38 respectively.

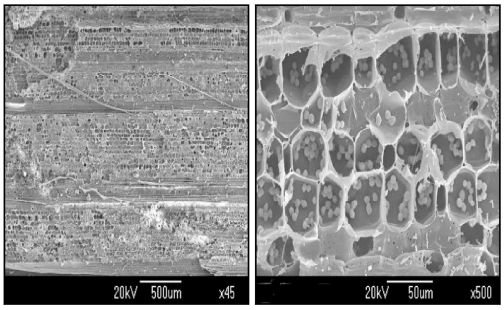

(a) (b)

Figure 3: SEM for BB by different revolution (a) and (b) for porous surface

Physicochemical properties of Bamboo biochar, such as pH, surface potential, and surface area, are important factors controlling their environmental applications [12]. In this work, the surface potential measurements indicated that Bamboo biochar has more negative surface charge which may be related to its higher surface area and pore volume. These data seems to suggest a greater potential to adsorb abundant positively charged heavy metals[13]. The values of charge can be shown in (Table 1). The biochar structures were not homogeneous and irregular pores with different shapes and sizes were observed [14].

Table 1: Zeta potential charge for different adsorbents.

Adsorbents	Zeta Potential (mv)
BB	-56
HAP + BB + CS	-2
HAP + BB	-19

The pH of the Bamboo biochar samples was measured by combining it with DI water in a mass ratio of 1:20. The solution was then hand stirred and allowed to stand for 5 min before measurement with a pH meter [13]. The pH was 8.00 for Bamboo biochar.

Sorption study:

Effect of initial metal concentration in adsorption equilibrium

For kinetics and isotherms equilibrium in all adsorbents used different initial concentrations from 50 to 150 ppm. It means 4 concentrations (50, 75, 100 and 150) used 50 ml in every experiment for 40 mentis after that measured the remaining metal from initial concentration. Sorption capacities of adsorbents HAP&CS and BB& CS for adsorption of Zn(II) and Cd(II) metal ions function in initial concentration of solution metal ions used Zn(II) and Cd(II) solution concentration in rang 50–150 mg/L, showed that clearly in figure 4(a), and figure 4(b), blow for HAP&CS and BB&CS respectively.

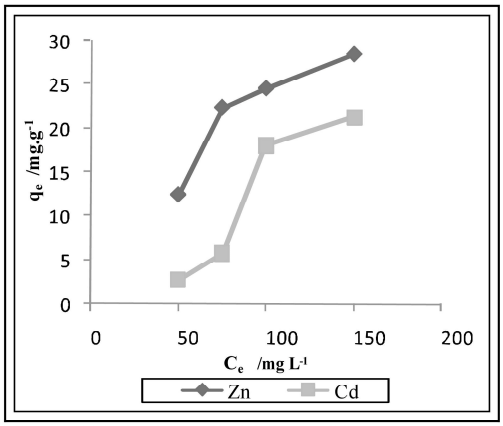

Figure 4(a): Effect of initial metal ion concentration in HAP&CS.

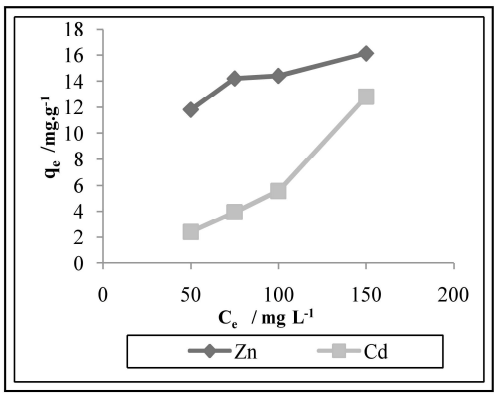

Figure 4(b): Effect of initial metal ion concentration of Zn and Cd in BB&CS.

In all the initial concentrations of Zn(II) and Cd(II), sorption capacities raises immediately in initial state, before rich in saturation and looked in space and empty site in adsorbents. The results are presented in

figure 4(b), for Zn^{+2} and Cd^{+2} adsorption capacity of the adsorbents HAP& CS and BB& CS in the beginning increased with increasing the initial concentration of metal ion and then reached a saturation values at about greater than 150 mg L^{-1} for both in HAP& CS and BB&CS, the maximum equilibrium uptake for Zn^{+2} and Cd^{+2} were 25 mg Zn^{+2}/g of HAP&CS, 18.05 mg Cd^{+2}/g of HAP&CS, and 14.42mg Zn^{+2}/g of BB&CS, 8.04 mg Cd^{+2}/g of BB&CS.

Effect of contact time in removal of metal

Effect of contact time between adsorbent and heavy metal solutions by different time period started from 0 to 40 min, with different initial concentrations.

The plot of Cd and Zn removed by HAP&CS and BB&CS adsorbents against time min, Result can be seen in figure 5(a), and figure 5(b), when it chose the concentration 100mg/L of metal to do the adsorption by HAP& CS and BB& CS.

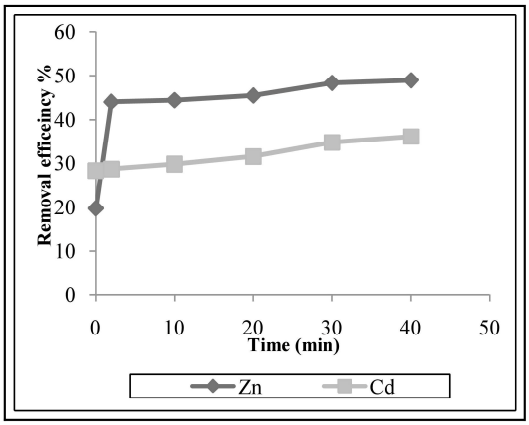

Figure 5(a): Effect of contact time in removal metal ion concentration in HAP& CS.

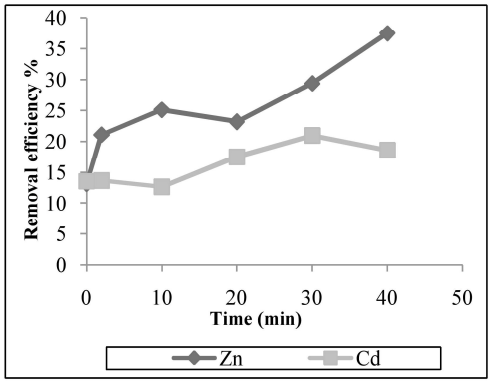

Figure 5(b): Effect of contact time in removal metal ion concentration in BB& CS.

The results elucidate that near to 50 % of Zn and 40% of Cd of metal ions by HAP&CS, were removed in the first 30 min, and 30% of Zn and more than 20% of Cd by BB&CS. It means that under same conditions of experiments no expressing adsorption was seen after 40 min.

Sorption kinetics

Sorption of Zn(II) and Cd(II) by HAP&CS and BB&CS adsorbents as function of contact time was explicated in figure 6(a) and figure 6(b) respectively. Kinetics sorption studies were applied by pseudo-

second order equation in this study. The results kinetics removal of Zn^{+2} and Cd^{+2} by this two adsorbents can be divided into two periods, fast 20 min, forward by a slow rise until equilibrium was about 40 minutes.

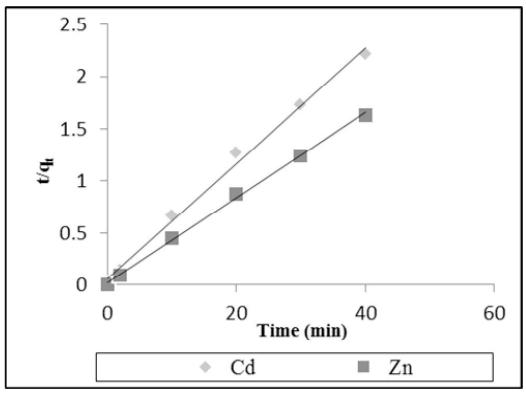

Figure 6(a): Kinetic model for removal of Zn and Cd ions in adsorbent (HAP&CS) in a pseudo-second model.

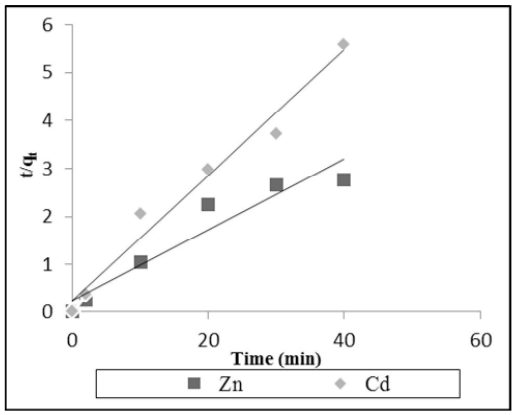

Figure 6(b): Kinetic model for removal of Zn and Cd for adsorbents (BB&CS) in pseudo- second order.

The rate constants K_2 and $q_{e(Cal)}$ of pseudo-second order kinetic model were determined from figure 6(a) and figure 6(b), by the slope and intercept of the linear plot of time versus t/q_t for both adsorbents. It can be seen in (Table 2) that the linear correlation coefficients for second-order model are good and based on the comparison between experimental and theoretically calculated q_e values; it was found that the pseudo second-order model fitted for the removal of Zn(II) and Cd(II) by HAP&CS and BB&CS adsorbents.

Table 2: Adsorption kinetic model rate constants for Zn (II) and Cd (II) removal

Adsorbent		q_{eExp} mg/g_{ad}	Pseudo second order		
			$q_{e(Cal)}$mg/g	K_2	R^2
HAP&CS	Zn	24.47	24.51	0.073	0.99
	Cd	18.05	18.018	0.0502	0.994
BB&CS	Zn	14.423	13.51	0.023	0.923
	Cd	8.0423	7.6452	0.0729	0.975

The calculated (Cal) value of q_e from the pseudo second-order kinetics model provides a near-perfect match between the theoretical and experimental q_e values. And the pseudo second order model provide high correlation coefficients (R^2 >0.99) for Zink and cadmium. By taking K_2 as the adsorption velocity, the constant K_2 0.073, 0.050 for HAP&CS is higher than those of BB&CS, 0.02, 0.07 for both metals.

Adsorption isotherms

For determining the capacity of adsorbents HAP&CS and BB&CS, we used high concentration of Zn^{+2} and Cd^{+2}. The maximum adsorbent capacity for this heavy metals used adsorption isotherms. Langmuir and Freundlich isotherm models were applied. The constants b and q_m can be determined from the slope and intercept of the linear plot $1/q_e$ versus $1/C_e$. Can show that in figure 7(a), and figure 7(b), for adsorbent HAP&CS and BB&CS respectively.

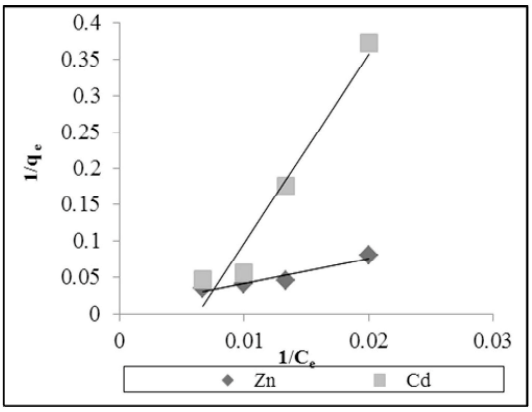

Figure 7(a): Langmuir isotherm for the adsorption of Zn and Cd in adsorbent HAP&CS.

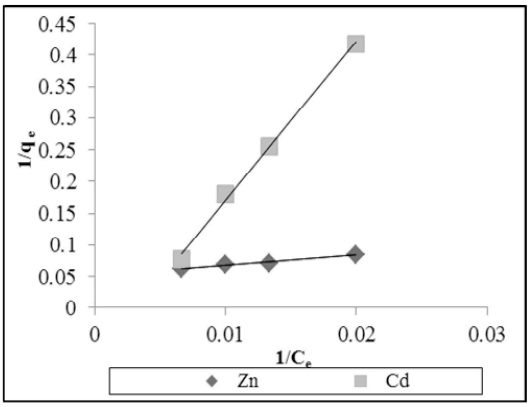

Figure 7(b): Langmuir isotherm for the adsorption of Zn and Cd in adsorbent BB&CS

The results were shown that values of correlation coefficient for the adsorption of Zn^{2+} and Cd^{2+} on HAP&CS and BB&CS adsorbents were 0.909, 0.951 and 0.959, 0.997 respectively, which demonstrated the good fitting of experimental data by this model. The Langmuir constant for Zn^{2+} and Cd^{2+} was 0.01, 0.04 and 0.002, 0.003 respectively, which illustrated that they had better adsorption affinity for Cd^{2+} than for Zn^{2+} since the Langmuir constant was proportional to the binding energy. The q_m values for the adsorption of Cd^{2+} and Zn^{2+} by the HAP&CS were 21.28 and 28.57mg/g, respectively and for BB&CS, 16.13mg/g for Zn^{2+} and 12.82 mg/g for Cd^{2+}.

The empirical Freundlich isotherms model, constants n and K_f can be determined from the slope and intercept of the linear plot log q_e versus log C_e. The plots can be shown in figure 8(a), and figure 8(b), for HAP&CS and BB&CS, adsorbents respectively. Results showed that the values of correlation coefficient for the adsorption of Zn^{2+} and Cd^{2+} on HAP&CS and BB&CS adsorbents were 0.8616, 0.9096 and 0.931, 0.9782 respectively, which clearly for compering between two models, Langmuir is good fitting more than Freundlich model. All the results can be shown in (Table 3). Maximum sorption capacity represents the monolayer coverage of sorbent with sorbate [15]. Comparing to other kinds of adsorbents, the adsorption capacity of Zn and Cd on BB&CS is highest than many adsorbents, as shown in (Table 4).

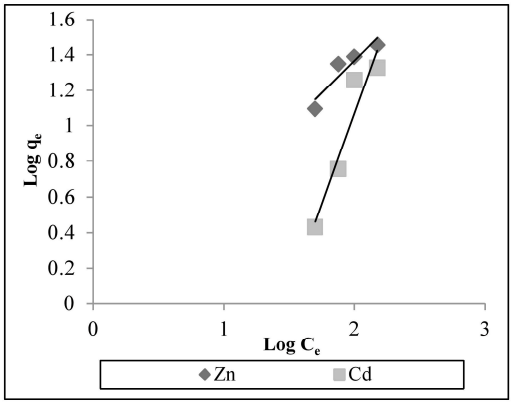

Figure 8(a): Freundlich isotherm for the adsorption of Zn and Cd ions in all adsorbent HAP&CS.

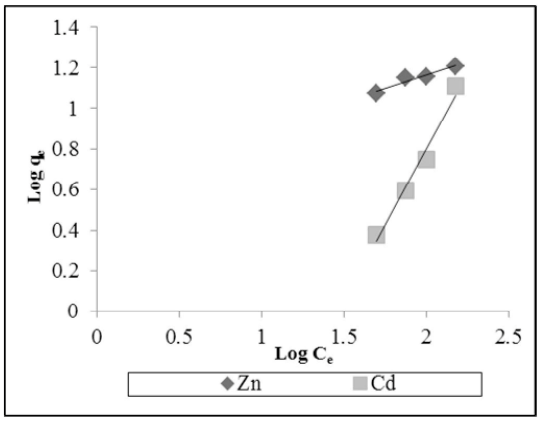

Figure 8(b): Freundlich isotherm for the Adsorption of Zn and Cd ions in adsorbent BB&CS.

Table 3: Isotherms parameters for sorption of Zn(II) and Cd(II) by different adsorbents.

Adsorbent		Langmuir			Freundlich		
		b	K	R^2	K_f	n	R^2
HAP&CS	Zn	28.57	0.01	0.9096	0.82	1.4	0.8616
	Cd	21.28	0.002	0.951	0.001	0.496	0.9096
BB&CS	Zn	16.13	0.04	0.9595	4.23	3.7	0.931
	Cd	12.82	0.003	0.9972	0.006	0.65	0.9782

Table 4: Comparison of Zn(II) and Cd(II) adsorption capacities of different adsorbents

Metal	adsorbents	q_e	Reference
Zn	Dairy manure biochar	32.8	[16]
Cd	Dairy manure biochar	51.4	[16]
Cd	Cocoa shell	4.94	[17]
Zn	Cocoa shell	2.92	[17]
Zn	Banana peel	5.8	[18]
Cd	Rice husk	2	[19]
Cd	Cassava Waste	18.05	[20]
Zn	Cassava waste	11.06	[20]
Cd	Jackfruit	52.08	[21]
Zn	Orange peel	5.25	[18]

Zn	HW450	4.54	[14]
Cd	BC500	13.24	[22]
Cd	Coffee residue- clay	39.5	[23]
Zn	Coffee residue- clay	13.4	[23]
Cd	Bagasse	2	[24]
Zn	Coal	1.2	[25]
Zn	GAC type C	20	[26]
Cd	CHAP	111.1	[27]
Cd	Chitosan–MAA nanoparticles	1.84	[11]
Zn	HAP&CS	24.47	This study
Cd	HAP&CS	18.05	This study
Zn	BB&CS	14.42	This study
Cd	BB&CS	8.042	This study

Conclusion

HAP&CS and BB&CS were able to substantially remove Zn and Cd from aqueous solutions. The adsorbent capacity of HAP&CS were 24.47 mg Zn(II)/g of HAP&CS, 18.05 mg Cd(II)/g of HAP&$CaSO_4$,14.423mg Zn(II)/g of BB&CS, and 8.0423 mg Cd(II)/g of BB&CS. It means that the removal efficiency for HAP&CS was defiantly higher than other adsorbent but if used other adsorbent like BB still can affect to remove Zn and Cd ions. In this work discovered BB and CS can played same function of adsorption of Zn and Cadmium from water and wastewater, however the efficiency not like HAP&CS but acceptable to replaced it as low cost adsorbent.

Acknowledgments

The Authors are grateful to Prince of Songkla University for funding fundamental to support this research. The author would like to thank chemical engineering department, Discipline of excellence in chemical engineering for performing the chemical analyses.

References

1. Kurniawan. T. A, Chan. G. Y. S, Lo. Wh, Babel. S. ''Comparisons of low-cost adsorbents for treating wastewaters laden with heavy metals'', Science of The total Environment, 2006; 366: 409-426.
2. Oliva. J, De Pablo. J, Cortina. J. L, Cama. J, Ayora. C. ''Removal of cadmium, copper, nickel, cobalt and mercury from water by Apatite II™: Column experiments'', Journal of Hazardous Materials., 2011; 194: 312-323.
3. Suzuki. Y, Mochidzuki. K, Takeuchi. Y, Yagishita. Y, Fukuda. T, Amakusa. H, Abe. H. ''Biological activated carbon treatment of effluent water from wastewater treatment processes of plating industries'', Separations Technology., 1996; 6: 147-153.
4. Kadirvelu. K, Thamaraiselvi. K, Namasivayam. C. ''Removal of heavy metals from industrial wastewaters by adsorption onto activated carbon prepared from an agricultural solid waste'', Bioresource Technology., 2001; 76: 63-65.
5. Yahaya. NK. EM, Abustan. I, Mohamed Latiff. M. F. P, Bello. O. S., Ahmad. M. A. ''Fixed-bed column study for Cu (II) removal from aqueous solutions using rice husk based activated carbon'', International Journal of Engineering & Technology., 2011; 11: 186-190.
6. Kumar. S, Loganathan. V. A, Gupta. R. B., Barnett. M. O. ''An Assessment of U (VI) removal from groundwater using biochar produced from hydrothermal carbonization'', Journal of Environmental Management., 2011; 92: 2504-2512.
7. Lehmann. J. ''A handful of carbon'', j. Nature, 2007; 447: 143-144.
8. Hua. L, Wu. W, Liu. Y, McBride. M. B. Chen. Y. ''Reduction of nitrogen loss and Cu and Zn mobility during sludge composting with bamboo charcoal amendment'', J Environmental Science and Pollution Research., 2009; 16: 1-9.
9. Krestou. A, Xenidis. A, Panias. D. ''Mechanism of aqueous uranium (VI) uptake by hydroxyapatite'', Minerals Engineering., 2004; 17: 373-381.

10. Febrianto. J, Kosasih. A. N, Sunarso. J, Ju. YH, Indraswati. N, Ismadji. S. ''Equilibrium and kinetic studies in adsorption of heavy metals using bio sorbent: A summary of recent studies'', Journal of Hazardous Materials., 2009; 162: 616-645.
11. Heidari. A, Younesi. H, Mehraban. Z, Heikkinen. H. ''Selective adsorption of Pb(II), Cd(II), and Ni(II) ions from aqueous solution using chitosan–MAA nanoparticles'', International Journal of Biological Macromolecules., 2013; 61: 251-263.
12. Inyang. M, Gao. B, Pullammanappallil. P, Ding. W, Zimmerman. A. R. ''Biochar from anaerobically digested sugarcane bagasse'', Bioresource Technology., 2010; 101: 8868-8872.
13. Inyang. M, Gao. B, Ying Yao. Y, Yingwen Xue. Y, Zimmerman. A. R, Pullammanappallil. P, Cao. X. ''Removal of heavy metals from aqueous solution by biochars derived from anaerobically digested biomass'', Bioresource Technology., 2012; 110: 50-56.
14. Chen. X, Chen. G, Chen. L, Chen. Y, Lehmann. J, McBride. M. B, Hay. A. G. ''Adsorption of copper and zinc by biochars produced from pyrolysis of hardwood and corn straw in aqueous solution'', Bioresour Technol., 2011; 102: 8877–8884.
15. Zhu. R, Yu. R, Yao. J, Dan Mao. D, Xing. C, Wang. D. ''Removal of Cd^{2+} from aqueous solutions by hydroxyapatite'', Catalysis Today., 2008; 139: 94-99.
16. Xu. X, Cao. X, Zhao. L, Wang. H, Yu. H, Gao. B. ''Removal of Cu, Zn, and Cd from aqueous solutions by the dairy manure-derived biochar'', Environmental Science and Pollution Research., 2013; 20: 358-368.
17. Meunier. N, Laroulandie. J, Blais. J. F, Tyagi. R. D. ''Cocoa shells for heavy metal removal from acidic solutions'', Bioresource Technology., 2003; 90: 255-263.
18. Annadurai. A, Juang. R. S, Lee. D. J. ''Adsorption of heavy metals from water using banana and orange peels'', Water Sci Technol., 2002; 47: 185–190.
19. Ajmal. M, Rao. R. A. K, Anwar. S, Ahmad. J, Ahmad. R. ''Adsorption studies on rice husk: removal and recovery of Cd(II) from wastewater'', Bioresource Technology., 2003; 86: 147-149.
20. Abia. A. A, Horsfall J. M, Didi. O. ''The use of chemically modified and unmodified cassava waste for the removal of Cd, Cu and Zn ions from aqueous solution'', Bioresource Technology., 2003; 90: 345-348.
21. Inbaraj. B. S, Sulochana. N. ''Carbonised jackfruit peel as an adsorbent for the removal of Cd(II) from aqueous solution'', Bioresource Technology., 2004; 94: 49-52.
22. Kim. WK, Shim. T, Kim. YS, Hyun. S, Changkook R. C, Park. YK, Jung. J. ''Characterization of cadmium removal from aqueous solution by biochar produced from a giant Miscanthus at different pyrolytic temperatures'', Bioresource Technology., 2013; 138: 266-270.
23. Boonamnuayvitaya. V, Chaiya. C, Tanthapanichakoon. W, Jarudilokkul. S. ''Removal of heavy metals by adsorbent prepared from pyrolyzed coffee residues and clay'', Separation and Purification Technology., 2004; 35: 11-22.
24. Gupta. V. K, Jain. C. K, Ali. I, Sharma. M, Saini. V. K. ''Removal of cadmium and nickel from wastewater using bagasse fly ash—a sugar industry waste'', Water Research., 2003; 37: 4038-4044.
25. Karabulut. S, Karabakan. A, Denizli. A, Yürüm. Y. ''Batch removal of copper (II) and zinc (II) from aqueous solutions with low-rank Turkish coals'', Separation and Purification Technology., 2000; 18: 177-184.
26. Ramos. R. L, Jacome. L. A. B, Barron. J. M, Rubio. L. F, Coronado. R. M. G. ''Adsorption of zinc(II) from an aqueous solution onto activated carbon'', Journal of Hazardous Materials., 2002; 90: 27-38.
27. Zheng. W, Li. Xm, Yang. Q, Zeng. Gm, Shen. Xx, Zhang. Y, Liu. Jj. ''Adsorption of Cd(II) and Cu(II) from aqueous solution by carbonate hydroxylapatite derived from eggshell waste'', Journal of Hazardous Materials., 2007; 147: 534-539.

*****

Appendix B

The publications of circulation fluidize bed column

Appendix B1

Journal Paper

A. H. Alamin, L. Kaewsichan, ‘‘Sorption of 2, 4-Dichlorophenol onto 2 mixtures: Bamboo biochar plus Calcium sulphate (BC) and Hydroxyapatite plus Bamboo biochar plus Calcium sulphate (HBC), in fluidized bed circulation column’’, **this manuscript had been accepted to publish in Polish Journal of Chemical Technology.**

Sorption of 2, 4-Dichlorophenol onto 2 mixtures: Bamboo biochar plus Calcium sulphate (BC) and Hydroxyapatite plus Bamboo biochar plus Calcium sulphate (HBC), in fluidized bed circulation column

Ahmed Hassan Alamin [1]*, Lupong Kaewsichan [2]

[1,2] Department of Chemical Engineering, Faculty of Engineering , Prince of Songkla University, Hat Yai, Songkhla, 90112, Thailand.

* Corresponding author, e-mail: (ahmed.10000@yahoo.com)

Abstract: Sorption studies were carried out to investigate removal of 2, 4-Dichlorophenol (2, 4-DCP) from aqueous solution in a fluidized bed by two types of adsorbent mixtures: BC (Bamboo char plus Calcium sulphate), and HBC (Hydroxyapatite plus Bamboo char plus Calcium sulphate); both manufactured in ball shape. The main material Bamboo char was characterized by FTIR, DTA and SEM. The adsorption experiments were conducted in a fluidized bed circulation column. Adsorption, isotherms and kinetic studies were established under 180-min operating process time, at different initial 2, 4- DCP solution concentrations ranging from 5-10 mg/l, and at different flow rates ranging from 0.25-0.75 l/min. The data obtained fitted well for both the Langmuir and Freundlich isotherm models; indicating favorable condition of monolayer adsorption. The kinetics of both adsorbents complies with the pseudo2ndorder model. BC was proven a new effective composite and low cost adsorbent which can be applied in the field of wastewater treatment, and it could also play an important role in industry water treatment.

Keywords: 2, 4-Dichlorophenol, Bamboo biochar, Hydroxyapatite, Calcium sulphate, Adsorption

INTRODUCTION

Phenolic compounds pose a major worldwide environmental health problem concerning industries handling phenol and metal process. Chlorophenol is a group of chemical, of which chlorines (between one and five) have been added to phenol[1]. Main pollution sources containing chlorophenols are wastewaters from pesticide, paint, solvent, pharmaceutics, wood, paper and pulp industries, as well as water disinfecting process[2]. In addition, phenolic derivatives are largely used as intermediates in productions of plastics, colors, pesticides, insecticides, etc.[3]. However, phenol containing water - when chlorinated during disinfection of water - results in formation of chlorophenol[4].

Chlorophenols and related compounds are toxic to humans and aquatic lives, which are carcinogenic, mutagenic, and resistant to biodegradation. Results of phenolic compound discharging into the environment, affected to the contamination the environment and living organisms[5]. Phenols are considered as priority pollutants since they are harmful to organisms at low concentrations and many of them have been classified as hazardous pollutants because of their potential to harm human health. The United States Environmental Protection Agency (USEPA) and the European Union (EU) have designated phenols as priority pollutants[6]. Thus, removal of phenol from drinking water is of great importance, and has been receiving particular concerns in the last few decades[7].

Treatment technologies, depending on the load of phenol compound in wastewater, are either physiochemical or biological[8]. Some conventional methods used to remove phenol from aqueous solutions are: adsorption, precipitation and coagulation, ion exchange, filtration, membrane separation, chemical oxidation, sedimentation, and reverse osmosis[9].

Phenol could be removed effectively through adsorption process using a variety of adsorbents[10], but without mentioning the use of Bamboo biochar. Preservative of various functional groups on Bamboo biochar surface can contribute a unique and specific preferential for different molecules uptake by active carbons[11]. Furthermore, it is well known that nano-size adsorbents, including Hydroxyapatite, possess excellent surface properties, such as large accessible internal and external surface[12], and Bamboo biochar is a nano-size absorbent.

A new composite material made from Bamboo biochare plus Calcium sulphate (BC), can be used as an adsorbent in that Calcium sulphate plays a role on its hydrophilic property. Hydroxyapatite, by itself or together with calcium sulphate – better known for their combined properties in the medical profession, particularly in bone surgery and bone treatment – has reportedly been used more in the removal of heavy metals, but less so in the removal of phenols. And literature is yet to be found on the use of Hydroxyapatite plus Calcium sulphate plus Bamboo biochar (HBC) in the removal of phenols either.

Fluidized-bed reactor has received considerable attention and wide utilization in wastewater treatment due to several advantages. First, this reactor renders a more intensive contact between liquid and solid phase causing high mass transfer, high reaction rate, and small external mass transfer resistance between solid and liquid phase. Second, it could eliminate operating problems such as bed clogging and high pressure drop, which occur in packed-bed operations. Third, it is a high efficient, simple, stable and economical operation compared to other reactor configurations[13]. Thus it was chosen as a tool in this adsorption study.

The objective of this study was to investigate adsorption of 2, 4-dichlorophenol (2, 4-DCP) in aqueous solution onto two types of ball-shape adsorbents: BC and HBC, in a

fluidized-bed circulation column. Adsorption isotherm of Langmuir and Freundlich were investigated. Moreover, adsorption kinetics pseudo-first and pseudo-second order were simulated for comparison.

MATERIALS AND EXPERIMENTAL METHODS

Preparation of Adsorbent and Properties

Bamboo biochar (BB), used in this work as the main material, was obtained by pyrolysis process at 500°C in nitrogen atmosphere. Hydroxyapatite (HAP), and 2, 4-DCP were purchased from Sigma-Aldrich Co. LLC**,** while Calcium sulphate (CS) was from Aldrich Chemicals. BB was ground and sieved through mesh number 20, and mixed with CS to form an adsorbent composite BC, and with HAP and CS to form another adsorbent composite HBC. The weight ratio of BB:CS is 0.62:0.38, and that of BB:HAP:CS is 0.46:0.27:0.27. A glue, prepared from polyvinyl alcohol (PVA) having a molecular weight MW of 22,000, was added to the mixtures to manufacture ball-shape adsorbents. The concentration of residual phenol was determined using a double beam UV–Vis spectrophotometer (Shimadzu UV-1601 Spectrophotometer, Japan) at wave length 765 nm. Fourier transforms infrared spectroscopies (FTIR) (Bomem, MB 100) were carried out to identify the functional groups of the biochar. DTA for thermal stability of BB was analyzed. Scanning electron microscopy (SEM) was conducted with a Hitachi JSM-6700F SEM to observe the surface microstructures of the fresh Bamboo biochar.

Properties and Preparation the Adsorbate

A stock solution of 2, 4-DCP was obtained by dissolving it in double distilled water. Desired solution of phenol was prepared using appropriate subsequent dilutions of the stock solution. The range of concentration of the phenol prepared from the standard solution varied between 5–10 mg/l. The pH of the solutions was adjusted to 6.5 by 0.1 N NaOH and 0.1N HCl solutions.

Experimental Method

Study of 2, 4-DCP adsorption was carried out in laboratory scale; circulation fluidized bed reactor was used as the adsorption system to improve mixing and homogeneity. The experimental system consisted of a reactor column, a water reservoir and a peristaltic pump. The reactor’s outside diameter is 50mm and its height is 240 mm. This reactor of the fluidized-bed column, having an effective volume of 470 ml, was made from transparent acrylic. A conical distributor was placed at the bottom to ensure proper distribution of fluid. Aqueous solution of phenol was continuously fed upward to the reactor at different flow rates, starting from 250 to 750ml/min. The liquid effluent stream was recycled to the hold-up tank. Three liters of the phenolic aqueous solution was treated with adsorbent of 3 g for each adsorbent.

Adsorptions of the 2, 4-DCP onto adsorbent BC and adsorbent HBC were compared. The suspensions in all studies were filtered through 0.45µm syringe membrane filters. All the experiments were conducted in triplicates for statistical analysis.

RESULTS AND DISCUSSION

FTIR Analysis

The progress from pyrolysis process method of the BB was fast and can be conveniently investigated by FTIR. The sample discs were prepared by mixing oven-dried (at 105 °C) BB samples with spectroscopy-grade KBr in an agate mortar. Infrared spectra (4000-400cm^{-1}) were recorded using a Nicolet IR100 FTIR spectrometer that was equipped with a TGS/PE detector and a silicon beam splitter with 1 cm^{-1} resolution. Figure 1 shows the FTIR spectra of the BB. Biochar produced at 500°C clearly revealed changes of functional groups on the surfaces. With increasing pyrolysis temperature, bands assigned to O-H stretching vibration should be close to 3400 cm^{-1} wave number. For the BB sample the O-H stretching vibration band of hydroxyl group was found at 3461cm^{-1}, and severe peak at wave number 2830cm^{-1} is assigned to C-H stretching vibration of aldehydes. Aliphatic was dwindled markedly by C-H stretching vibration (2921.21-2855 cm^{-1}), indicating dwindle of labile aliphatic compounds in the biochar with the rise in pyrolysis temperature and a possible occurrence of demethoxylation, demethylation, and dehydration of lignin.

The loss of OH and aliphatic groups explain the enhanced pore formation within a synchronous efflorescence of fused–ring entity, exceptionally for a high pyrolysis temperature; and this hypothesis was consistent with the results of increased surface area. The two functional groups, asymmetric (2921.21 cm^{-1}) and symmetric (2855 cm^{-1}) C-H stretching bands, were associated with aliphatic functional groups. Intense bands for aliphatic CH_2 dwindle with rising temperature; denoting dwindles in the contents of nonpolar groups.

Intensity of the band at 1690–1591.73 cm^{-1} (aromatic C=C stretching and C=O stretching of conjugated ketones and Quinone's) also diminished with rising temperature. The peak at 1513.55 cm^{-1} represents the C=C ring stretching vibration of lignin, while the bands at 1434.91cm^{-1}(aromatic C=C stretching) and 885cm^{-1} (out–of–plane deformation by aromatic C–H groups) might be caused by carbonates. Severe peaks at 1248.6–1000 cm^{-1} were assigned to C-O and C-C stretching, and these peaks markedly dwindle, probably due to the loss of polysaccharides during pyrolysis. Moreover, sharp band at 1372 cm^{-1} confirmed the existence of a C-O bond on BB, reinforcing the interaction with carboxyl groups.

DTA Analysis

Thermal stability of the BB was investigated by DTA analysis; and the analysis curve was shown in Figure 2. The BB sample generally showed three main peaks for weight loss in the temperature range 25–800°C. The first strong peak among the three peaks, at 75–96.17°C, should be assigned to the evaporation procedure of adsorbed water molecules. The second weak peak in the range 280–294°C is as imputed for a degeneration method of the surfaces. And the third broad peak, appearing in the range 402–570°C, could originate from the further carbonization process of this material. Above this range, a new peak near 814°C was introduced.

Scanning Electron Microscope Images (SEM)

SEM result on BB characteristics showed its morphology and elemental composition. Figure 3(a) and Figure 3(b) at different magnifications revealed its large internal surface and porous structure**.** Figure 3(c), at x500 magnification, showed an average porous space of 38.67µm. Elemental percent compositions of the BB were evaluated by SEM mapping technique; results on C, S, K, Cl were 58.61, 1.55, 30.46, 9.38, respectively.

Effect of Initial pH Solution of 2, 4-DCP Adsorption

Adsorbent behaviour of BC and HBC on the adsorption of 2, 4-DCP were studied from adjustment effect of the initial pH between 3 to 10 at room temperature of 28°C while the initial concentration of 2, 4-DCP solution of 10mg/l was constantly maintained for both adsorbents. As shown in Figure 4, the removal rates of the 2, 4-DCP were lower on both ends of the pH region. Different behavior trends were observed for the two different adsorbents. For HBC adsorbent, the maximum 2, 4-DCP percent removal of 60 was at pH 6, and its rates declined to 45-50 on either side. For BC adsorbent, the maximum removal percent of nearly 40 was at pH 8, but was rather stable between pH 6-10, though with a sharp drop at pH 4. The drop in adsorption percent was sharper for HBC in the alkaline region while the drop was a little sharper for BC in the acidic region. Chlorophenols are weakly acidic, and pH has a significant effect on the degree of ionization of 2, 4-DCP and the adsorbent surface properties[14].

The surface charge on the BC and HBC, as a matter of fact, was negative in range of pH 3-10. The ionic fraction of Chlorophenol ions increases with increasing pH, and Chlorophenol could be expected to become negatively charged as pH increases[14]. Non-dissociated form activated by the OH^- and Cl^- dominates the overall sorption of chlorinated phenols on organic sorbents[2]. The slow and low removal percent of 2, 4-DCP at highest pH could have been resulted from competition between the OH^- ions and the ionic species of 2, 4-DCP, hence reducing the 2, 4-DCP removal[1].

Effect of Contact Time of Fluidization

The efficiency of percentage removal of 2, 4-DCP by adsorption onto adsorbents BC and HBC was studied on the effect of contact time of fluidization at various time intervals between 0 to 180 min at room temperature. At initial stage time the adsorbents have more vacuous number of available surface sites, and hence were ready for adsorption. Adsorption gradually increases depending on the accumulation of phenol on the adsorbents surface during this time. As a result, the remaining vacant surface sites are difficult to be occupied due to formation of repulsive forces between the phenol molecules on the solid surface and in the bulk phase[15]. Besides, phenol molecules are very small in size and can easily diffuse into internal pores until they become saturated; which will reduce the driving force for mass transfer between the bulk liquid phase and the solid phase over time[11]. Figure 5 depicts the effect of time on the percentage removal and the result was that the equilibrium time for either adsorbent was reached at approx. 180 min; the authors had conducted up to 6 hrs and found no significant increase in percentage removal. However, adsorption of 2, 4-DCP employing either BC or HBC increased slowly to equilibrium, particularly the BC. At equilibrium, the removal percent were approx. 68% for HBC, and 53% for BC.

Effect of Flow Rate of 2, 4-DCP Solution

The effect of different flow rate was investigated for adsorption of 2, 4-DCP from aqueous solution employing the two adsorbents. Experiments were carried out at room temperature with flow rate in range of 250–750 ml/min while other variables were kept constant (solute pH of 6.5, 3g of adsorbent, 7.5 mg/l of the 2, 4-DCP initial concentration.) From Figure 6, the percentage removal of the 2, 4-DCP solution using BC adsorbent declined with increasing flow rate of the solution, whereas for HBC it was the opposite. The behavior for the BC can be explained by insufficient residence time of the solute in the column; the residence time decreased with increasing flow rate, leading to insufficient time for diffusion of the solution into the pores of the BC adsorbent and thus limiting the number of available active sites for adsorption, reducing the adsorbed amount of the aqueous solution since much solute left the column before equilibrium occurs[16]. In case of adsorbent HBC, the removal capacity increased imperceptibly below flow rate of 500 ml/min, except at 250 to 300 ml/min. Beyond flow rate of 500 ml/min the removal capacity rose rapidly to another plateau; the reason is that at higher flow rate, the rate of mass transfer tends to increase.

Effect of Initial Concentration of 2, 4-DCP Solution

Studies were carried out at room temperature to investigate the effect of initial concentrations, from 5-10mg/l of 2, 4-DCP, on adsorption at fixed parameters: pH of 6.5, adsorbent weight of 3g, flow rate of 500 ml/min. It can be noted from Figure 7 that at lower initial concentration the capacities of sorption for both BC and HBC increased with increasing initial concentration, then rose slowly (for BC) or plateau off (for HBC). This is due to the raising of the mass transfer driving force and thus

the rate at which 2, 4-DCP molecules pass from the bulk solution to the particle surface. However, when the initial concentration went beyond 9 mg/l the absorbents behaved differently; the percentage of removal for the BC rose up a little, whereas for the HBC it dropped.

From the experiment, the highest percentage of removal for HBC was approx. 75% at 7.5mg/l initial concentration. For adsorbent BC, the maximum percentage of removal was at 56% at 10mg/l. The performance of adsorbent HBC is better than BC because the former has more specific surface area and more macro porous structures. However, BC performance is at approx. 75% of that obtained using HBC.

Adsorption Kinetics

Adsorption kinetics models, pseudo-first order and pseudo-second order, were used to investigate, at room temperature, the 2, 4-DCP adsorption kinetics by adsorbents BC and HBC.

The pseudo-first order equation can be explained using Lagergren equation:

$$\log(q_e - q_t) = \log(q_e) - \frac{k_1}{2.303}\, t \qquad (1)$$

Where q_e and q_t are the amounts of 2, 4-DCP, adsorbed at equilibrium and at time t in mg/g, respectively, and k_1 is the pseudo-first order rate constant in g/mg h.

From the first order equation, the values of $\log(q_e - q_t)$ for 2, 4-DCP were calculated and plotted versus time as shown in Figure 8, while the calculated data of the pseudo-first order model are shown in Table 1. If the plotted line is linear with good correlation coefficient, Lagergren equation is appropriate; and it can be clearly seen that BC did not fare well. Though with respectable R^2, HBC does not fit well in this model either, because the q_e calculated is very different from q_e experimental.

The pseudo-second order kinetic model equation, based on equilibrium adsorption, is:

$$\frac{t}{q_t} = \frac{t}{q_e} + \frac{1}{k_2 q_e^2} \qquad (2)$$

Where q_e and q_t are as described in Equation 1; and k_2 is the rate constant of second-order adsorption in g/mg h.

Equation 2 was found to be easier to predict the kinetics behaviour of adsorption over the whole range; the linear plot of t/q_t versus t, shown in Figure 9 and in Table 1 as well, was used to find the slope $1/q_e$, and the intercept $\frac{1}{k_2 q_e^2}$. From Table 1, agreements between calculated values of q_e and experimental values was clear; 5.68 vs. 5.56 for BC, and 5.90 and 6.25 for HBC. Moreover, both correlation coefficients derived from the second-order kinetics model were higher for those obtained from the first-order model. Thus, the second-order kinetics model is proven better than the first-

order model to predict and describe the adsorption system of 2, 4-DCP onto both adsorbents.

Adsorption Isotherms:

Isotherms are very important and essential for the understanding of adsorption system mechanism, and two models, Langmuir and Freundlich, were applied in this study to investigate the performance of the BC and HBC adsorbents.

The Langmuir model is based on assumptions of adsorption homogeneity such as equal available adsorption sites, monolayer surface coverage, and no interaction between adsorbed species[17], and is described in Equation 3:

$$\frac{C_e}{q_e} = \frac{1}{b\,q_{max}} + \frac{C_e}{q_{max}} \qquad (3)$$

Where q_e and q_{max} are the observed and maximum uptake capacities in mg g^{-1}; C_e is the equilibrium concentration in mg L^{-1}; and b is the equilibrium constant in Lmg^{-1}.

The plots of $\frac{1}{q_e}$ versus $\frac{1}{C_e}$ are shown in Figure 10, and the calculated results in Table 2. It can be seen from the Table that the correlation coefficients were good for both adsorbents; with HBC a little better. And hence the Langmuir isotherm model is acceptable.

Freundlich isotherm model describes the logarithmic relation between the energy of sorption and the increase in bending sites. The model can be applied to non-ideal sorption on heterogeneous surfaces as multilayer sorption[17]. The Freundlich equation is:

$$Ln q_e = Ln K_f + \frac{1}{n} Ln C_e \qquad (4)$$

Where q_e is the equilibrium capacity of sorption in mg/g; C_e is the equilibrium concentration of the 2,4-DCP in mg/l; K_f is the sorption capacity coefficient; and n is a coefficient related to the sorption intensity.

The values of K_f and n were obtained from the intercept and the slope of the plots between $\ln(q_e)$ versus $\ln(C_e)$ in Figure 11 and shown in Table 2 together with other parameters from the Langmuir model.

The correlation coefficients R^2 for the Freundlich isotherm model were found to be higher than those found from the Langmuir model. Both models thus gave R^2 of at least 0.9461 and are both well-fitted for the experimental results. The Freundlich model, however, yielded a better fitting for describing the adsorption of 2, 4-DCP onto both adsorbents BC and HBC since the R^2 obtained were relatively higher and the computed coefficient n values were less than unity.

Comparison of the adsorption capacity of phenolic compounds onto BC and HBC to other types of adsorbents is shown in Table 3. From the 16 selected experimental results, HBC ranks the 11th highest on the list, and BC in the lower six. It can be safely stated that HBC is a very good adsorbent comparing to many others, while BC is

moderate in comparison. However, the fact that BC performs better than quite a few others it means BC is promising to be used, particularly when its low cost is taken into consideration.

CONCLUSION

Bamboo biochar plus Calcium sulphate (BC), and Hydroxyapatite plus BC were investigated for their capacity in the removal of 2, 4-dichlorophenol (2, 4-DCP) in aqueous solution. The time of fluidization, adsorption kinetics and isotherms, among others, were studied. The fluidization time was found to be best at 180 min. For the adsorption kinetics, the pseudo–second order model gave a better fit. Comparison of the adsorption efficiency between BC and HBC showed that the two adsorbents are of similar quality, albeit with a lower quality value for the BC. In the isotherms investigation it was found that all data fitted well into the Langmuir and Freundlich models, and that the Freundlich model gave a better fit than the Langmuir model. Both adsorbents were compared with others in performance, and are found to be well placed for the HBC, while the BC is acceptably good. HBC and BC adsorbents are thus suitable and acceptable for the removal of 2,4-DCP from aqueous solutions at parameters it depended like the pH, the initial concentration of 2,4-DCP, the flow rate of the solution and the time of fluidization. Taken its low cost into consideration, BC could be regarded as a new, moderately effective adsorbent that can be applied in the field of wastewater treatment and industries.

ACKNOWLEDGEMENTS

The authors are grateful to the Prince of Songkla University (PSU) for her financial assistance and support to this research. We would also like to thank the PSU Department of Chemical Engineering and the Discipline of Excellence (DoE) in Chemical Engineering for assistance in the carrying out of needed chemical analyses.

Tables:

Table 1: Adsorption kinetic model rate constants for 2, 4-DCP removal by different adsorbents

Adsorbent	q_{eExp} mg/g_{ad}	Pseudo-first order			Pseudo-second order		
		$q_{e(cal)}$ mg/g	k_1	R^2	$q_{e(cal)}$ mg/g	k_2	R^2
BC	5.56	4.140	0.0260	0.7810	5.68	0.0190	0.9925
HBC	6.25	1.317	0.0046	0.9421	5.90	0.0311	0.9916

Table 2 Isotherm parameters for sorption of 2, 4-DCP by different adsorbent

Adsorbent	Langmuir			Freundlich		
	q_{max}	b	R^2	K_f	n	R^2
BC	10.69	0.0350	0.9461	0.302	0.79	0.9650
HBC	16.37	0.0315	0.9699	0.410	0.80	0.9827

Table 3 Comparison of phenolic compounds adsorption capacities of different adsorbents

Phenolic compounds	Adsorbents	Capacity (mg/g)	Reference
Phenol	Activated carbon	49.72	21
P-Chlorophenol	Rice husk char	36.23	20
Phenol	Multi walled carbon nanotubes	32.23	9
2,4 DCP	Palm pith carbon	19.16	18
Phenol	Palm seed coat activated carbon	18.30	19
2,4-DCP	HBC (Hydroxyapatite plus BC)	16.37	This study
p-chlorophenol	Rice husk char	14.36	20
3-Chlorophenol	Rice straw-based carbon	14.20	24
Phenol	Fly ash	13.16	8
2,4-DCP	Mycelial pellets of *P chrysosporium*	11.62	14
2,4-DCP	BC (Bamboo biochar plus Calsium sulphate)	10.69	This study
Phenol	Hydroxyapatite nano powders	10.33	12
Chlorophenol	Biofilm of A. viscous supported on granular activated carbon	9.70	23
P-Chlorophenol	Petroleum coke	9.34	20
4-Chlorophenol	Anaerobic granular sludge	6.32	2
Phenol	Activated coal	1.48	22

Figures:

Figure 1 Characteristics of BB from FTIR Analysis

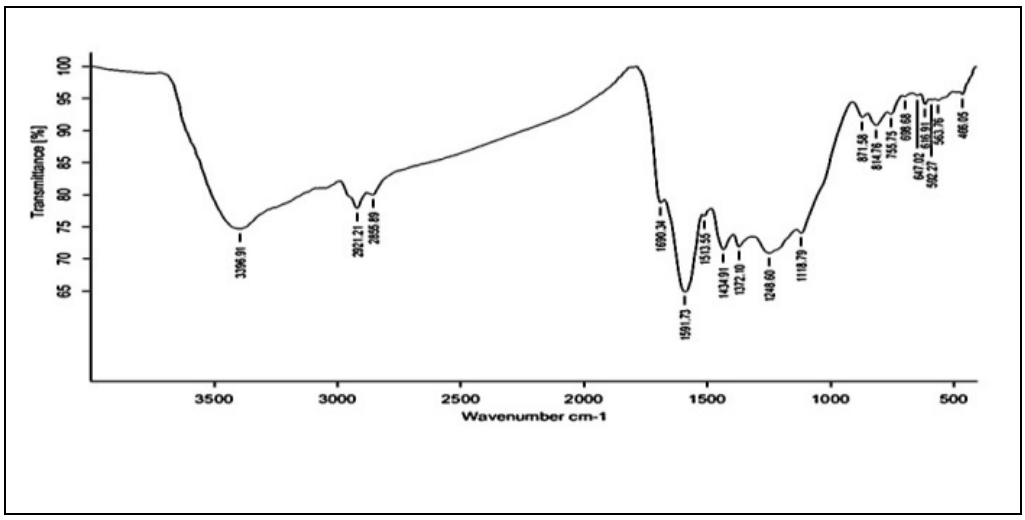

Figure 2 Characteristics of BB from DTA Analysis

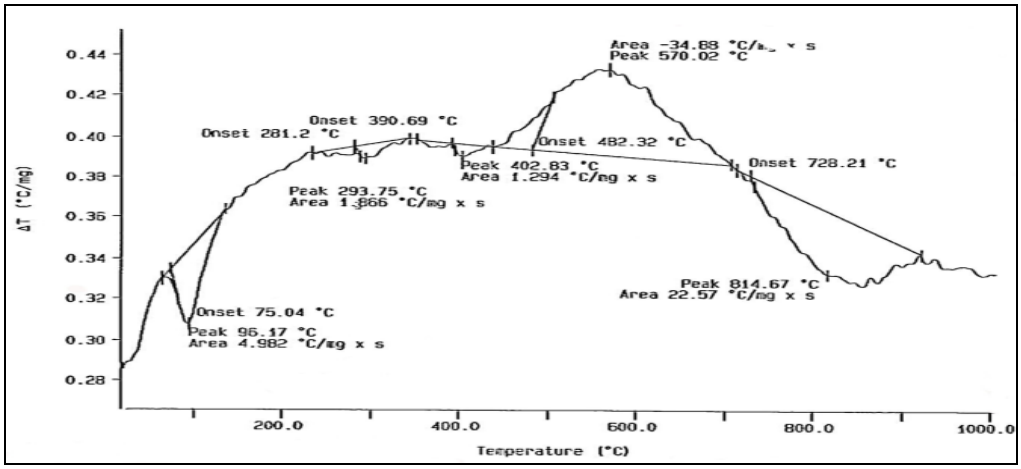

Figure 3 SEM of the Bamboo biochar

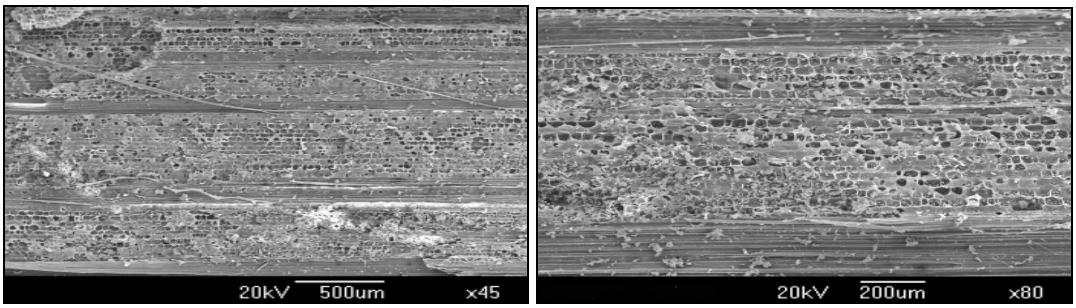

(a) (b)

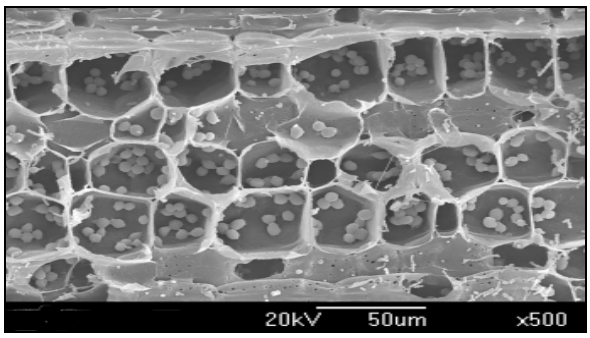

(c)

Figure 4 Initial pH solution of 2, 4-DCP adsorption vs. Percentage of removal

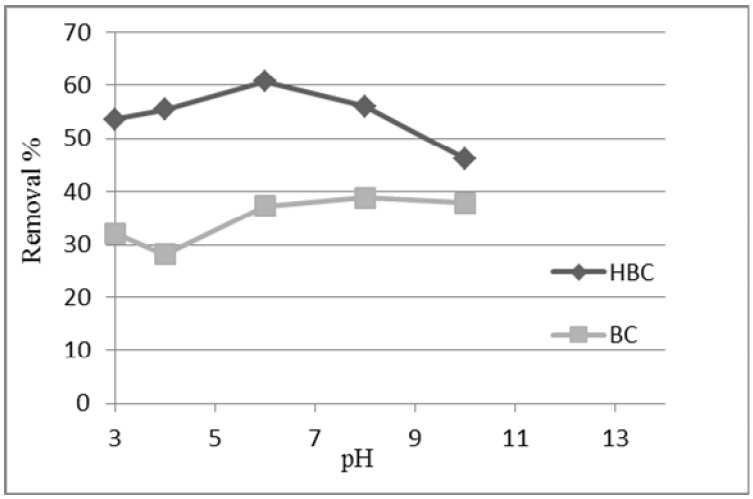

Figure 5 Contact time of circulation fluidization vs. Percentage of removal

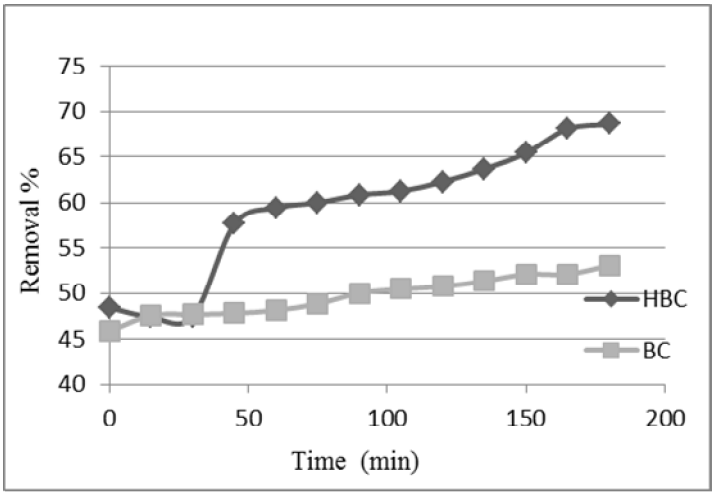

Figure 6 Flow rate of 2, 4-DCP solution vs. Percentage removal

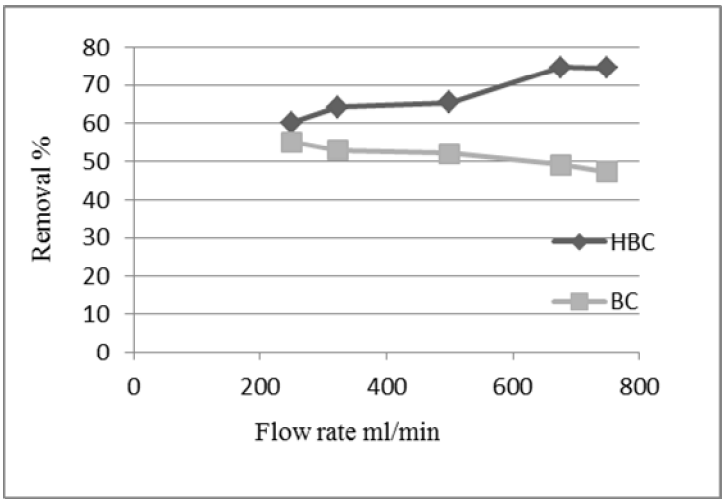

Figure 7 Initial concentration of 2, 4-DCP solutions vs. Percentage of removal

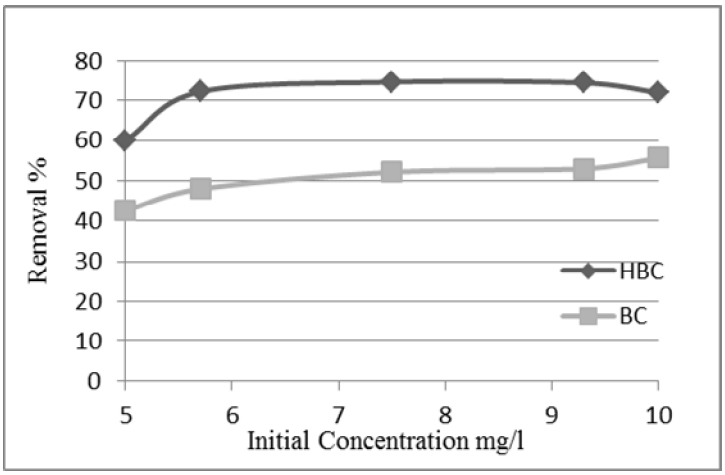

Figure 8 Results from pseudo-first order kinetic model for the removal of 2, 4-DCP

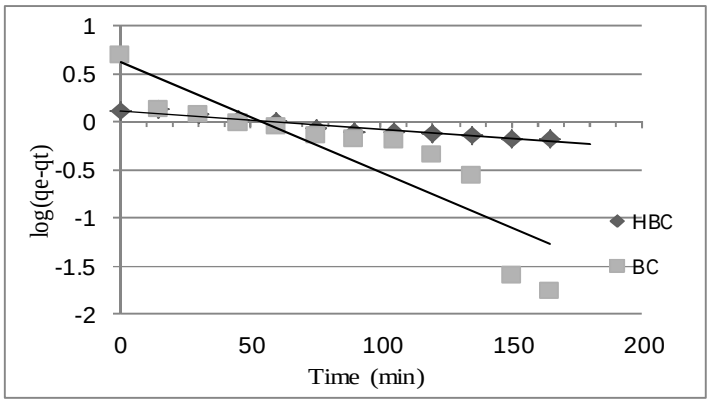

Figure 9 Results from pseudo-second order kinetic model for the removal of 2, 4-DCP

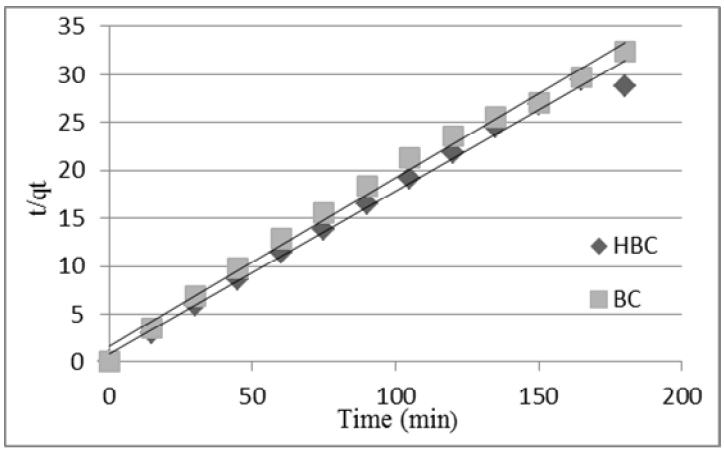

Figure 10 Langmuir isotherms (1/qe) vs. 1/Ce for the adsorption of 2, 4-DCP

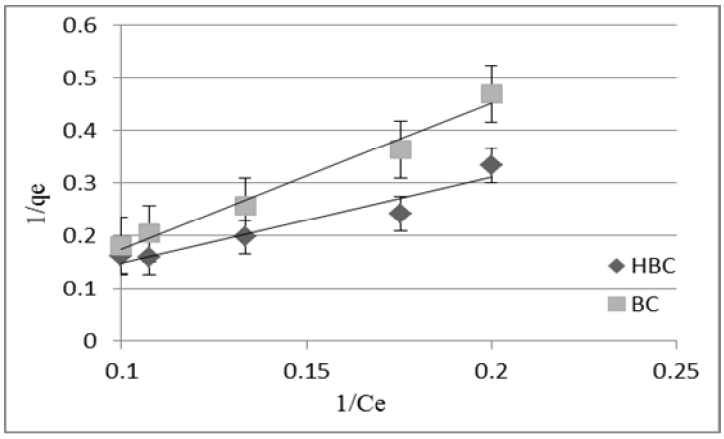

Figure 11 Freundlich isotherm ln(qe) vs. 1n(Ce) for the adsorption of 2, 4-DCP

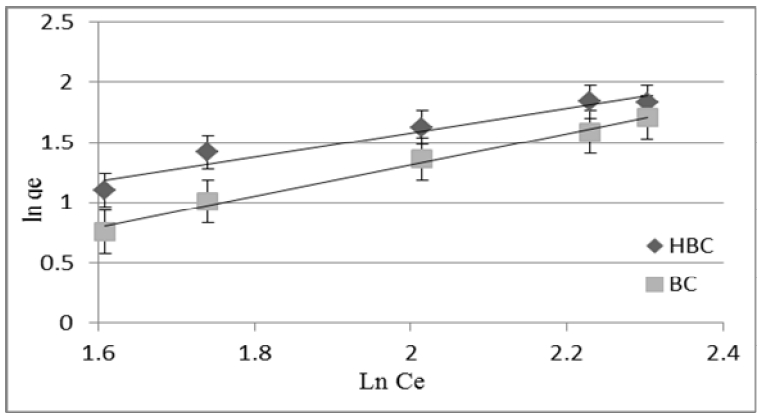

REFERENCES

1. Tan. I. A. W, Ahmad. A. L, Hameed. B. H. (2009). Adsorption isotherms, kinetics, thermodynamics and desorption studies of 2, 4, 6-trichlorophenol on oil palm empty fruit bunch-based activated carbon. *J. Hazard. Mater*. 164(2-3), 473-482. DOI: 10.1016/j.jhazmat.2008.08.025.

2. Gao. R, Wang. J. (2007). Effects of pH and temperature on isotherm parameters of chlorophenols biosorption to anaerobic granular sludge. *J. Hazard. Mater.* 145(3), 398-403. DOI: 10.1016/j.jhazmat.2006.11.036.

3. Hameed. B. H, Chin. L. H, Rengaraj. S. (2008). Adsorption of 4-chlorophenol onto activated carbon prepared from rattan sawdust. *Desalination*. 225(1-3), 185-198, DOI: 10.1016/j.desal.2007.04.095.

4. Aksu. Z, Akpınar. D. (2000). Modelling of simultaneous biosorption of phenol and nickel(II) onto dried aerobic activated sludge. *Sep. Purif. Technol*. 21(1-2), 87-99. DOI: 10.1016/S1383-5866(00)00194-5.

5. Xuequan. Z, Xiankai. W, Huixiang. S, Dahui. W. (2009). Adsorption of 2,4-dichlorophenol from aqueous solution onto microwave modified activated carbon: Kinetics and equilibrium. *Transactions of Tianjin University*. 15(6), 408-414. DOI: 10.1007/s12209-009-0071-9.

6. Hamdaoui. O, Naffrechoux. E, Suptil. J, Fachinger. C. (2005). Ultrasonic desorption of p-chlorophenol from granular activated carbon. *Chem. Eng. J*. 106(2), 153-161. DOI: 10.1016/j.cej.2004.10.010.

7. Yan. M, Naiyun. G, Wenhai. C, Cong. L. (2013). Removal of phenol by powdered activated carbon adsorption. *Frontiers of Environmental Science & Engineering*. 7(2), 158-165. DOI: 10.1007/s11783-012-0479-7.

8. Sarkar. M, Acharya. P. K. (2006). Use of fly ash for the removal of phenol and its analogues from contaminated water. *J. Waste Manage.* 26(6), 559-570. DOI: 10.1016/j.wasman.2005.12.016.

9. Abdel-Ghani. N. T, El-Chaghaby. G. A, Farag S. Helal. F. S. (June 2014). Individual and competitive adsorption of phenol and nickel onto multiwalled carbon nanotubes. *Journal of Advanced Research*. Retrieved June 6, 2014, from ScienceDirect database on the World Wide Web, www.sciencedirect.com. DOI: 10.1016/ S2090123214000757.

10. Wang. J. P, Feng. H. M, Yu. H. Q. (2007). Analysis of adsorption characteristics of 2,4-dichlorophenol from aqueous solutions by activated carbon fiber. *J. Hazard. Mater*. 144(1-2), 200-207. DOI: 10.1016/j.jhazmat.2006.10.003.

11. Mohd Din. A. T, Hameed. B. H, Ahmad. A. L. (2009). Batch adsorption of phenol onto physiochemical-activated coconut shell. *J. Hazard. Mater.* 161(2-3), 1522-1529. DOI: 10.1016/j.jhazmat.2008.05.009.

12. Lin. K, Pan. J, Chen. Y, Cheng. R, Xu. X. (2009). Study the adsorption of phenol from aqueous solution on hydroxyapatite nanopowders. *J. Hazard. Mater*. 161(1), 231-240. DOI: 10.1016/j.jhazmat.2008.03.076.

13. Mowla. D, Ahmadi. M. (2007). Theoretical and experimental investigation of biodegradation of hydrocarbon polluted water in a three phase fluidized-bed bioreactor with PVC biofilm support. *Biochem. Eng. J.* 36(2), 147-156. DOI: 10.1016/j.bej.2007.02.031.

14. Wu. J, Yu. H. Q. (2006). Biosorption of 2, 4-dichlorophenol from aqueous solution by *Phanerochaete chrysosporium* biomass: Isotherms, kinetics and thermodynamics. *J. Hazard. Mater*. 137(1), 498-508. DOI: 10.1016/j.jhazmat.2006.02.026.

15. Mall. I. D, Srivastava. V. C, Agarwal. N. K. (2006). Removal of Orange-G and Methyl Violet dyes by adsorption onto bagasse fly ash-kinetic study and equilibrium

isotherm analyses. *Dyes and Pigment*. 69(3), 210-223. DOI: 10.1016/j.dyepig.2005.03.013.

16. Hanen. N and Abdelmottaleb.O. (2013). Modeling of the Dynamics Adsorption of Phenol from an Aqueous Solution on Activated Carbon Produced from Olive Stones. *International Journal of Chemical Engineering and Applications.* 4(4), 254-261. DOI:10.7763/IJCEA.2013.V4.306.

17. Zhang. Z. B, Cao. X. H, Liang. P, Liu. Y. H. (2013). Adsorption of uranium from aqueous solution using biochar produced by hydrothermal carbonization. *J. Radioanalytical and Nuclear Chemistry*. 295(2), 1201-1208. DOI: 10.1007/s10967-012-2017-2.

18. Sathishkumar. M, Binupriya. A. R, Kavitha. D, Yun. S. E. (2007). Kinetic and isothermal studies on liquid-phase adsorption of 2,4-dichlorophenol by palm pith carbon. *Bioresource Technology*. 98(4), 866-873. DOI: 10.1016/j.biortech.2006.03.002.

19. Rengaraj. S, Moon. S. H, Sivabalan. R, Arabindoo. B, Murugesan. V. (2002). Agricultural solid waste for the removal of organics: adsorption of phenol from water and wastewater by palm seed coat activated carbon. *Waste Management*. 22(5), 543-548. DOI: 10.1016/S0956-053X(01)00016-2.

20. Ahmaruzzaman. M, Sharma. D. K. (2005). Adsorption of phenols from wastewater, *J. Colloid. Interf. Sci*. 287(1), 14-24. DOI: 10.1016/j.jcis.2005.01.075.

21. Özkaya. B. (2006). Adsorption and desorption of phenol on activated carbon and a comparison of isotherm models. *J. Hazard. Mater*. 129(1-3), 158-163. DOI:10.1016/j.jhazmat.2005.08.025.

22. Vázquez. I, Iglesias. J. R, Marañón. E, Castrillón. L, Álvarez. M. (2007). Removal of residual phenols from coke wastewater by adsorption. *J. Hazard. Mater*. 147(1-2), 395-400. DOI: 10.1016/j.jhazmat.2007.01.019.

23. Quintelas. C, Sousa. E, Silva. F, Neto. S, Tavares. T. (2006). Competitive biosorption of ortho-cresol, phenol, chlorophenol and chromium (VI) from aqueous solution by a bacterial biofilm supported on granular activated carbon. *Process Biochemistry*. 41(9), 2087-2091. DOI: 10.1016/j.procbio.2006.04.014.

24. Wang. S. L, Tzou. Y. M, Lu. Y. H, Sheng. G. (2007). Removal of 3-chlorophenol from water using rice-straw-based carbon. *J. Hazard Mater*. 147(1–2), 313-318. DOI: 10.1016/j.jhazmat.2007.01.031.

Appendix B2

Journal Paper

A. H. Alamin, L. Kaewsichan, ‘‘Sorption of Pb(II) onto 2 mixtures: Bamboo biochar plus Calcium sulphate (BC) and Hydroxyapatite plus Bamboo biochar plus Calcium sulphate (HBC), in fluidized bed circulation column’’, **This manuscript have been submitted to International Journal of Chemical Engineering.**

Sorption of Pb(II) onto 2 Mixtures: Bamboo Biochar Plus Calcium Sulphate (BC) and Hydroxyapatite Plus Bamboo Biochar Plus Calcium Sulphate (HBC), in Fluidized Circulation Column

Ahmed H. Alamin[*1], Lupong. Kaewsichan[2]

[1,2] *Department of Chemical Engineering, Faculty of Engineering, Prince of Songkla University, Hat Yai, Songkhla, 90112, Thailand.*

[*1] Email: ahmed.10000@yahoo.com

ABSTRACT: Sorption characteristics were carried out to investigate removal of Pb(II), from aqueous solution in a circulation fluidized column by two types of adsorbent mixtures: BC (Bamboo biochar plus Calcium Sulphate), and HBC (Hydroxyapatite plus Bamboo biochar plus Calcium Sulphate); both made in ball shape. The main material Bamboo biochar (BB) was characterized by FTIR, and SEM. The adsorption experiments were carried out in a fluidized circulation column. Adsorption, isotherms and kinetic studies were established under 180-min operating process time, at different initial Pb(II) solution concentrations ranging from 30-70 mg/l, and at different flow rates ranging from 250-750 ml/min. The kinetics of both adsorbents complies with the pseudo-second order model. The data obtained from experiment fitted well for both the Langmuir and Freundlich isotherm models. BC was proven a new effective composite and low cost adsorbent which can be applied in the field of wastewater treatment, and it could also play an important role in industrial water treatment.

KEYWORDS: Pb(II), Bamboo biochar, Hydroxyapatite, Calcium Sulphate, Adsorption

1. Introduction

Heavy metal pollution has been under microscope the world over, and is catching increasing international awareness since industries are on the growth and oftentimes wastes are discharged to the environment without any precautions. These discharges are mainly introduced into the environment as point sources such as from mining, metal plating, battery, and paper industries. Heavy metal pollution caused by Lead, copper, chromium, cadmium, nickel and arsenic is much serious to the human body [1]. Ion of these metals are toxic to living organisms in water, but also cause harmful

effects to land animals including humans through food chain transfers, and heavy metal ions particularly bind to nucleic acids, proteins, and small metabolites in living organisms [2]. Pollution of Pb(II) has also been of great concerns through their adverse effects on human and aquatic life [3].

The removal of heavy metal ions is an important problem in the field of water purification [1]. Many methods have been developed to discuss these stringent environmental regulations that necessitate removal of this ion compound from wastewater [4]. Among these different techniques, adsorption is highly effective because of the ease of operation and its low cost [5]. Display quotations of over 40 words, or as needed.

Nanomaterials have gradually developed important roles to resolve this problem because of their high surface area, enhanced active sites, and abundant functional groups on the surfaces [6], and have been used as adsorbents. Adsorbents in form of biochar produced from agricultural wastes or by-products were thought to be inexpensive materials for the removal of Pb(II) [7]. Biochar converted from agricultural residue wastes has a large adsorption capacity for lead removal from wastewater [8]. Bamboo is one outstanding renewable biomass resource due to its fast growing speed and short growth cycle [9, 10]; an inexpensive and environmentally friendly adsorbent. Bamboo char has been commercially used in water purification, dehumidification, odour adsorbents and health products, at low prices as $400–600 per ton in 2012 China [10]. Hydroxyapatite (HAP) nano powders have high biocompatibility and adsorption properties, and have been widely used as carriers for drugs, adsorbents for chromatography to separate proteins, and removal of heavy metal ions to recover the contaminated soils, wastewater and fly ashes, etc.[11, 12].

Preliminary investigations by the authors revealed generally higher heavy metals adsorbing efficiencies when either the low-cost bamboo biochar (BB) or the relatively expensive Hydroxyapatite (HAP) was used as mixtures together with Calcium Sulphate (CS). Furthermore, HAP&CS composites have been described for use as resorbable biomaterials in bone surgery [13], but have never been used for adsorbing heavy metals from polluted water [14].

In this study, we combined BB obtained from pyrolysis process of Bamboo wood with CS to produce a good adsorbent (BC) for Pb(II), removal from aqueous solution and compared it with HBC; a mixture containing HAP, BB and CS.

Circulation fluidized-bed reactor has received considerable attention for its wide-range utilization in field such as wastewater treatment due to at least four features. First, this type of reactor maintains excellent contacts between solid and liquid phases yielding high mass transfer, high reaction rate, and low external mass transfer resistance between the two phases. Second, it eliminates many operating problems such as bed clogging and high pressure drop, which often occur in packed-bed operations. Third, it renders a highly efficient, simple, stable and economical operation

compared to other types of reactor. Fourth, it is possible for partial replenishment of the fluidized-bed without interrupting the operation [15]. For all these reasons circulation fluidized-bed reactor was selected as an instrument system in this study.

The main aim of this research was to investigate adsorption of Pb(II), in aqueous solution onto two types of ball-shape adsorbents: BC and HBC, in a fluidized circulation column. Two Sorption isotherm models, Langmuir and Freundlich were investigated. Moreover, pseudo-first and pseudo-second order sorption kinetics were simulated for comparisons.

2. Materials and Method

2.1. Preparation of Adsorbent. Bamboo biochar (BB) is used in this study as the main material. Calcium Sulphate (CS) was purchased from Aldrich Chemicals. Hydroxyapatite (HAP), purchased from Sigma-Aldrich Co. LLC, is of a commercial type. Purchased from Boss official limited partnership in Thailand were the $Pb(No_3)_2$ standard samples. All solutions were prepared from analytical reagents (AR) and distilled water. Bamboo biochar was prepared in the laboratory by pyrolysis process at 500° C, ground, sieved and mixed with CS at a ratio of 0.62:0.38 to form adsorbent composite BC, and with HAP and CS at a ratio of 0.46:0.27:0.27 to form adsorbent composite HBC. A glue, made from polyvinyl alcohol (PVA) having molecular weight (MW) of 22,000, was added to the mixtures to make ball-shape adsorbents. The concentration of residual Pb(II), was analysed using a Perkin Elmer thermos scientific S-series model (AAnalyst100), flame atomic absorption spectrometer (AAS). Fourier transform infrared spectroscopy (FTIR) (Bomem, MB 100) was conducted to identify the functional groups of the biochar. Scanning electron microscopy (SEM) was conducted with a Hitachi JSM-6700F SEM to observe surface microstructures of the fresh biochar and the adsorbent balls after the adsorption process.

2.2. Properties and Preparation the Adsorbate. The 1,000-ppm solution of $Pb(NO_3)_2$ was prepared by diluting a stock standard solution of $Pb(NO_3)_2$ to the desired concentration. A stock solution was obtained by dissolving 1.59 g of Lead nitrate in 1 litre distilled water. The range of concentration of the Pb(II) prepared from the standard solution varied between 30-70 mg/l. The pH of the solutions was adjusted to 6.5 by 0.1 N NaOH and 0.1 N HCl solutions.

2.3. Experimental Methodology. Study of Pb(II) adsorption was carried out at laboratory scale; fluidized reactor was used as the adsorption system to improve mixing and homogeneity. The experiment setup consisted of a fluidized column, a water reservoir, a peristaltic pump, as shown in Figure 1. The 5 cm-outside-diameter and 24 cm-height reactor with an effective volume of 470 ml was made from

transparent acrylic. A mesh screen was fit at the top of the fluidized circulation column in order to capture the solid coming out of the column. One conical distributor was placed at the bottom to ensure proper distribution of the fluid. Aqueous solution of Pb(II) was continuously fed upward to the reactor at different flow rates, starting from 250 to 750 ml/min. The liquid effluent stream was recycled to the hold-up tank. Three liters of the Lead aqueous solution was treated with adsorbents of 3 g for either adsorbent. Adsorption of Pb(II) onto adsorbents BC and adsorbent HBC were compared. The suspensions in all studies were filtered through 0.45µm syringe membrane filters. All experiments were conducted in triplicates for statistical analysis.

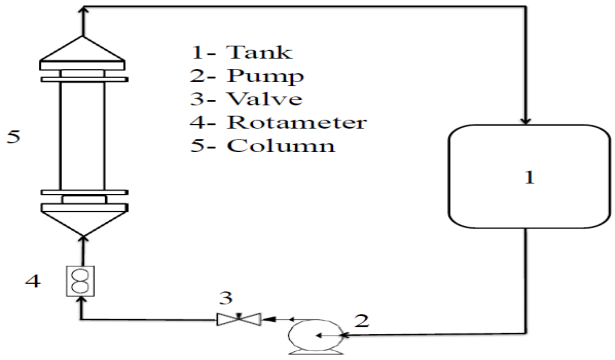

FIGURE 1: Process Diagram

3. Results and Discussions

3.1. Fourier Transforms Infrared Analysis (FTIR). Fourier Transform Infrared (FTIR) spectra were investigated in range of 500 to 4000 cm^{-1} wave number in the transmission mode. Different functional groups of this investigation are shown in Figure 2, inclusive of the wavenumber measured. The broad band at 3396 cm^{-1} was assigned to the hydroxyl functional groups; this peak could be assigned to O–H stretching. The bands at 2921 cm^{-1} and 2855 cm^{-1}, apparently the aliphatic methyl and methylene bands, indicate that the sample was highly aromatized. An unsymmetrical peak at 1690 cm^{-1} presents due to C=O stretching. This peak comprised a variety of C=O diminished with rising temperature; it contains functional groups including that of carboxylic acids esters, ketones and quinones. The bands at 1434, and 1590 cm^{-1} indicate alkyl C=C stretching and the presence of an aromatic C−H bond derived from original aromatic rings in the lignin of biochar. The band at1361cm^{-1} is due to the stretching vibrations of CO_2^{-3}. The M–O and O–M–O (M=Mg or Al) vibration bands appear in the 400 to 800 cm^{-1} region.

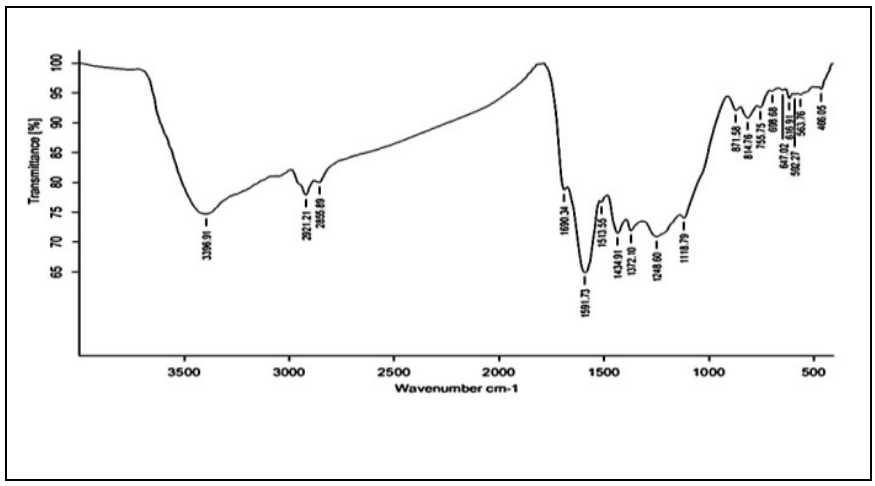

FIGURE 2: Characteristics of Bamboo biochar from Fourier Transform Infrared Analysis

3.2. Scanning Electron Microscope Image (SEM). SEM characteristic results on the fresh BB, and on the ball-shape adsorbents after adsorption, revealed its morphology and elemental compositions. Figure 3(a), at x80 magnification, depicts the internal surface and porous structures of the BB. Figure 3(b), at x500 magnification, reveals an average porous diameter of 38µm. Figure 3(c) and 3(d) for the BC, and Figure 3(e) and 3(f) for the HBC, show the pores on, respectively, the surface and the cross section of the ball-shape adsorbents. Elemental compositions of the ball-shape adsorbents after adsorption are shown in Figure 3(g) and 3(h) for the BC, and in Figure 3(i) and 3(j) for the HBC, again for the surface and cross section respectively. These four graphs show clearly the Pb ions available on the surface and on the cross section (the inside) of the balls.

Solutions at a mass ratio of 1:20 (BB:DI water) were hand stirred and allowed to stand for 5 min before measurements were taken for their pH [4]. The pH was found to be 8.00, a little to the alkaline side.

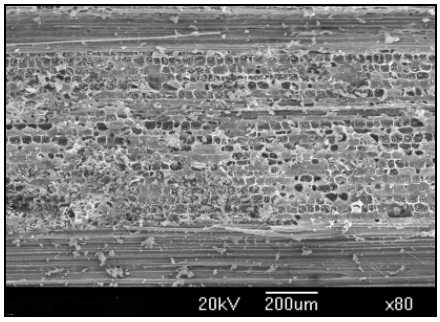

(a)

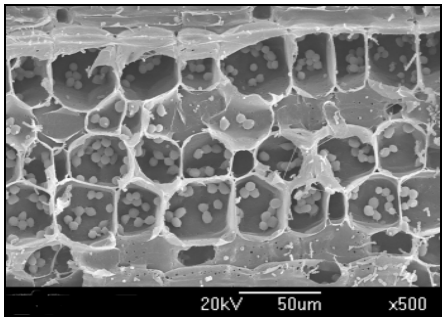

(b)

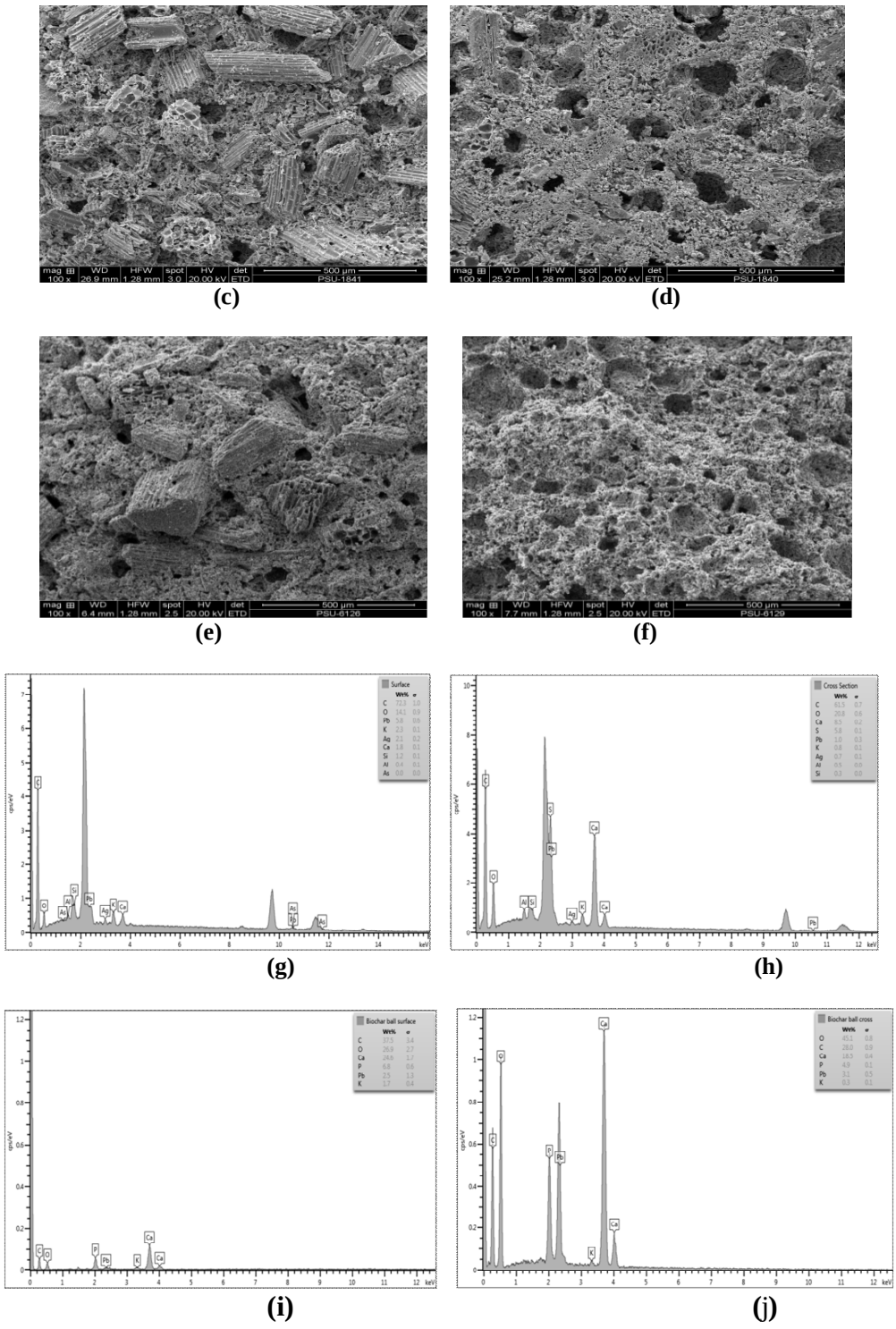

FIGURE 3: SEM of the Bamboo biochar [(a) and (b)], and of the ball-shape adsorbent after adsorption [(c) through (j)]

3.3. Effect of Initial pH Solution of Pb(II) Adsorption. A factor indicating removal efficiency of contaminants from aqueous solution is the pH. For the adsorption of Pb(II) aqueous solution onto BC and HBC adsorbents, this effects were studied from

adjustment of initial pH between 3 to 10 at room temperature while the initial concentration of Pb(II) solution of 70 mg/l was constantly maintained.

Different behaviour trends were observed for the two adsorbents as shown in Figure 4. At low pH, BC is positively charged due to surface group protonation [16], that it is from biochar. Electrostatic attraction between positively charged adsorbent surfaces and positively charged metal ion surfaces is not possible; thus some non-electrostatic forces are involved in adsorption, and while in acidic solution, the surface being positively charged, the adsorption of Pb(II) and $Pb(OH)^+$ species are not favoured [17]. For the BC adsorbent, the maximum Pb(II) removal percentage of 94 occurred at pH 10, and its rate decreased dramatically to be 15% at the weak acidic pH of 6.

This efficiency, however, increased back again to just above 80% at pH 3. Hence, for the BC, the solution needs to be either very basic or acidic, and not at anywhere near neutrality.

At pH below 4, uptakes of lead increase with the increase of H_3O^+ ions in the solution [18]. For the HBC adsorbent in the experiment the lead removal percentage increased from just above 60% at pH 3 to over 90% at pH 4. At low pH values, the surface of the adsorbent is closely associated with hydronium ions (H_3O^+) and holds mainly protonated sites, as a result the surface maintains a net positive charge [19, 2]. In the case of high pH values (pH = 6-10), however, there are several lead species with different charges like $Pb(OH)^+_2$ and $Pb(OH)_2$ and thus the removal of lead is possibly accomplished by simultaneous precipitation of $Pb(OH)_2$ and sorption of $Pb(OH)_2$ [20, 21]. In our HBC investigation, a maximum lead removal percentage of nearly 95% occurred at pH 10, and was rather stable between pH 8-10, though with a sharp drop at pH 6.

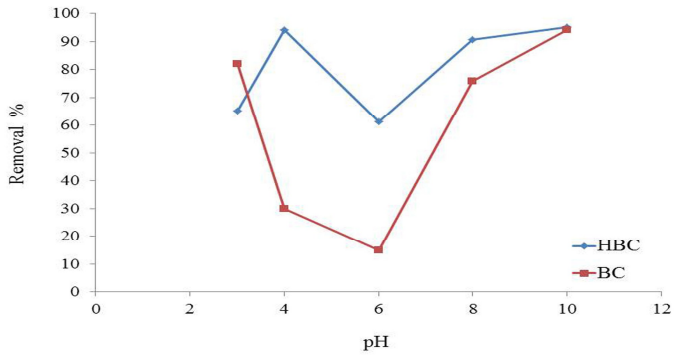

FIGURE 4: Initial pH of Pb(II) vs. Percentage of removal

3.4. Effect of Contact Time of Fluidization. Percentage removal of Pb(II) by adsorption onto adsorbents BC and HBC was investigated on the effect of contact time of fluidization at different time intervals from 0 to 180 minutes. Experiments were conducted at room temperature while others variables were kept constant (solute pH of 6.5, 3g of adsorbents, 250 ml/min flow rate, 50 mg/l of the Pb(II) initial concentration). Available adsorption studies reported reveal that the uptake of adsorbate species is fast at the initial stage of the contact period, and thereafter it becomes slower near the equilibrium [22]. Figure 5 describes the effect of contact time on the lead percentage removal, and the time of equilibrium for both adsorbents was apparently 180 minutes. Adsorption of Pb(II) employing either BC or HBC increased slowly to equilibrium, however, especially for the BC. The removal rates were approx. 57% for the BC, and 69% for the HBC at equilibrium.

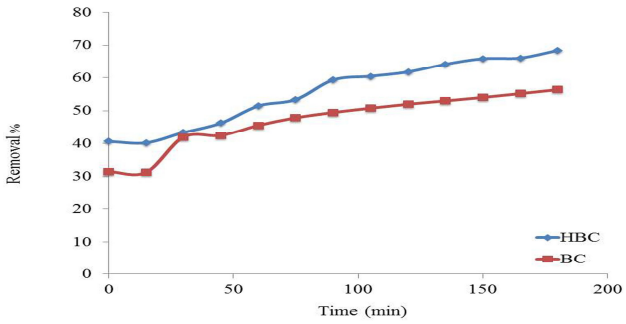

FIGURE 5: Contact time of circulation fluidization vs. Percentage of removal

3.5. Effect of Flow Rate of Pb(II) Solution. The effect of various flow rates was studied for adsorption of Pb(II) from aqueous solution using BC and HBC adsorbents. Experiments were carried out at flow rate in range of 250-750 ml/min at room temperature while other parameters were kept constant (3g of adsorbents, solute pH of 6.5, 50 mg/l of the Pb(II) initial concentration). Figure 6 depicts the effect of flow rate on the percentage removal; that, for either adsorbent, an increase in the former decreases the latter. In case of a lower flow rate, the residence time was increased in the column, and the opposite occurred at a higher flow rate. In a column operation, the volume element of the solution is in contact with a given layer of the bed for a limited period of time, usually insufficient for attainment of equilibrium [23]. In case of an increase in the flow rate the resistance of the film in the external transfer which causes an improvement in the kinetics of adsorption reduces [24]. Generally at a lower flow rate, the liquid hold-up of the bed is lower, and the liquid mal-distribution has serious effects upon the effectiveness of the process [23]. From the experiments, the highest percentages of removal were approx. 57% for BC, and 69% for HBC, at 250 ml/min flow rate.

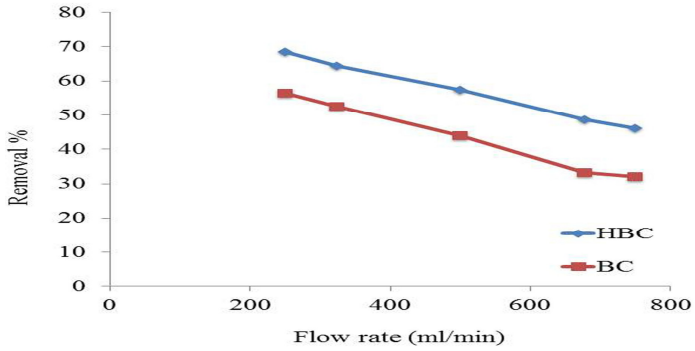

FIGURE 6: Flow rate of Pb(II) solution vs. Percentage removal

3.6. Effect of Initial Concentration of Pb(II) Solution. The effect of initial concentration is important. Experiments were executed at room temperature to investigate this effect at range of 30-70 mg/l of Pb(II) solution, whilst other variables were fixed constant (adsorbent weight of 3g, pH of 6.5, and flow rate of 500 ml/min). Figure 7 shows the effect of initial concentration on the removal percentage of Pb(II). From the Figure, the removal percentage of Pb(II) decreases with an increase in initial concentration of the solution for both adsorbents. The capacities of sorption for BC and HBC behave similarly. For this effect, an increase in initial concentration was followed by an increase in loading rate of Pb(II). Though the pore size and shape of BC and HBC adsorbents differ, these are constants, meaning that at low initial concentration, diffusion is greater. These results demonstrate that, a change in the concentration gradient affects the saturation rate and the equilibrium time, or in other words, the diffusion process is concentration dependent [25]. At low initial concentrations, for both adsorbents, there were more available pores for adsorption, and these were saturated at high initial concentrations.

From the experiment, the highest percentages of removal were 53% for BC, and 77% for HBC, at 30 mg/l initial concentration. Adsorbent HBC performed better than BC because it has more macro porous-structures and high specific surface area. However, the performance of adsorbent BC achieved approx. 70% of that using HBC.

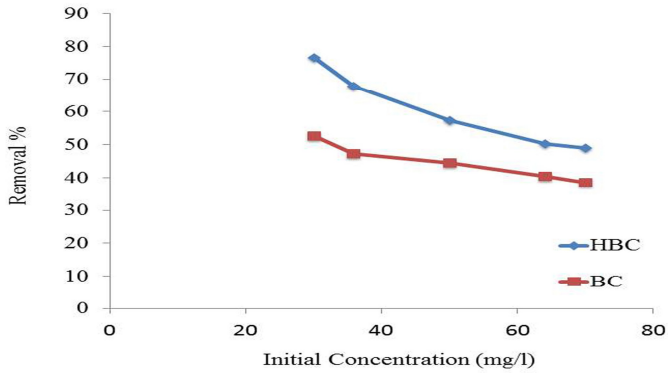

FIGURE 7: Initial concentration of Pb(II) solutions vs. Percentage of removal

3.7. Adsorption Kinetics. The adsorption mechanism was expounded by the kinetic sorption characteristics. Kinetic models, pseudo-first order and pseudo-second order, were used to investigate the Pb(II), adsorption kinetics by adsorbents BC and HBC.

The first order equation (Lagergren equation) was written as:

$$\log(q_e - q_t) = \log(q_e) - \frac{k_1}{2.303} \quad 1 \qquad (1)$$

Where q_e and q_t are the amounts in mg/g of Pb(II) adsorbed at equilibrium and at time t, respectively, and k_1 is the pseudo-first order rate constant in g/mg min.

From the first order equation, the values of k_1 and q_e were calculated from the slope and the intercept of the plot of $\log(q_e - q_t)$ versus time t, shown in Figure 8, while the calculated data of the pseudo-first order model are shown in Table 1. If a linear line from the plot yields a good correlation coefficient, it means the first order equation is appropriate, and both adsorbents did fairly well with values more than 0.9. However, it can be clearly seen this model is not quite suitable because the value of q_e calculated (7.98 for BC, and 20.77 for HBC) differed much from q_e experimental (40.29 for BC, and 41.20 for HBC.)

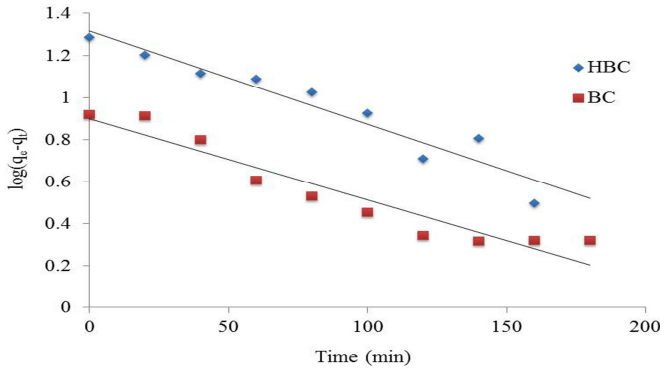

FIGURE 8: Results from Pseudo-first order kinetic model for the removal of Pb(II)

TABLE 1: Adsorption kinetic model rate constants for Pb(II) removal by different adsorbents

Adsorbent	q_{eExp} mg/g_{ad}	Pseudo-first order			Pseudo-second order		
		$q_{e(cal)}$ mg/g	k_1	R^2	$q_{e(cal)}$ mg/g	k_2	R^2
BC	40.29	7.98	0.009	0.9116	40.98	0.0075	0.9994
HBC	41.20	20.77	0.01	0.9209	40.98	0.0015	0.9719

The pseudo-second order kinetic model equation, based on adsorption equilibrium, can be described in equation (2):

$$\frac{t}{q_t} = \frac{t}{q_e} + \frac{1}{k_2 q_e^2} \quad (2)$$

Where q_t is the amount of metal ions adsorbed in mg/g at any given time t in min; q_e the amount of metal ion adsorbed in mg/g at equilibrium; and k_2 the second order reaction rate constant for adsorption in g/mg min.

For Pb(II) ion adsorption onto BC and HBC, the pseudo-second order kinetic model constant, k_2 and $q_{e\ cal}$, values were determined from the slope $1/q_e$ and the intercept $\frac{1}{k_2 q_e^2}$ of the linear plot of t/q_t versus t, shown in Figure 9, and in Table 1 as well. From

Table 1, the correlation coefficients derived from the second order kinetics model for BC and HBC adsorbent were higher than those gained from the first order model. Furthermore, correspondence between the experimental values of q_e and the calculated values was clearly close; 40.29 vs. 40.98 for BC, and 41.20 vs. 40.98 for HBC. Thus, it could be stated that the adsorption of Pb(II) aqueous solution onto BC and HBC were able to be better predicted and described by the pseudo-second order kinetic model than the pseudo-first order kinetic model.

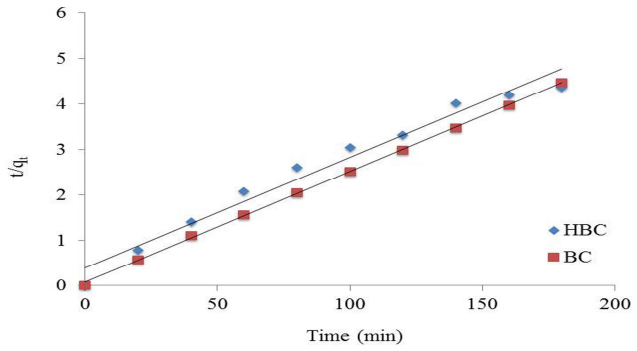

FIGURE 9: Results from Pseudo-second order kinetic model for the removal of Pb(II)

3.8. Adsorption Isotherms. Isotherms data are considered in accurate formula of adsorption equlibrium used for design purposes. Two selected isotherm models, Langmuir and Freundlich, were applied here in the investigation of the BC and HBC adsorbents.

Langmuir model assumes monolayer adsorption on the surface of adsorbent, and no interaction between the adsorbed species. The linear equation form of the model is discribed in equation (3):

$$\frac{C_e}{q_e} = \frac{C_e}{q_{max}} + \frac{1}{K_L q_{max}} \qquad (3)$$

Where q_e and q_{max} are respectively the equilibrium and maximum monolayer adsorption capacity of the adsorbent in mg/g, C_e the equilibrium concentration in mg/L of Pb(II) in the solution, and K_L is the Langmuir isotherm constant in L/mg.

The liner plot of $1/q_e$ versus $1/C_e$ is shown in Figure 10, and the calculated results in Table 2. In the Table the values of q_{max} and K_L are evaluated from the slope and the intercept of the liner plot. The correlation coefficients obtained were good for both the BC and HBC adsorbents, hence the Langmuir isotherm model is convenient.

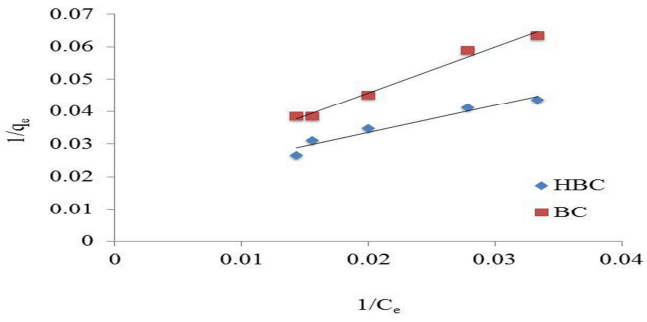

FIGURE 10: Langmuir isotherms (1/qe) vs. 1/Ce for the adsorption of Pb(II)

TABLE 2: Isotherm parameters for sorption of Pb(II) by different adsorbent

Adsorbent	Langmuir			Freundlich		
	q_{max}	K_L	R^2	K_F	n	R^2
BC	57.47	0.012	0.9857	1.77	1.56	0.9853
HBC	59.52	0.020	0.9466	3.49	1.83	0.9517

Freundlich isotherm model assumes heterogeneous surfaces and multilayer on adsorbents, and describes the logarithmic relation between the increase in bending sites and the energy of sorption. The equation of the Freundlich model is:

$$\ln q_e = \frac{1}{n} \ln C_e + \ln K_F \quad (4)$$

Where q_e is the equilibrium capacity of sorption in mg/g; C_e is the equilibrium concentration of Pb(II) in mg/L; K_F is the Freundlich adsorption isotherm constant in L/g, and n is a coefficient related to the sorption intensity.

The values K_F and n, were obtained from the slope and the intercept of the plots of $\ln(q_e)$ versus $\ln(C_e)$ in Figure 11 and shown in Table 2, both with variables from the Langmuir isotherm model.

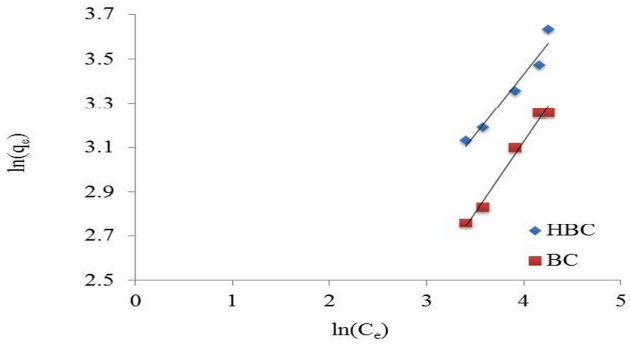

FIGURE 11: Freundlich isotherm ln(qe) vs. 1n(Ce) for the adsorption of Pb(II)

The values of 1/n are less than 1 for both adsorbents, indicative of the degree of nonlinearity between the solution concentration and amount of metal ion adsorbed [26]. Furthermore, high value of K_F indicates that the Pb(II) adsorption capacity of HBC is high; the low 1/n suggests that any large change in the equilibrium concentration of Pb(II) ions would not result in a change in the amount of metal adsorbed by the HBC. The correlation coefficients R^2 for the Freundlich isotherm model were found to be very close to those found from the Langmuir model. Both models gave correlation coffecient R^2 of more than 0.94 and thus the expremintal results are well-fitted. However, the Freundlich isotherm model showed a better fit in predicting or describing the adsorption of Pb(II) onto BC and HBC adsorbents, since the R^2 gained were a little higher.

Comparison of the adsorption capacity of Pb(II) onto BC and HBC, and onto other types of adsorbents is shown in Table 3. From the 19 selected experimental results, HBC ranks the 7th highest on the list, and BC the 8th. It can be safely stated that HBC and BC are very good adsorbents comparing with many others. However, the fact that BC performs better than eleven others in the Table indicates that it is promising to be used, particularly when its low cost is taken into consideration.

TABLE 3: Comparison of Lead adsorption capacities using different adsorbents

Adsorbent	Capacity (mg/g)	Reference No.
Biochar-alginate capsule	263.20	[8]
Dithiocarbamate-anchored n polymer /organosmectite composites	170.70	[26]
HA (50 wt%)/polyurethane composite foam	150.00	[27]
Natural Palygorskite clay	104.28	[28]
Calcined phosphate	85.60	[18]
Streptoverticillium cinnamoneum	70.44	[29]
HBC	59.52	This Study
BC	57.47	This Study
Carbon Nanotube/Bamboo Charcoal (CNT/BC)	47.40	[30]
Carbon Aerogel	34.72	[31]
Moringa oleifera Bark	34.60	[32]
Modified activated carbon (AC–S).	29.44	[25]
Activated carbon prepared from coconut shell	26.50	[17]
Olive mill product	21.56	[33]
Sphagnum moss peat	19.90	[34]
Carbon nano tubes	12.41	[35]
Chitosan–MAA nanoparticles	11.30	[36]
Bituminous coal	8.89	[37]
Kaolinite clay	2.35	[38]

4. Conclusion

Bamboo biochar plus Calcium sulphate (BC) and BC plus Hydroxyapatite (HBC) were investigated for their capacity in the removal of Pb(II) in aqueous solution. The initial pH of the solution, the time of circulation in the column, the flow rate, initial concentration, adsorption kinetics and isotherms, were studied. The suitable time of circulation in the column was found to be 180 min. In the kinetics investigation, the pseudo-second order model was preferred to represent the time-dependent adsorption characteristics in which both the adsorbents gave agreeable regression parameters. For the isotherms study, the Langmuir and the Freundlich adsorption model, on their time-independent adsorption characteristics, both fitted well. However, the Freundlich

model yielded a little better fit which implied some additional layers on the surface, especially for the HBC. Compared with many others in performance both adsorbents were found to be well positioned in the middle range, with HBC one rank higher than BC. Both adsorbents are thus suitable for the removal of Pb(II) from aqueous solution at variables they depended such as the initial concentration of Pb(II), the pH, the time of circulation in the column and the flow rate of the solution. Nevertheless, HBC is much more expensive than BC; approx. 20 times in Thailand at present. Hence it can be concluded that BC offers a new effective and low cost adsorbent that can be applied in the field of wastewater treatment and industry.

Acknowledgments

The authors are thankful to the Prince of Songkla University (PSU) for her financial assistance and support to this research study. We would also like to thank the PSU Department of Chemical Engineering and the Discipline of Excellence (DoE) in Chemical Engineering for assistance in the carrying out of needed chemical analyses.

References

[1] S-Y. Wang, M. H. Tsiu, S. F. Lo, M. J. Tsai, "Effects of manufacturing conditions on the adsorption capacity of heavy metal ions by Makino bamboo charcoal", *Bioresource Technology*, vol. 99, no. 15, pp. 7027-7033, 2008.

[2] A. A. Farghali, M. Bahgat, A. Enaiet Allah, M. H. Khedr, "Adsorption of Pb(II) ions from aqueous solutions using copper oxide nanostructures", *Beni-Suef University Journal of Basic and Applied Science*, vol. 2, no. 2, pp. 61-71, 2013.

[3] H. Lu, W. Zhang, Y. Yang, X. Huang, S. Wang, R. Qiu, "Relative distribution of Pb^{2+} sorption mechanisms by sludge-derived biochar", *Water Research*, vol. 46, no. 3, pp. 854-862, 2012.

[4] M. Inyang, B. Gao, Y. Yao, Y. Xue, A. R. Zimmerman, P. Pullammanappallil, X. Cao, "Removal of heavy metals from aqueous solution by biochars derived from anaerobically digested biomass", *Bioresource Technology*, vol. 110, no. 1, pp. 50-56, 2012.

[5] S. R. Popuri, Y. Vijaya, V. M. Boddu, K. Abburi, "Adsorptive removal of copper and nickel ions from water using chitosan coated PVC beads", *Bioresource Technology*, vol. 100, no. 1, pp. 194-199, 2009.

[6] G. Zhao, J. Li, X. Ren, C. Chen, X. Wang, "Few-layered graphene oxide nanosheets as superior sorbents for heavy metal ion pollution management", *Environmental Science &Technology*, vol. 45, no. 24, pp. 10454-10462, 2011.

[7] S. E. Bailey, T. J. Olin, R. M. Bricka, D. D. Adrian, "A review of potentially low-cost sorbents for heavy metals", *Water Research*, vol. 33, no. 11, pp. 2469-2479, 1999.

[8] X-H. Do, and B-K. Lee, "Removal of Pb^{2+} using a biochar-alginate capsule in aqueous solution and capsule regeneration", *Journal of Environmental Management*, vol. 131, pp. 375-382, 2013.

[9] N. Siddiqui, J. Don, K. Mondal, and A. Mahajan, "Development of bamboo-derived sorbents for mercury removal in gas phase", *Environmental Technology*, vol. 32, no. 4, pp. 383-394, 2011.

[10] Z. Tan, J. Xiang, S. Su, H. Zeng, C. Zhou, L. Sun, S. Hu, J. Qiu, "Enhanced capture of elemental mercury by bamboo-based sorbents", *Journal of Hazardous Materials*, vol. 239, pp. 160-166, 2012.

[11] A. Ślósarczyk, J. S. Oleksiak, B. Mycek, "The kinetics of pentoxifylline release from drug-loaded hydroxyapatite implants", *Biomaterials*, vol. 21, no. 12, pp. 1215-1221, 2000.

[12] B. Sandrine, N. Ange, B. A. Didier, C. Eric, S. Patrick, "Removal of aqueous lead ions by hydroxyapatites: Equilibria and kinetic processes", *Journal of Hazardous Materials*, vol. 139, no. 3, pp. 443-446, 2007.

[13] N. Evaniew, V. Tan, N. Parasu, E. Jurriaans, K. Finlay, B. Deheshi, M. Ghert, "Use of a Calcium Sulfate-Calcium Phosphate Synthetic Bone Graft Composite in the Surgical Management of Primary Bone Tumors", *Orthopedics*, vol. 36, no. 2, pp. 216-222, 2013.

[14] N. Belaicha, W. Lemlikchi, M. O. Mecherri, P. Sharrock, A. Nzihou, "Composite Material with Calcium Sulfate and Calcium Phosphate for Heavy Metals Retention", *Procedia Engineering*, vol. 83, pp. 403-406, 2014.

[15] D. Mowla, and M. Ahmadi, "Theoretical and experimental investigation of biodegradation of hydrocarbon polluted water in a three phase fluidized-bed bioreactor with PVC biofilm support", *Biochemical Engineering Journal*, vol. 36, no. 2, pp. 147-156, 2007.

[16] D. Mohan, S. Rajput, V. K. Singh, P. H. Steele, C. U. Pittman Jr, "Modeling and evaluation of chromium remediation from water using low cost bio-char, a green adsorbent", *Journal of Hazardous Materials*, vol. 188, no. 1-3, pp. 319-333, 2011.

[17] M. Sekar, V. Sakthi, S. Rengaraj, "Kinetics and equilibrium adsorption study of lead(II) onto activated carbon prepared from coconut shell", *Journal of Colloid and Interface Science*, vol. 279, no. 2, pp. 307-313, 2004.

[18] A. Aklil, M. Mouflih, S. Sebti, "Removal of heavy metal ions from water by using calcined phosphate as a new adsorbent", *Journal of Hazardous Materials*, vol. 112, no. 3, pp. 183-190, 2004.

[19] K. S. Low, C. K. Lee, A. C. Leo, "Removal of metals from electroplating wastes using banana pith", *Bioresource Technology*, vol. 51, no. 2-3, pp. 227-231, 1995.

[20] V. K. Gupta, S. Agarwal, T. A. Saleh, "Synthesis and characterization of alumina-coated carbon nanotubes and their application for lead removal", *Journal of Hazardous Materials*, vol. 185, no. 1, pp. 17-23, 2011.

[21] S.T. Ramesh, N. Rameshbabu, R. Gandhimathi, K. M. Srikanth, P. V. Nidheesh, "Adsorptive removal of Pb(II) from aqueous solution using nano-sized hydroxyapatite", *Applied Water Science*, vol. 3, no. 1, pp. 105-113, 2013.

[22] I. D. Mall, V. C. Srivastava, N. K. Agarwal, "Removal of Orange-G and Methyl Violet dyes by adsorption onto bagasse fly ash-kinetic study and equilibrium isotherm analyses", *Dyes and Pigments*, vol. 69, no. 3, pp. 210-223, 2006.

[23] M. A. Stylianou, V. J. Inglezakis, K. G. Moustakas, S. P. Malamis, M. D. Loizidou, "Removal of Cu(II) in fixed bed and batch reactors using natural zeolite and exfoliated vermiculite as adsorbents", *Desalination*, vol. 215, no. 1-3, pp. 133-142, 2007.

[24] H. Nouri, and A. Ouederni, "Modelling of the Dynamics Adsorption of Phenol from an Aqueous Solution on Activated Carbon Produced from Olive Stones", *International Journal of Chemical Engineering & Application*, vol. 4, no. 4, pp. 254-261, 2013.

[25] J. Goel, K. Kadirvelu, C. Rajagopal, V. K. Garg, "Removal of Lead(II) by adsorption using treated granular activated carbon: Batch and column studies", *Journal of Hazardous Materials*, vol. 125, no. 1-3, pp. 211-220, 2005.

[26] R. Say, E. Birlik, A. Denizli, A. Ersöz, “Removal of heavy metal ions by dithiocarbamate-anchored polymer/organosmectite composites”, *Applied Clay Science*, vol. 31, no. 3-4, pp. 298-305, 2006.

[27] S. H. Jang, B. G. Min, Y. G. Jeong, W. S. Lyoo, S. C. Lee, “Removal of lead ions in aqueous solution by hydroxyapatite/polyurethane composite foams”, *Journal of Hazardous Materials*, vol. 152, no. 3, pp. 1285-1292, 2008.

[28] H. Chen, and A. Wang, “Kinetic and isothermal studies of lead ion adsorption onto palygorskite clay”, *Journal of Colloid and Interface Science*, vol. 307, no. 2, pp. 309-316, 2007.

[29] P. R. Puranik, and K. M. Paknikar, “Influence of co-cations on biosorption of lead and zinc-a comparative evaluation in binary and multimetal systems”, *Bioresource Technology*, vol. 70, no 3, pp. 269-276, 1999.

[30] Z-H. Huang, F. Zhang, M-X. Wang, R. Lv, F. Kang, “Growth of carbon nanotubes on low-cost bamboo charcoal for Pb(II) removal from aqueous solution”, *Chemical Engineering Journal*, vol. 184, pp. 193-197, 2012.

[31] J. Goel, K. Kadirvelu, C. Rajagopal, V. K. Garg, “Removal of lead(II) from aqueous solution by adsorption on carbon aerogel using a response surface methodological approach”, *Industrial & Engineering Chemistry Research*, vol. 44, no. 7, pp. 1987-1994, 2005.

[32] D. H. K. Reddy, K. Seshaiah, A. V. R. Reddy, M. M. Rao, M. C. Wang, “Biosorption of Pb^{2+} from aqueous solutions by Moringa oleifera bark: Equilibrium and kinetic studies”, *Journal of Hazardous Materials*, vol. 174, no. 1-3, pp. 831-838, 2010.

[33] S. H. Gharaibeh, W. Y. Abu-el-sha'r, M. M. Al-Kofahi, “Removal of selected heavy metals from aqueous solutions using processed solid residue of olive mill products”, *Water Research*, vol. 32, no. 2, pp. 498-502, 1998.

[34] J. K. Mclellan, and C. A. Rock, “Pretreating landfill leachate with peat to remove metals”, *Water, Air, and Soil Pollution*, vol. 37, no. 1-2, pp. 203-215 1988.

[35] Y-H. Li, Z. Di, J. Ding, D. Wu, Z. Luan, Y. Zhu, “Adsorption thermodynamic, kinetic and desorption studies of Pb^{2+} on carbon nanotubes”, *Water Research*, vol. 39, no. 4, pp. 605-609, 2005.

[36] A. Heidari, H. Younesi, Z. Mehraban, H. Heikkinen, “Selective adsorption of Pb(II), Cd(II), and Ni(II) ions from aqueous solution using chitosan-MAA nanoparticles”, *International Journal of Biological Macromolecules*, vol. 61, pp. 251-263, 2013.

[37] S. Dhanesh, and N. S. Rawat, “Sorption of Pb (II) by bituminous coal”, *Indian Journal of Chemical Technology*, vol. 2, no. 1, pp. 49-50, 1995.

[38] M-Q. Jiang, X. Y. Jin, X. Q. Lu, Z. L. Chen, “Adsorption of Pb(II), Cd(II), Ni(II) and Cu(II) onto natural kaolinite clay”, *Desalination*, vol. 252, no. 1-3, pp. 33-39, 2010.

Appendix C

The publication of fixed bed column adsorption

Appendix C1

Journal Paper

A. H. Alamin, L. Kaewsichan, ‘‘Adsorption of Pb(II) Ions from Aqueous Solution in Fixed Bed Column by Mixture of Clay plus Bamboo Biochar’’, **This manuscript had been accepted to publish in Walailak Journal of Science and technology.**

WALAILAK JOURNAL
http://wjst.wu.ac.th (Article)

Adsorption of Pb(II) Ions from Aqueous Solution in Fixed Bed Column by Mixture of Clay plus Bamboo Biochar

Ahmed Hassan ALAMIN[1,a] and Lupong KAEWSICHAN [1,b]

[1] Department of Chemical Engineering, Prince of Songkla University, Hat Yai, Songkhla, Thailand

(*Corresponding author e-mail: [a] ahmed.10000@yahoo.com)

Received: xxx, Revised: xxx, Accepted: xxx

Running title
Column Adsorption Pb by Clay& Bamboo char

Abstract

Fixed bed column experiments were conducted to investigate adsorption potential of adsorbent mixture containing natural Clay from Sudan (CS) and Bamboo Biochar (BB) to form CB adsorbent for the removal of Pb(II) from aqueous solution. Characterization of CS was performed using FTIR, XRD, and XRF techniques; and for BB, FTIR and SEM. Effects of solution flow rate (10-20 ml/min), bed height (10-40 mm) and initial Pb(II) concentration (5-30 mg/L) on the breakthrough characteristics of the adsorption process were investigated. The adsorption process system was found to be better performed at low feed flow rate, low CB bed height and high Pb(II) inlet concentration. Bed depth service time (BDST) model was used in the column performance experimental data, and model parameters were evaluated. Three other models were used to fit the adsorption data: Adams-Bohart, Thomas, and Yoon-Nelson. All models are good but the coefficient of determination for the first and the two latter models were found to yield a better fit than the Adams-Bohart model and hence these were used to predict the adsorption of Pb(II) ions in the fixed bed column. The CB mixture was shown to be a suitable adsorbent for adsorption, or removal, of Pb(II).

Keywords: Fixed bed, clay, Bamboo biochar, adsorption, Pb(II).

Introduction

Heavy metals pose an important issue in worldwide environmental problem. Effluents from a wide range of industrial applications, e.g., microelectronics, electroplating, battery manufacturing, metal finishing, mining and metallurgical products, dyestuffs, tannery, chemicals and pharmaceuticals, contain heavy metals and are responsible for pollution of the environment [1]. Presence of heavy metals in natural water body poses health problems with animals, plants and human beings, and numerous metals such as Sb, Cr, Cd, Pb, Mn, Hg, have toxic effects on man and environment [2]. Exposure to Pb(II), a highly toxic substance, produces a wide range of adverse health effects for both adults and children [3]. Lead poisoning causes severe damage to organs and leads to deadly diseases, thereby posing one greatest danger to the living [4]. Common methods available for the removal of Pb(II) from aqueous solutions are: ion exchange, solvent extraction, membrane process, chemical precipitation and adsorption [5], along with their advantages and disadvantages. Conventional precipitation method does not always provide a satisfactory removal rate to meet the pollution control standards and synthetic ion-exchange resins are often expensive [6]. Adsorption is one of the important procedures for removal of heavy metals [7]; ion-exchange and adsorption mechanisms of various adsorbents have been used to remove a variety of heavy metal ions from aqueous solution [1].

Adsorbents such as minerals, organic of biological origins, zeolites, industrial by-products, agricultural wastes, biomass, and polymeric materials had been used for removal of heavy metals from

water [8]. Clays, abundant and readily available in nature, can also be used as adsorbents due to their high surface area, chemical and mechanical stabilities and their surface and structural properties [9]. Many soil adsorbents have been studied for the removal of heavy metals, such as Chinese loess [10], clay [11] and bentonite [12]. In general the ability of clay is in its readiness to expand and effectively increase in surface area to accommodate more metal ions [13]. Lead metal was found to be easily adsorbed onto montmorillonite, both in its raw form and its acid activated derivatives [14]. The removal of Lead by Sudan clay is particularly extractive because it is natural; local product; therefor, cheap and easily available source aluminosilicate [15]. Moreover its adsorption capacity can be improved via mix with other adsorbent such as Bamboo biochar.

Biochar, an important renewable source for securing future energy supply from environmentally benign systems [16], is also recognized as an effective sorbent for potentially organic compounds and heavy metals [17]. Recent studies also suggested that surface modification processes, such as growing/adding/depositing nanomaterials on biochar surfaces (biochar nanocomposites), could dramatically improve sorption ability to various water pollutants, including heavy metals, organics, phosphate, nitrate, etc. [18,19].

Preliminary investigations by the authors revealed generally higher Pb(II) adsorbing efficiencies when the bamboo biochar (BB) was used as mixtures together with Sudanese clay (CS). Furthermore, there appears to be limited information on the wastewater treatment using mixed adsorbents, although Pb(II) removal using such adsorbents have not be reported.

In this study, removal efficiency of Pb(II) from aqueous solution employing fixed bed column using a mixture of Sudan clay plus Bamboo biochar was investigated. Principal design parameters: solution flow rate, column bed height and inlet concentration of Pb(II) solution, were evaluated using a laboratory scale apparatus and the effect of operation conditions on the removal percentage of Pb(II) was investigated.

Materials and methods

Adsorbents

Sudanese clay (CS) used in this experiment was from the Nile river region in Sennar state, Sudan. Standard metal of $Pb(No_3)_2$ was purchased from Boss Official Limited Partnership, Thailand. Bamboo biochar (BB) was prepared at laboratory scale by pyrolysis process at 500°C, grinded and sieved through mesh number 20 and mixed with clay at a ratio of 1:1 to form adsorbent mixture CB. All solutions were prepared from analytical reagents (AR) and double distilled water. The mixture of adsorbents was put in circular rubber foam rings acting as holders to be fixed in a column to make a bed of varying height. Concentration of residual Pb(II) was analysed using a Perkin Elmer thermos scientific S-series model (AAnalyst100) flame atomic absorption spectrometer (AAS). Fourier transform infrared spectroscopy (FTIR) (Bomem, MB 100) was conducted to identify the functional groups of the clay and biochar. The mineralogical composition of the CS was determined using X-Ray Diffraction (XRD), and the chemical composition was determined by thermos ARL-9800 model X-Ray Fluorescence (XRF) spectrometer and wet analysis.

Adsorbate

Standard solution of $Pb(No_3)_2$ (1000 mg/L) was obtained by dissolving 1.59 (g) of lead nitrate in 1 litre double distilled water. Stock solutions were prepared by diluting the standard solution to various concentrations in the rage of 5-30 (mg/L).

Experimental setup and procedure

Schematic diagram for the fixed bed column system is shown in **Figure 1**. The column was made of glass tube having 35 (mm) inside diameter and 240 (mm) in height. At the bottom of the column, a stainless steel sieve was attached, followed by a layer of glass wool. A known quantity of the prepared mixture of CS and BB, to form CB, was put in the circular rubber foam ring and was packed in the column to obtain the desired bed height of the adsorbent at ranges of 10-40 (mm), equivalent to 0.8 to 3.2

(g) of CB, to study the effect of bed height. The column was connected to a distributer in order to provide a uniform flow of the solution through the column. Solution of Pb(II) of known concentrations at ranges of 5-30 (mg/L) was pumped downward through the column at varied flow rate at ranges of 10-20 (ml/min) controlled by a peristaltic pump to investigate the effects of initial concentration, effects of flow rate and effects of bed height. Samples of the outlet solution were collected at the exit of the column at time intervals and their concentrations were determined using a flame atomic adsorption spectrophotometer (AAS). In order to ensure the accuracy and reproducibility of all the data, all column adsorption experiments were conducted in triplicate, and mean values were used in the analysis.

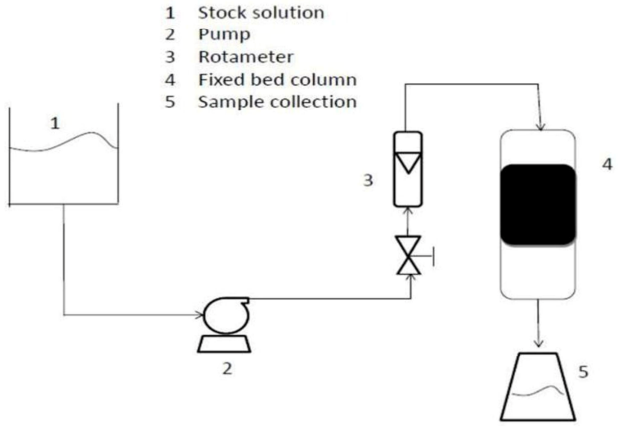

Figure1 The fixed bed experimental setup

Analysis of column data

Characteristics of importance in determining the operation and dynamic response of an adsorption fixed bed column are the time of breakthrough appearance and the shape of the breakthrough curve. The breakthrough curves will reveal the loading behavior of Pb(II) to be removed from the solution and is usually expressed in terms of adsorbed Pb(II) concentration (C_{ad}), inlet Pb(II) concentration (C_o), outlet Pb(II) concentration (C_t) or normalized concentration defined as the ratio of outlet Pb(II) concentration to the inlet Pb(II) concentration (C_t/C_o), as a function of time or volume of effluent for a given bed height [20]. Effluent volume (V_{eff}) can be calculated from Eq. (1):

$$V_{eff} = Qt_{total} \quad (1)$$

Where t_{total} and Q are the total flow time (min) and the volumetric flow rate (ml/min).

The area under the breakthrough curve (A), obtained by integrating the adsorbed concentration (C_{ad} in mg/L) versus t (min), can be used to find the total adsorbed Pb(II) quantity (maximum column capacity). The total adsorbed metal quantity (q_{total} in mg) in the column for a given feed concentration and flow rate (Q) can be calculated from Eq. (2):

$$q_{total} = \frac{Q\,A}{1000} = \frac{Q}{1000}\int_{t=0}^{t=t_{total}} C_{ad}\,dt \quad (2)$$

The total amount of metal ions dispatched to the column (M_{total}) can be calculated using Eq. (3):

$$M_{total} = \frac{C_0\,Qt_{total}}{1000} \quad (3)$$

The total removal is calculated from Eq. (4):

$$\text{Total removal } (\%) = \frac{q_{total}}{M_{total}} \times 100 \quad (4)$$

The equilibrium metal uptake q_{eq}, or the maximum capacity of the column is defined by Eq. (5) as the total amount of metal sorbed q_{total} per g of adsorbent (X) at the end of the total flow time:

$$q_{eq} = \frac{q_{total}}{X} \quad (5)$$

Column breakthrough curve modelling

Successful design and operation of laboratory-scale fixed bed column adsorption can be explained by simple mathematical models. Breakthrough curves yielded for flow rate, initial concentration and bed height were predicted by models such as bed-depth service-time (BDST), Adams-Bohart, Thomas, and Yoon-Nelson models.

The breakthrough curves using the BDST model is based on measuring the bed capacity at different percentage of breakthrough values. The model is based on an assumption that the rate of adsorption is controlled by the surface reaction between the adsorbate and the unused capacity of the adsorbent. Constants from the model can be easily scaled up for different concentration and flow rate without conducting more experiments. Moreover, it can be used to predict the fixed bed column performance at any bed height. The linear relationship between bed depth and service time is given by Eq. (6) [21]:

$$t = \frac{NZ}{C_0 v} - \frac{1}{K_\alpha C_0} \ln\left[\left(\frac{C_0}{C}\right) - 1\right] \quad (6)$$

Where C is the breakthrough Pb(II) concentration (mg/L); N the adsorption capacity of the bed (mg/L); Z the depth of the column bed (cm); v the linear flow velocity of lead solution through the bed (ml/cm^2 h); and K_α the rate constant (L/mg h).

Adams-Bohart model [22] is commonly used for description of the initial part of the breakthrough curve [23], and the model equation is expressed as Eq. (7):

$$\ln \frac{C_t}{C_0} = k_{AB} C_0 t - k_{AB} N_0 \frac{Z}{F} \quad (7)$$

Where C_0 and C_t (mg/L) are the inlet and effluent Pb(II) concentration; k_{AB} (L/mg min) the kinetic constant; F (mm/min) the linear velocity calculated by dividing the flow rate by the column section area; Z (mm) the bed depth of column; and N_0 (mg/L) the saturation concentration.

One of the most popular and widely used models for describing the process theory of adsorption in a fixed bed column is the Thomas model [24]. This model assumes plug flow behavior in the bed, and uses Langmuir isotherm for equilibrium and second-order reversible reaction kinetics. The model equation is expressed as Eq. (8):

$$\ln\left(\frac{C_0}{C_t} - 1\right) = \frac{k_{Th} q_0 W}{Q} - k_{Th} C_0 t \quad (8)$$

Where k_{Th} (ml/min mg) is the Thomas rate constant; q_0 (mg/g) the equilibrium Pb(II) uptake per g of the adsorbent; C_o (mg/L) the inlet Pb(II) concentration; C_t (mg/L) the outlet concentration at time t; W (g) the mass of adsorbent; Q (ml/min) the flow rate; and t (min) the flow time.

Yoon and Nelson [25] had developed a model based on the assumption that the rate of decrease in the probability of adsorption of adsorbate molecule is proportional to the probability of the adsorbate adsorption and the adsorbate breakthrough on the adsorbent. The linear form of the equation as Eq. (9):

$$\ln\left(\frac{C_t}{C_0 - C_t}\right) = k_{YN} t - \tau k_{YN} \quad (9)$$

Where k_{YN} (min^{-1}) is the Yoon–Nelson proportionality constant; and τ (min) the time required for retaining 50% of the initial sorbate.

Results and discussion

Characteristics of the Sudanese Clay

Fourier Transformed Infrared Spectroscopy (FTIR) of the Clay

FTIR spectrum curves for the clay sample in **Figure 2** showing changes in the functional groups can be observed in all frequency range. The spectrum of the clay exhibits a broad shoulder at around 3700-3400 cm^{-1}; the range of frequencies usually assigned to surface hydroxyl groups and sorbed water. Absorption band observed at 3622 cm^{-1} for clay is attributable to hydroxyl group vibrations in Mg-OH-Al, Al-OH-Al, and Fe-OH-Al units in the octahedral layer. This poorly resolved shoulder consists of overlaps of two components: Si-OH at 3622 cm^{-1}, and Mg-OH at 3697 cm^{-1} stretching vibrations. The band at 3448 cm^{-1} is due to the O-H stretching vibration of the silanol Si-OH groups and HO-H vibration of the water adsorbed by the silica surface. The spectrum also contains a broad band at 1457 cm^{-1} related to the stretch vibrations of C=O group due to calcite impurity. The broad band near 1034 cm^{-1} is related to the stretch vibrations of the Si-O groups. The band appeared at 1457 cm^{-1} corresponds to that of carbonate [calcite ($CaCO_3$) or dolomite (Ca, $Mg(CO_3)_2$)]. In the low energy region, the spectrum shows one band around 685 cm^{-1} due to O-H bending vibration from the adsorbed water, and one band at 535 cm^{-1} assigned to Mg-O vibration. The bands appeared at 468 cm^{-1} correspond to SiO Mg.

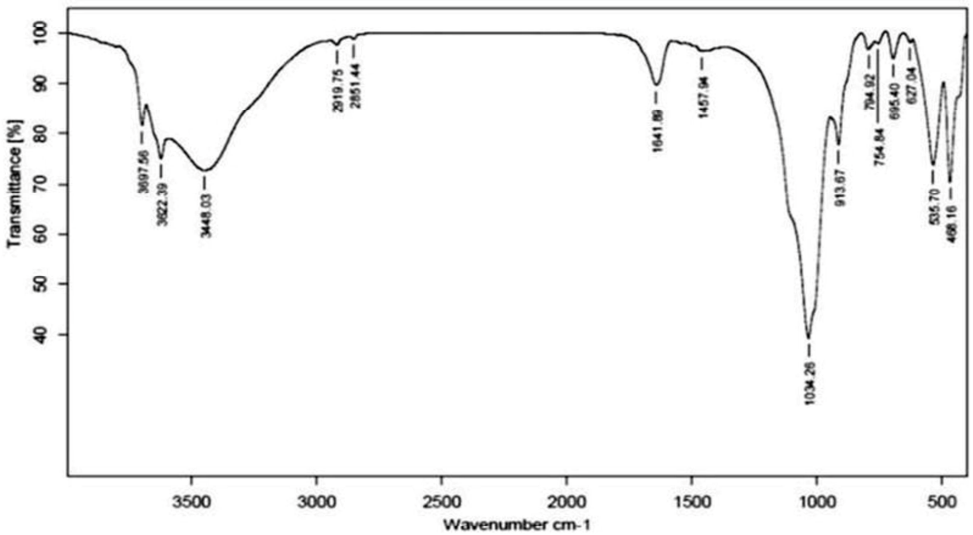

Figure2 FTIR Analysis on the Sudanese clay

X-ray Diffraction (XRD), X-ray Fluorescence (XRF), and SEM of the Clay

XRD measurements show that the Sudanese clay is mainly composed of (Albite, calcian, ordered), besides quartz, kaolinite and montmorillonite; significant peaks are identified on the XRD spectrum in **Figure 3**. Chemical compositions of the clay are tabulated in **Table 1**.

Scanning Electron Microscopy (SEM) for Bamboo biochar and clay

The BB morphological characteristics by scanning electron microscopy (SEM) showed large internal surface and porous structure with an approximate porous space of 38.67μm; as shown in **Figure 4** (a) and (b) with different magnitude. Furthermore, SEM on elemental composition in the BB sample was shown in **Table 2**.

The SEM analysis of clay was investigated to study the surface as shown in **Figure 4** (c) and (d). It is reviled clear from the image that the surface has porous. In general way materials with porous acted as adsorbents.

Characteristics of the Bamboo Biochar

FTIR spectrum analysis of the Bamboo biochar sample (figure not shown) revealed many functional groups on its surfaces: the bands assigned to O–H stretching; aliphatic C-H stretching; intense bands of aliphatic CH_2; intensity of aromatic C=C stretching and C=O stretching of conjugated ketones and quinones; C=C ring stretching vibration of lignin; and C–O and C–C stretching.

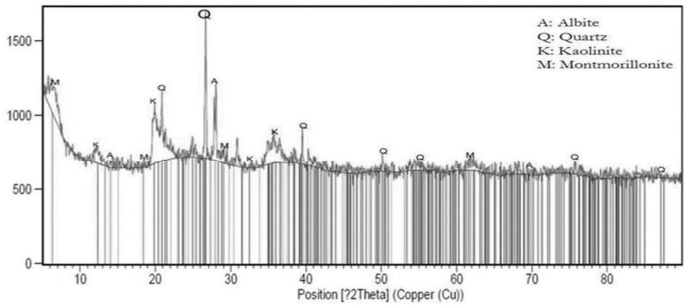

Figure 3 XRD Chart on the Sudanese clay

Table 1 Characteristics of the Sudanese Clay

Chemical composition of the Clay (%)	
Na_2O	1.437
MgO	2.106
Al_2O_3	20.637
SiO_2	47.612
K_2O	0.310
CaO	1.972
TiO_2	1.393
MnO	0.159
Fe_2O_3	11.219
SrO	0.015
ZrO_2	0.023
Others	13.117
Other Parameters:	
Organic Matters	12.82 ± 0.44 g/kg
pH	9.98 ± 0.01
Conductivity	514 ± 3.06 µS/cm
Particle size	139.4µm
Density	2.275±0.003 g/cm^3

Table 2 Characteristics of the Bamboo char

Chemical composition of the Bamboo char (%)	
C	58.61
K	30.46
Cl	9.38
S	1.55
Other Parameters:	
pH	8.00 ± 0.01
Density	0.394±0.005 g/cm^3

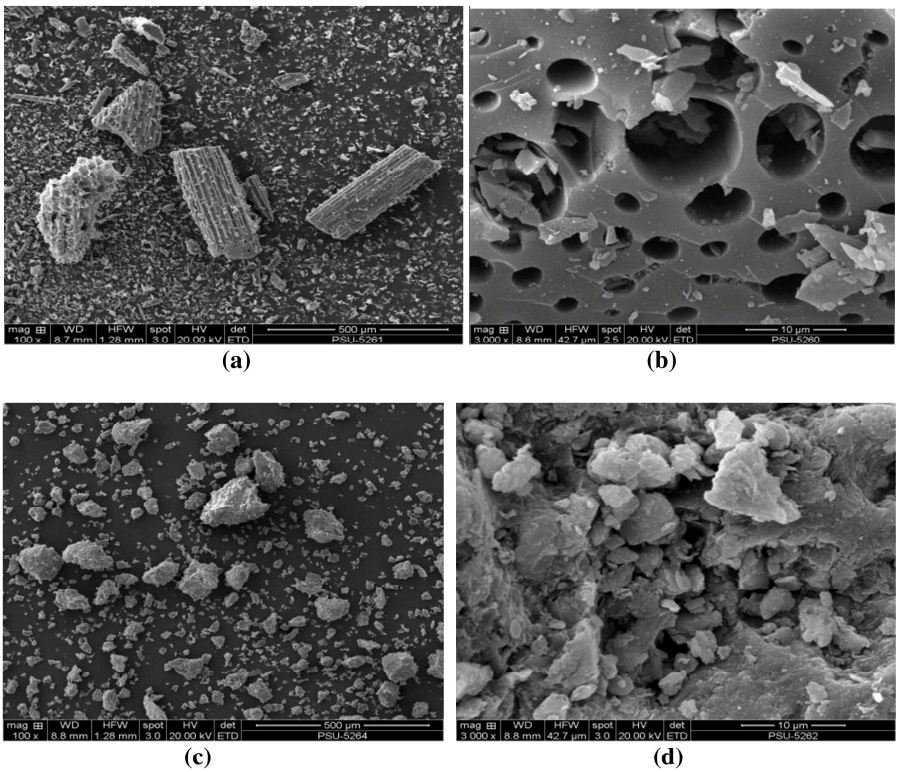

(a) **(b)**

(c) **(d)**

Figure 4 SEM of the Bamboo biochar [(a) and (b)], and of the Clay adsorbent [(c) and (d)]

Effect of Pb(II) Solution Flow Rate

The effect of flow rate on adsorption of Pb(II) using the CB adsorbent was investigated under various flow rates in the range of 10-20 ml/min, whilst other variables were fixed (adsorbent bed height of 25 (mm) and an inlet Pb(II) concentration of 17.5 (mg/L)). Breakthrough curves obtained are shown in **Figure 5**. Generally the breakthrough occurred slower with lower flow rate. Similarly, the breakthrough time to reach saturation decreased significantly with increasing flow rate. The curves represented at high flow rate were much sharper than that in the case of low flow rate. This can be explained to the fact that at low flow rate the residence time of Pb(II) ions in the column increases, hence the Pb(II) ions have more

time to diffuse into the pores of the CB through intraparticle diffusion resulting in a longer breakthrough time and saturation time [26].

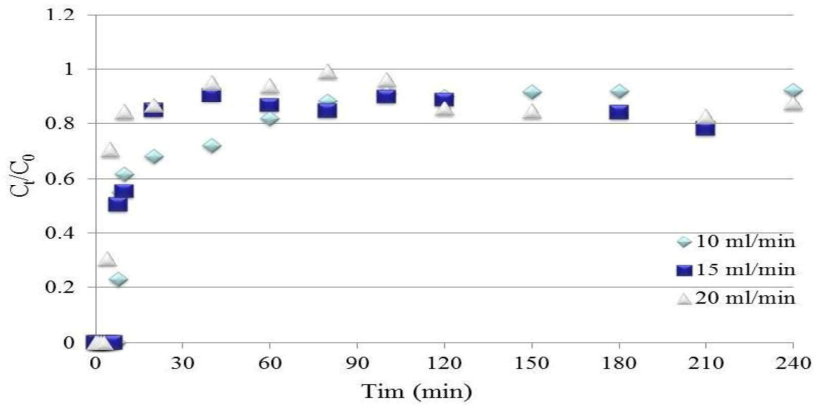

Figure 5 Breakthrough curves for Pb(II) adsorption on the CB at different flow rate (at constant inlet Pb(II) concentration of 17.5 (mg/L) and bed height of 25 (mm))

Effect of Initial Pb(II) Concentration

The effect of initial metal concentration on adsorption of Pb(II) by the CB adsorbent were investigated using different inlet Pb(II) concentration in the range of 5-30 (mg/L) while other parameters were kept constant (adsorbent bed height of 25 (mm) and solution flow rate of 15 (ml/min)). **Figure 6** shows the breakthrough curves obtained from various concentration of Pb(II). From the adsorption data, the breakthrough time, the removal efficiency and the saturation time decreased with the increase in initial concentration of the Pb(II) ions. The diffusion happens when there is a concentration gradient, diffusion will normally proceed from an area of higher concentration to an area of lower concentration and at the end of time equilibrium will occur. There is several factors affect in the rate of diffusion, one of these, concentrations of the solution. The major difference in concentration would be more rapid in rate of diffusion. The second factor is mass of the molecules diffusing, heavier molecules move more slowly; therefore, they diffuse more slowly, and the reverse is true for lighter molecules. This can be explained by the fact that a lower concentration causes a slower transport due to the decrease in the diffusion coefficient or mass transfer coefficient [23]. The Pb(II) ions adsorbed onto the CB adsorbent increased from 306 to 887 and 905 (mg), respectively with the inlet initial concentration of 5, 17.5 and 30 (mg/L). The increase in inlet concentration of Pb(II) ions has an effect on the metal uptake capacity of the CB due to saturation of column. The increase in the Pb(II) uptake capacity of the CB is due to the fact that a higher inlet concentration provides a higher driving force for the transfer process to overcome the mass transfer resistance [27].

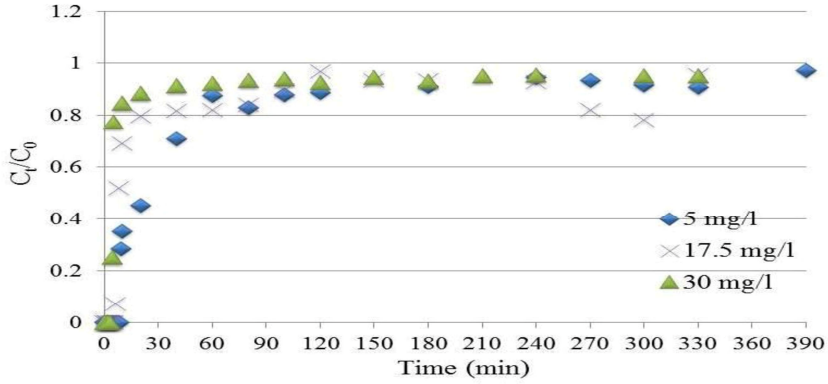

Figure6 Breakthrough curves for Pb(II) adsorption on the CB at different inlet Pb(II) concentrations (at constant bed height of 25 (mm) and flow rate of 15 (ml/min))

Effect of Adsorbent Bed Height

Removal of Pb(II) in the adsorption process using CB adsorbent was studied under the effect of bed height while flow rate and inlet concentration of Pb(II) were kept constant, respectively at 15 (ml/min) and 17.5 (mg/L). The breakthrough curves for bed heights of 10, 25 and 40 (mm) are shown in **Figure 7**. The breakthrough curves obtained were steeper with lower bed height. When bed height increased, the removal efficiency, the breakthrough time and the saturation time increased. This increase in removal efficiency of Pb(II) ions onto the CB adsorbent is due to the higher number of adsorption sites available and the increase in volume influent. The slope of the breakthrough curve decreased with increasing bed height, resulting in a broadened mass transfer zone [23]. Highest adsorption capacity was observed at the highest bed height due to an increase in the surface area of adsorbent, which provided more binding sites for the adsorption [28].

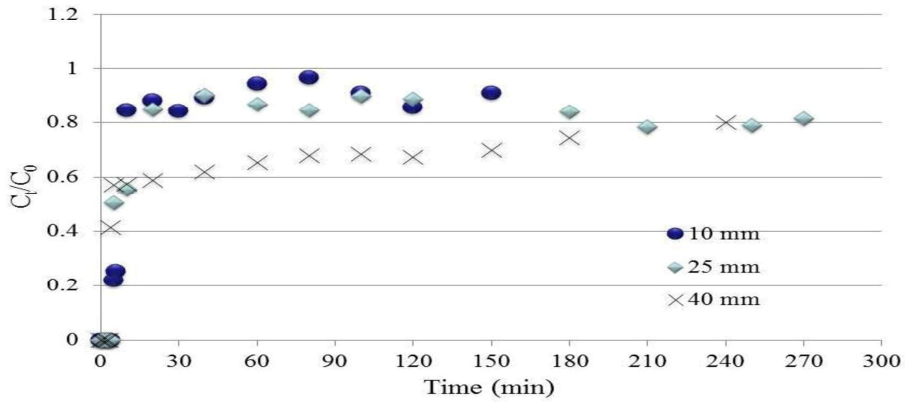

Figure 7 Breakthrough curves for Pb(II) adsorption on the CB at different bed height (at constant inlet Pb(II) concentration of 17.5 (mg/L) and flow rate of 15 (ml/min))

Dynamic Adsorption Models Employed

Variables from the breakthrough curves can be used to predict the design column efficiency. Four mathematical models used here to predict the efficiency of laboratory-scale column and its dynamic

behaviour are: the bed-depth service time (BDST), the Adams-Bohart, the Thomas, and the Yoon-Nelson models.

The Bed Depth Service Time (BDST) Model

The BDST model plot of service time versus bed depth at flow rate of 15 ml/min was linear, as shown in **Figure 8**. The correlation coefficient value R^2 of 0.9959 is very high, pointing to very good validity of the model. The calculated values of the model parameters (N) and (K_α) are 393.75 (mg/L) and 0.037 (L/mg h), respectively. In case of large (K_α) value, a short bed is enough to avoid breakthrough, but as (K_α) gets smaller, as in this study, a progressively deeper bed is required to avoid breakthrough [29].

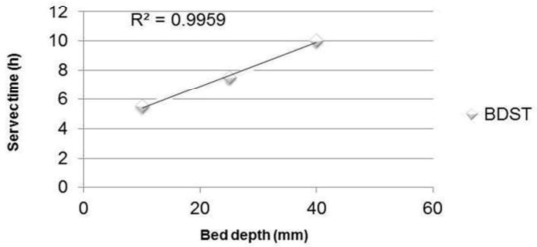

Figure 8 BDST plot for Pb(II) adsorption on CB

The Adams–Bohart Model

Adams-Bohart model was applied to the experimental data and the value of adsorption capacity for adsorbent (N_0) and the kinetic constant of the model (k_{AB}) were calculated and presented in **Table 3**, together with the correlation coefficients (obtained in range of 0.9182 to 0.9788) . According to this model, the equilibrium is not instantaneous and the rate of sorption Pb(II) on CB adsorbent is proportional to fraction of sorption capacity [27]. Although, Adams-Bohart models gives a simple and comprehensive approach for evaluating column dynamics, its validity of adsorption process of Pb(II) by CB is limited to the range of condition used [30]. From the Table, (N_0) increased with increasing inlet concentration of Pb(II) and the flow rate, whereas the trend for (k_{AB}) was the opposite, indicating that the overall system kinetics was dominated by external mass transfer in the initial part of adsorption in the column [31]. On bed height parameter, (N_0) increased with increasing bed height while (k_{AB}) decreased.

The Thomas Model

The experimental data were fitted to the Thomas model. The calculated rate constant (k_{Th}), the maximum sorption capacity (q_0), and the correlation R^2 (obtained in range of 0.8839 to 0.9838) are listed in **Table 4**. From the Table, k_{Th} decreased with increasing inlet concentration of Pb(II) due to the increase in mass transport resistance while the values of (q_0) were increasing. This is attributable to the driving force of adsorption for the difference in concentrations between Pb(II) on the CB adsorbent surface and in the solution [32]. Thus the higher driving force due to the higher lead concentration resulted in larger q_0 [33]. The maximum sorption capacity q_0 decreases with increasing bed height and flow rate. That means q_0, affected by increase in CB mass, these are due to more adsorption sites being available for Pb(II) ions as the amount of CB increased. At lower flow rates, there is a longer contact time between the Pb(II) ions and CB adsorbent and therefore, a higher value of the rate constant suggested that the adsorption capacity will reach the equilibrium value faster [34]. The rate constant of Thomas model k_{Th} also decreased with increasing bed height. It was demonstrated that Pb(II) adsorption onto CB followed pseudo-second order reaction and both external and intraparticle diffusion were involved in the adsorption process . These mean that Thomas model was suitable for adsorption processes where external and internal diffusions were not the limiting step [35].

The Yoon–Nelson Model

The fourth, and final model applied to the experimental data is the Yoon-Nelson model. The Yoon–Nelson proportionality constant (k_{YN}) and the time required for retaining 50% (τ) calculated for all data of the breakthrough curves with corresponding correlation coefficient are shown in **Table 5**. The range of R^2 between 0.9287 and 0.9904 obtained from this model represents a better fit than the Adams-Bohart and the Thomas model, but not the BDST. The rate constant was significant increases with increase in flow rate and decreases with increase in bed height. In case of high flow rate the number of Pb(II) molecules passing through a particular CB adsorbent was more, which increase the rate. Also at higher bed height the Pb(II) molecules has more time to immigrate through the column which results in the reduced adsorption rate [36]. The time retaining 50% (τ) was found to be significantly decreasing with the increase in inlet Pb(II) concentration and the flow rate of the solution. This is due to the fact that saturation of the column was rapidly achieved, while τ increased with the increase in bed height because saturation was slower in thicker bed height.

Table 3 Adams-Bohart model result from linear regression analysis

Initial concentration (mg/L)	**Flow rate** (ml/min)	**Bed height** (mm)	**k_{AB} (L/mg min)**	**N_0 (mg/L)**	**R^2**
5	15	25	0.0024	298.26	0.9267
17.5	15	25	0.000262857	939.68	0.9263
30	15	25	0.0002	1090.66	0.9544
17.5	10	25	0.000297143	891.63	0.9788
17.5	15	25	0.0002	1090.66	0.9544
17.5	20	25	0.000182857	1283.8	0.9506
17.5	15	10	0.000411429	478.81	0.9182
17.5	15	25	0.000262857	939.68	0.9263
17.5	15	40	6.28571E-05	2827.58	0.9501

Table 4 Thomas model result from linear regression analysis

Inlet concentration (mg/L)	Flow rate (ml/min)	Bed height (mm)	k_{Th} (L/mg min)	q_0 (mg/g)	R^2
5	15	25	0.003780000	7352.58	0.8839
17.5	15	25	0.000542857	9319.21	0.9763
30	15	25	0.000610000	12313.52	0.9795
17.5	10	25	0.000577143	18018.94	0.9552
17.5	15	25	0.002834286	9852.22	0.8841
17.5	20	25	0.000542857	9319.21	0.9763
17.5	15	10	0.000942857	25444.60	0.9832
17.5	15	25	0.000577143	18018.94	0.9552
17.5	15	40	0.000377143	2682.20	0.9586

Table 5 Yoon–Nelson model result from linear regression analysis

Inlet concentration (mg/L)	Flow rate (ml/min)	Bed height (mm)	k_{YN} (L/mg min)	τ (min)	R^2
5	15	25	0.0196	221.62	0.9670
17.5	15	25	0.0124	197.84	0.9849
30	15	25	0.0183	54.73	0.9795
17.5	10	25	0.0101	205.93	0.9552
17.5	15	25	0.0124	197.84	0.9849
17.5	20	25	0.0101	67.73	0.9904
17.5	15	10	0.0165	77.55	0.9832
17.5	15	25	0.0124	197.84	0.9849
17.5	15	40	0.0028	123.11	0.9900

Conclusions

Clay and Bamboo biochar are capable of treatment heavy metal from aqueous solution particularly when the mixed together. CB, a mixture of Sudanese clay plus Bamboo biochar (a low cost material), was employed as adsorbent for removal of Pb(II) ions from aqueous solution in a fixed bed column. Varying variables investigated were: initial inlet ion concentration, flow rate, and bed height. The system was found to better perform at low feed flow rate, low CB bed height and high Pb(II) inlet concentration. Bed depth service time (BDST) model was used in the column performance experimental data and model variables were calculated. The column data obtained fitted well with three other mathematical models: the Adams–Bohart, the Thomas and the Yoon-Nelson models. All models can be applicable, but the first and latter two models, the BDST, the Thomas and Yoon–Nelson, were found to better predicted the breakthrough curves than the Adams-Bohart. This work shown that CB adsorbent can play an important role in adsorption of Pb(II) from water in column. Taken its low cost into consideration, CB could be regarded as a new, moderately effective adsorbent that can be applied in the field of industrial wastewater treatment.

Acknowledgements

The authors are grateful to the Prince of Songkla University (PSU) for her financial assistance and support to this research. We would also like to thank the PSU Department of Chemical Engineering and the Discipline of Excellence (DoE) in Chemical Engineering for assistance in the carrying out the needed chemical analyses.

References

[1] SH Lin, SL Lai, HG Leu, Removal of Heavy Metals from Aqueous Solution by Chelating Resin in a Multistage Adsorption Process. J. Hazard. Mater. 2000, DOI: 10.1016/S0304-3894(00)00207-7.

[2] VCT-Costodes, H Fauduet, C Porte, A Delacroix, Removal of Cd(II) and Pb(II) Ions, from Aqueous Solutions, by Adsorption onto Sawdust of Pinus sylvestris. J. Hazard. Mater. 2003, DOI: 10.1016/j.jhazmat.2003.07.009.

[3] AA Farghali, M Bahgat, A E-Allah, MH Khedr, Adsorption of Pb(II) Ions from Aqueous Solutions using Copper Oxide Nanostructures. Beni-Suef Univ. J. Basic Appl. Sci. 2013, DOI: 10.1016/j.bjbas.2013.01.001.

[4] V Singh, S Tiwari, AK Sharma, R Sanghi, Removal of Lead from Aqueous Solutions using Cassia Grandis Seed Gum-graft-Poly(methylmethacrylate). J. Colloid Interface Sci. 2007, DOI: 10.1016/j.jcis.2007.07.061.

[5] MM Kumar, Removal of Pb(II) from Aqueous Solution by Adsorption using Activated Tea Waste. Korean J. Chem. Eng. 2010, DOI: 10.1007/s11814-009-0304-6.

[6] CW-Chung and FT-Ping, Adsorption/ion-exchange Behavior between a Water-insoluble Cationic Starch and 2-Chlorophenol in Aqueous Solutions. J. Appl. Polym. Sci. 1998, DOI: 10.1002/(SICI)1097-4628(19980207)67:6<1085::AID-APP16>3.0.CO;2-.

[7] A Sarı, M Tuzen, D Cıtak, M Soylak, Adsorption characteristics of Cu(II) and Pb(II) onto expanded perlite from aqueous solution. J. Hazard. Mater. 2007, DOI: 10.1016/j.jhazmat.2007.02.052.

[8] TA Kurniawan, GYS Chan, W Lo, S Babel, Comparisons of Low-cost Adsorbents for Treating Wastewaters Laden with Heavy Metals. Sci. Total. Environ. 2006, DOI: 10.1016/j.scitotenv.2005.10.001.

[9] P Liu. Polymer Modified Clay Minerals: A review. Appl. Clay Sci. 2007, DOI: 10.1016/j.clay.2007.01.004.

[10] X Tang, Z Li, Y Chen, Z Wang, Removal of Zn(II) from aqueous solution with natural Chinese loess: behaviors and affecting factors. Desalination. 2009, DOI: 10.1016/j.desal.2008.10.023.
[11] JUK Oubagaranadin, and ZVP Murthy. Adsorption of divalent lead on a montmorillonite- illite type of clay. Ind. Eng. Chem. Res. 2009; 48, 10627-10636.
[12] A Mellah, S Chegrouche, The removal of Zinc from aqueous solutions by natural bentonite. Water Res. 1997, DOI: 10.1016/S0043-1354(96)00294-1.
[13] MEI Ahmed, Selective Adsorption of Cadmium Species onto Organic Clay using Experimental and Geochemical Speciation Modeling Data. Inter. J. Eng. Technol. 2016, DOI: 10.7763/IJET.2016.V8.871.
[14] KG Bhattacharyya, SS Gupta, Pb(II) Uptake by Kaolinite and Montmorillonite in Aqueous Medium: Influence of Acid Activation of the Clays. Colloids Surface A. 2006, DOI: 10.1016/j.colsurfa.2005.11.060.
[15] MA Ismail, MAZ Eltayeb and SA Abdel Maged. Elimination of heavy metals from aqueous solutions using Zeolite LTA Synthesized from Sudanese clay. Res. J. Chem. Sci. 2013; 3, 93-98.
[16] Y Yu, and H Wu, Bioslurry as a Fuel. 2. Life-Cycle Energy and Carbon Footprints of Bioslurry Fuels from Mallee Biomass in Western Australia. Energ. Fuel. 2010, DOI: 10.1021/ef100957a.
[17] CT Chiou, and DE Kile, Deviations from Sorption Linearity on Soils of Polar and Nonpolar Organic Compounds at Low Relative Concentrations. Environ. Sci. Technol. 1998, DOI: 10.1021/es970608g.
[18] M Zhang, B Gao, Y Yao, Y Xue, M Inyang, Synthesis of Porous MgO-biochar Nanocomposites for Removal of Phosphate and Nitrate from Aqueous Solutions. Chem. Eng. J. 2012, DOI: 10.1016/j.cej.2012.08.052.
[19] M Inyang, B Gao, Y Yao, Y Xue, AR Zimmerman, P Pullammanappallil, X Cao, Removal of Heavy Metals from Aqueous Solution by Biochars Derived from Anaerobically Digested Biomass. Bioresour. Technol. 2012, DOI: 10.1016/j.biortech.2012.01.072.
[20] J Guo, AC Lua, Textural and Chemical Properties of Adsorbent Prepared from Palm Shell by Phosphoric Acid Activation. Mater. Chem. and Phys. 2003, DOI: 10.1016/S0254-0584(02)00383-8.
[21] RA Hutchins. New methods simplifies design of activated carbon system. Chem. Eng. 1973; 80, 133–138.
[22] GS Bohart, and EQ Adams, Some Aspects of the Behavior of Charcoal with Respect to Chlorine. J. Am. Chem. Soc. 1920, DOI: 10.1021/ja01448a018
[23] AA Ahmad, BH Hameed, Fixed-bed Adsorption of Reactive Azo Dye onto Granular Activated Carbon Prepared from Waste. J. Hazard. Mater. 2010, DOI: 10.1016/j.jhazmat.2009.10.003.
[24] HC Thomas, Heterogeneous Ion Exchange in a Flowing System. J. Am. Chem. Soc.1944, DOI: 10.1021/ja01238a017.
[25] YH Yoon, JH Nelson, Application of Gas Adsorption Kinetics. Part 1. A Theoretical Model for Respirator Cartridge Service Time. Am. Ind. Hyg. Assoc. J. 1984, DOI: 10.1080/15298668491400197.
[26] G Yan, T Viraraghavan, Heavy Metal Removal in a Biosorption Column by Immobilized M. rouxii Biomass. Bioresour. Technol. 2001, DOI: 10.1016/S0960-8524(01)00020-7.
[27] R Lakshmipathy, and NC Sarada, A fixed Bed Column Study for the Removal of Pb^{2+} Ions by Watermelon Rind. Environ. Sci. Water Res. Technol. 2015, http://dx.DOI: 10.1039/C4EW00027G.
[28] Z Zulfadhly, MD Mashitah, S Bhatia, Heavy Metals Removal in Fixed-bed Column by the Macro Fungus Pycnoporus Sanguineus. Environ. Pollut. 2001, DOI: 10.1016/S0269-7491(00)00136-6.

[29] I Mobasherpour, E Salahi and A Asjodi. Research on the batch and fixed-bed column performance of red mud adsorbents for Lead removal. Can. Chem. Trans. 2014; 2, 83-96.

[30] ZZ Chowdhury, SM Zain, AK Rashid, RF Rafique, and K Khalid, Breakthrough Curve Analysis for Column Dynamics Sorption of Mn(II) Ions from Wastewater by Using Mangostana garcinia Peel-Based Granular-Activated Carbon. J. Chem. 2013, DOI: 10.1155/2013/959761.

[31] R Han, L Zou, X Zhao, Y Xu, F Xu, Y Li, Y Wang, Characterization and Properties of Iron Oxide-Coated Zeolite as Adsorbent for Removal of Copper(II) from Solution in Fixed Bed Column. Chem. Eng. J. 2009, DOI: 10.1016/j.cej.2008.10.015.

[32] Z Aksu, F Gönen, Biosorption of Phenol by Immobilized Activated Sludge in a Continuous Packed Bed: Prediction of Breakthrough Curves. Process Biochem. 2004, DOI: 10.1016/S0032-9592(03)00132-8.

[33] EI Unuabonah, MI El-Khaiary, BI Olu-Owolabi, KO Adebowale, Predicting the Dynamics and Performance of A Polymer–Clay Based Composite in a Fixed Bed System for the Removal of Lead (II) ion. Chem. Eng. Res. Des. 2012, DOI: 10.1016/j.cherd.2011.11.009.

[34] AB Albadarin, C Mangwandi, AH Al-Muhtaseb, GM Walker, SJ Allen, MNM Ahmad, Modelling and Fixed Bed Column Adsorption of Cr(VI) onto Orthophosphoric Acid-activated Lignin, Chin. J. Chem. Eng. 2012, DOI: 10.1016/S1004-9541(11)60208-5.

[35] SS Baral, N Das, TS Ramulu, SK Sahoo, SN Das, GR Chaudhury, Removal of Cr(VI) by Thermally Activated Weed Salvinia Cucullata in a Fixed-bed Column. J. Hazard. Mater. 2009, DOI: 10.1016/j.jhazmat.2008.04.127.

[36] P Sivakumar, PN Palanisamy. Packed bed column studies for the removal of Acid blue 92 and Basic red 29 using non-conventional adsorbent. Indian. j. Chem. Technol. 2009; 16, 301-307.

Appendix C2

Journal Paper

A. H. Alamin, L. Kaewsichan, ‘‘Adsorption of Lead (II) from Aqueous Solution on Fixed-bed Column by Mixture of Clay and Biochar Using a Response Surface Method’’, **this manuscript is draft.**

Adsorption of Lead (II) from Aqueous Solution on Fixed-bed Column by Mixture of Clay and Biochar Using a Response Surface Method

Abstract:

New form of adsorbent was mixed clay from Sudan (CS) and Bamboo biochar (BB) using ratio 1:1 to form mixture (CB) as powder. Response surface methodology (RSM) was investigated for the adsorption of Pb(II) from aqueous solution on this new form of adsorbent and the process variables were optimized. Fixed-bed column mode experiments were carried out for adsorption equilibrium and determined the adsorbent capacity. Three important process variables including, flowrate of (10-20 ml/min), concentration of Pb(II) metal solution (5-30 mg/L), and adsorbent bed height (10-40 mm) on the adsorbent capacity were investigated and optimized to determine the best capacity yield of adsorbent. The experimental data obtained were analysed by analysis of variance (ANOVA). The results showed that the maximum adsorbent capacity yield was about 18.64 mg/g obtained by using 15 ml/min flowrate, 17.5 mg/L inlet Pb(II) concentration and 10 mm of bed height. From the analysis of variance (ANOVA), most influential factor for each experimental design response was identified. The optimum conditions for adsorption Pb(II) by CB adsorbent capacity (26 mg/g), from aqueous solution in fixed bed column were found as, 10 ml/min of flowrate, 14.53 mg/L solution concentration and 10 mm bed height.

Keywords: Clay, Bamboo biochar, Adsorption, Optimization, Pb(II).

Introduction:

The objective of control of water pollution in the industrial field applications is to removal or reduces of the hazard contaminations like heavy metals. Sometimes, wastewater with toxic organics and heavy metals is discharged into the surrounding environment even without purification and treatment [1]. Many industrial processes in the plating industry involve heavy metals for metal finishing and their effluent must be treated prior to discharge [2]. The rivers and groundwater are gradually polluted, resulting in serious threats on the safety of food supply and health of human beings [1]. In recent years Pb has been introduced into natural water from a variety of sources such as storage batteries, lead smelting, tetraethyl lead manufacturing, mining, plating, ammunition, and the ceramic glass industries [3]. But lead in drinking water can also cause a variety of adverse health effects. The permissible limit of lead in drinking water is 0.05 mg/L [4]. Lead toxicity effects on the nervous system, the blood circulation system, cardiovascular system, vital organs like the brain and the kidneys, and on restricted development of IQ, etc. have been well documented [5].

Precipitation, ion exchange, solvent extraction, and adsorption on many adsorbents were the conventional methods for the removal of heavy metal ions from aqueous solutions [6][7]. The adsorption process is used especially in the water treatment field and the investigation has been made to determine inexpensive and good adsorbents [8].

Natural materials that are available in large quantities, or certain waste products from industrial or agricultural operations, may have potential as inexpensive sorbents [9]. For this reason and objective used clay mixed with bamboo biochar as adsorbent in this present study. Both of them are inexpensive materials in many places in the world.

The clay mineral, being important constituents of soil, have been playing this role always by taking up various contaminants as water flows over soil or penetrates underground [10]. The chemical and pore structures of clays usually determine their adsorption ability [11]. Bentonite, which is predominantly montmorillonite clay, was used a wide range of industrial applications such as clarification of edible and mineral oils, paints, cosmetics and pharmaceuticals [12]. Since the natural clay minerals have the

relatively low adsorption capacity, they can be adding other material such as biochar to improve their adsorption ability and capacity.

Biochar is a pyrogenic carbon-rich material, derived from thermal decomposition of biomass in a closed system with little or no oxygen [13][14][15]. The use of biochar as a low-cost sorbent to remove metallic contaminants from aqueous solutions is an emerging and promising wastewater treatment technology, which has already been demonstrated in previous studies [16][17][18][19][20]. Biochars converted from agricultural residues, animal waste, and woody materials have been tested for their ability to sorb various heavy metals, including lead, copper, nickel, and cadmium [21][22]. A recent study indicated that biochar produced from Bamboo by pyrolysis process is an effective sorbent of lead than other type of biochar, but the capacity of adsorption it is low, while need to add other material such as clay for increased and improved the capacity. However, there has been no report on the application of clay plus Bamboo biochar as adsorbents.

Response surface methodology (RSM) is a collection of mathematical and statistical techniques useful for analysing the effects of several independent variables [23]. RSM can help in investigating the interactive effect of process variables and in building a mathematical model that accurately describes the overall process [24].

In this paper, adsorption of Pb(II) over adsorbent mixture contented form Sudanese clay plus Bamboo biochar will investigate in fixed-bed adsorption column system process. The effect of operating conditions on the adsorbent capacity is conducted. The optimum operating conditions such as flow rate of Pb(II) solution, initial concentration of metal solution and the bed height of adsorbent in the column, are analysed using design of experiments (DOE) and response surface methodology (RSM).

Material and methods:

Adsorbents

The clay (CS) was obtained from Sudan located in Nile river region in Sennar state, Sudan. Standard samples of $Pb(No_3)_2$ was purchased from Boss official limited partnership in Thailand. All solutions were prepared from analytical reagents (AR) and distilled water. Bamboo biochar (BB) was prepared in the laboratory scale by pyrolysis process at 500° C, grinded and sieved through mesh number 20 and mixed with clay at a ratio of 1:1 to form adsorbent mixture CB. The mixture of adsorbents was put in rubber foam ring as holder, and fixed in column to make bed. The concentration of residual Pb(II), was analysed using a Perkin Elmer thermos scientific S-series model (AAnalyst100), flame atomic absorption spectrometer (AAS).

Adsorbate

A stock solution concentration of $Pb(No_3)_2$ (1000 mg/l) was prepared by diluting a stock standard solution of $Pb(NO_3)_2$ to the varies concentration. A stock solution was obtained by dissolving 1.59 g of Lead nitrate in 1 litre distilled water. The range of concentration of the Pb(II) prepared from the standard solution varied between 5–30 mg/L.

Experimental setup and procedure

A schematic diagram for the fixed-bed column system is shown in Figure1. The fixed-bed column was made of glass tube of 3.5 cm inner diameter and 24 cm height. At the bottom of column, stainless steel sieve was attached followed by layer of glass wool. A known quantity of the prepared adsorbent mixture of CB was put in rubber foam ring and was packed in the column to obtain the desired bed height of adsorbent at range (10-40 mm) equivalent to (0.8-3.2 g) of mixture CB for study the effect of bed height. The column was then connected with distributer in order to provide a uniform flow of the solution through the column. Solution of Pb(II) of known concentrations at range (5-30 mg/L) was

pumped downward through the column at varies flowrate at range (10-20 ml/min) controlled by a peristaltic pump for investigate the effects of initial concentration and effects of flow rate. The samples of out let solution were collected at the exit of the column at different time intervals and the concentration of these samples was determined using a flame atomic adsorption spectrophotometer (AAS). In order to ensure the accuracy and reproducibility of all the data, all the column adsorption experiments were conducted in triplicate, and the mean values were used in the data analysis.

Experimental Design and Response Surface Methodology

Response surface methodology (RSM) is one of the techniques used for design experiments and to developed mathematical model to predict the optimum values of independent variables [25][26].

In this study the experiments were designed using essential regression and experimental design software. Three important factors, flowrate (ml/min), initial concentration of Pb(II) (mg/L) and bed height (mm), were chosen as independent variables that would be affect in adsorption capacity of CB adsorbent. These factors at ranges included three levels, low, central and high. 17 experimental runs were designed using Box-Behnken with three central pointes as shown in Table (1). The experiments were conducted to determine one quantity (response) as shown in that Table, the capacity of adsorbents (mg/g). The model used for predicting adsorbent capacity is quadratic equation as explained by:

$$Y = b_0 + b_1F + b_2C + b_3B + b_4F^2 + b_5C^2 + b_6B^2 + b_7FC + b_8FB + b_9CB$$

Where Y is the predicted response; b_0, b_1, b_2, b_3, b_4, b_5, b_6, b_7, b_8 and b_9 are the regression coefficients; and F, C, and B are the coded independent variables for flowrate, initial concentration and bed height, respectively.

Table 1. Experimental design matrix and results

Run	Flowrate ml/min	Concentration mg/l	Bed height mm	Resp_1	Predicted Resp_1	Residuals
1	15	17.5	25	6.55	6.84	-0.293
2	17.9	24.9	34	5.7	7.09	-1.390
3	12	10	16	13.3	14.30	-1.000
4	20	17.5	25	9.3	6.74	2.563
5	15	17.5	4	6.91	6.13	0.783
6	15	17.5	25	6.65	6.84	-0.190
7	12	10	34	4	3.86	0.145
8	15	17.5	10	18.64	16.04	2.597
9	12	24.9	16	12.13	13.55	-1.419
10	17.9	10	16	5	6.35	-1.352
11	15	17.5	25	6.75	6.84	-0.09363

12	12	24.9	34	3.7	4.74	-1.038
13	17.9	10	34	2.4	3.37	-0.972
14	17.9	24.9	16	5.9	8.44	-2.535
15	10	17.5	25	12.26	11.44	0.816
16	15	30	25	6.7	4.06	2.642
17	15	5	25	2.3	1.56	0.737

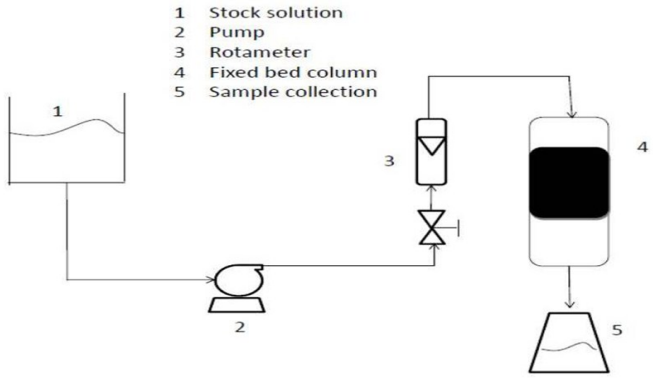

Figure1 The fixed bed experimental setup

Analysis of column data

The time for breakthrough appearance and the shape of the breakthrough curve are very important characteristics for determining the operation and the dynamic response of an adsorption fixed-bed column. The breakthrough curves show the loading behaviour of Pb(II) to be removed from solution in a fixed-bed column and is usually expressed in terms of adsorbed Pb(II) concentration (C_{ad}), inlet Pb(II) concentration (C_o), outlet Pb(II) concentration (C_t) or normalized concentration defined as the ratio of outlet Pb(II) concentration to inlet Pb(II) concentration (C_t/C_o) as a function of time or volume of effluent for a given bed height [27]. Effluent volume (V_{eff}) can be calculated as Eq. (1):

$$V_{eff} = Q\, t_{total} \quad (1)$$

Where t_{total} and Q are the total flow time (min) and volumetric flow rate (ml/min). The area under the breakthrough curve (A) obtained by integrating the adsorbed concentration (C_{ad}; mg/L) versus t (min) plot can be used to find the total adsorbed Pb(II) quantity(maximum column capacity). Total adsorbed metal quantity (q_{total}; mg) in the column for given feed concentration and flow rate (Q) is calculated from eq. (2):

$$q_{total} = \frac{QA}{1000} = \frac{Q}{1000}\int_{t=0}^{t=t_{total}} C_{ad}\, dt \quad (2)$$

Total amount of metal ion sent to column (M_{total}) is calculated from Eq. (3):

$$M_{total} = \frac{C_0\, Qr_{total}}{1000} \quad (3)$$

Total removal is calculated from Eq. (4):

$$\text{Total removal } (\%) = \frac{q_{total}}{M_{total}} \times 100 \quad (4)$$

Equilibrium metal uptake (q_{eq}) or maximum capacity of the column) is defined by Eq. (5) as the total amount of metal sorbed (q_{total}) per g of adsorbent (X) at the end of total flow time:

$$q_{eq} = \frac{q_{total}}{X} \quad (5)$$

Result and Discussion:

Optimization

The CB adsorbent ability for adsorption Pb(II) in this work was measured by capacity yield. Results of investigation are reported for the effects of three variables on a capacity yield of CB. RSM was used to predict the optimum values of the three variables. A mathematical model was developed based on the experimental design performed initially by essential regression software, as listed in Table 1. The experimental data was used to develop a quadratic regression model to predict the CB yield as a function of the three parameters including flowrate (F, ml/min), initial concentration of lead solution (C, mg/L), and bed height of adsorbent CB (H, mm), which was given by:

(CB adsorbent capacity) Resp_1 = 82.03 -5.487*F + 0.368*C -24.37H + 0.08984*F^2 -0.02582*C^2 +

1.885*H^2 + 0.03208*FC + 0.704*FH + 0.06167*CH (7)

The analysis of variance (ANOVA) summarized in Table 2 and 3, demonstrated that the models were highly significant at 95% confidence level, with high F-Value and very low F-significance. The regression coefficients and P-values were also shown; the latter were used to check the significance of each coefficient. From the significance test, it was found that flowrate (F) and bed height (H) were the most significant factors (p-values <0.05) affecting the CB capacity yield and the removal percentage of Pb(II) in CB. Additionally, as can be seen in Figure 2, the values predicted for CB capacity response by the mathematical model were in good agreement with the experimental results, confirming the fitness of the model.

The quality of the model developed was evaluated based on the correlation coefficient, R^2 and also standard deviation values [28]. From the Figure 2, the model's results fit well with the experimental results, as indicated by the determination coefficients (R^2) of 0.875 for the model's predictions of CB yield, as can be seen the points of data were well distributed near to a straight line, while suggested a good relationship between predicted and the experimental values of the response. This indicated that 87.5% of the total variation in the Pb(II) uptake in CB adsorbent. The R^2 from Eq.7 was considered as moderate to validate the fit validate, while may lead to large variation in CB adsorbent capacity yield predicted from the model.

Table 2 Analysis of variance (ANOVA) summarized

ANOVA						
Source	SS	SS%	MS	F	F Signif	df
Regression	262.51	88	29.17	5.446	0.01802	9
Residual	37.49	12	5.356			7
LOF Error	37.47	12 (100)	7.494	750.7820	0.00133	5
Pure Error	0.01996	0 (0)	0.00998			2
Total	300.00	100				16

Table 3 Continue analysis of variance (ANOVA) summarized

		P value	Std Error	-95%	95%	t Stat	VIF
b0	82.03	0.01664*	26.22	20.03	144.02	3.129	
b1	-5.487	0.06895*	2.556	-11.53	0.557	-2.147	147.24
b2	0.368	0.650	0.776	-1.466	2.202	0.474	84.75
b3	-24.37	0.00853*	6.735	-40.30	-8.442	-3.618	92.01
b4	0.08984	0.287	0.07799	-0.09458	0.274	1.152	124.51
b5	-0.02582	0.07732	0.01248	-0.05532	0.00369	-2.069	28.02
b6	1.885	0.06611	0.867	-0.164	3.934	2.175	39.23
b7	0.03208	0.415	0.03704	-0.05550	0.120	0.866	53.94
b8	0.704	0.05656*	0.309	-0.02584	1.434	2.281	57.89
b9	0.06167	0.633	0.123	-0.230	0.354	0.500	23.88

From the statistical results was shown that the models was adequate to predict the adsorbent capacity yield within the range of parameter investigated. In Figure 2 show the predicted values versus the experimental values for Pb(II) uptake by CB adsorbent, as expected the errors between predicted and experimental values were bigger. The possible reason for the higher error and lower notability of estimation given by the model, might be there are other parameters affecting for the adsorbent capacity yield, more than three variable, More study need to be carried out to verify this.

Essential regression software was used to optimize the conditions, and the results showed that the maximum value of capacity yield was about 26 mg/g for a flowrate of 10 ml/min, a bed height of 10 mm, and an initial concentration of 14.5 mg/L.

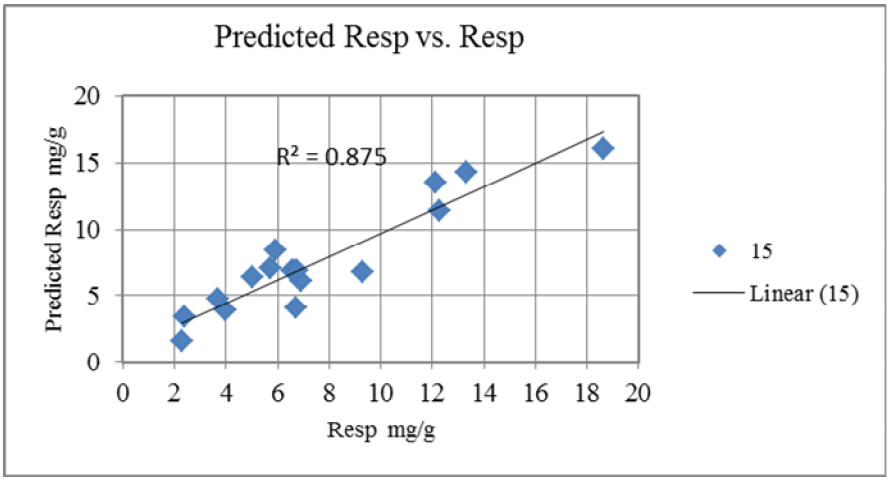

Figure. 2. Experimental results versus predicted values of

Effect of Pb(II) solution flowrate

Three-dimensional (3D) response surfaces and their corresponding 2-D contours in Figure 3 (a and b), display the interaction effects of most significant variables flowrate and bed height for the CB adsorbent capacity yield. The response surface can be used to determine the optimum levels of the parameters for the maximum response of capacity yield at the highest point of the surface. Figure 3(a) shows the mutual effects of the flowrate and bed height on the adsorbent capacity yield. The highest CB capacity yield was 20 mg/g obtained at around 10 ml/min of flowrate and decreased gradually to about 5 mg/g with increase of flowrate about 20 ml/min. However, there was a significant decrease in the capacity yield of adsorbent when the flowrate further increased from 10 ml/min to 20 ml/min. This might be

occurred due to short time (contact time between solution and adsorbent) in the column. From other words as the flow rate increased, the sorption capacity decreased because of insufficient residence time of Pb(II) metal solution in the column and reduced diffusion of adsorbate ions within the CB pores, and therefor earlier breakthrough time was obtained since equilibrium was not achieved [29].

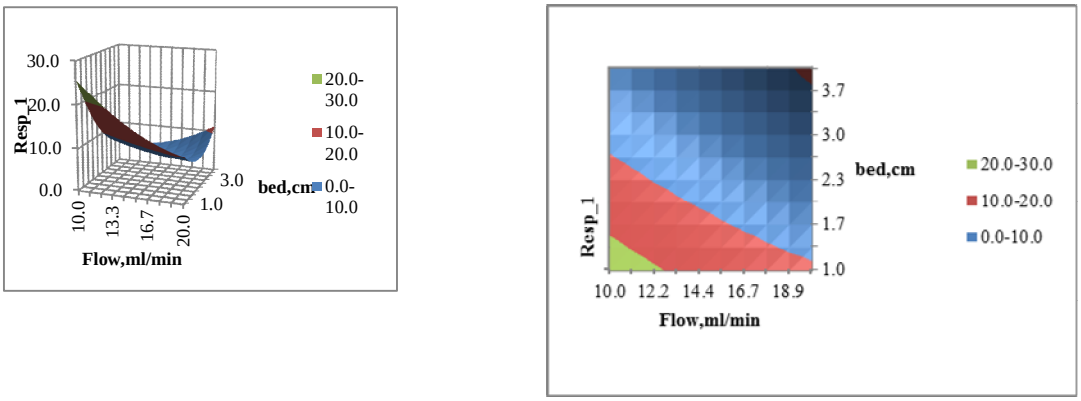

(a) (b)

Figure 3 response surfaces (a) 3D dimensional and (b) 2D contours, effects of variables flowrate and bed height for the CB adsorbent capacity yield

Effect of adsorbent bed height

The bed height effect was shown in Figure 4 (a and b), Also a highest CB capacity yield, i.e., about 25 mg/g, was achieved at around 10 mm bed height, then gradually dropped to about 5 mg/g with increasing bed height to 40 mm due to an increased flow rate of solution. The choice of the examined independent variables with their ranges seem appropriate with this process; however, the reduction of the flowrate (10 ml/min) is most likely needed, as it would probably enhance the column adsorption process, hence increasing the adsorbent capacity, which will therefore get the optimum values in the examined ranges.

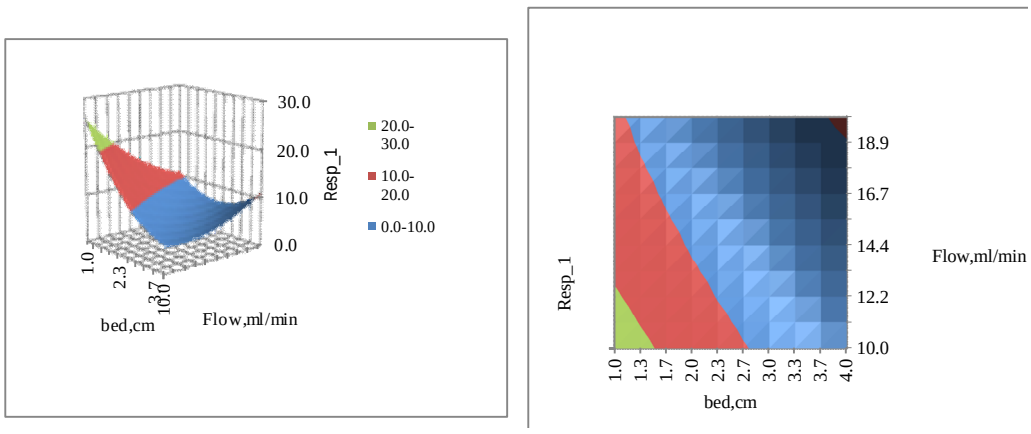

(a) (b)

Figure 4 response surfaces (a) 3D dimensional and (b) 2D contours, effects of variables flowrate and bed height for the CB adsorbent capacity yield

Conclusion:

1. It was demonstrated that adsorption process were generated by using mixed of clay and Bamboo biochar with ratio 1:1 in the column for adsorption Pb(II) from aqueous solution.
2. Flowrate and bed height were identified as the most significant factors affecting the adsorbent (CB) capacity yield. The model was adequate for predicting the CB capacity yield at less than 5% error. From RSM, a maximum value of 26 mg/g of the CB capacity yield was obtained at 10 ml/min of flowrate, 15mg/g of solution concentration, and bed height of 1 cm,
3. Experiments were conducted at the optimum conditions in order to verify the accuracy of the simulated optimum conditions. The CB capacity yield was 25mg/g as compared to simulated value of 26 mg/g (4 % error).

Acknowledgement:

The authors wish to thank the Prince of Songkla University (PSU) for its financial support under the DOE Discipline of Excellence (DOE) in Chemical Engineering for assistance in the carrying out of needed chemical analyses, and Scientific equipment centre (SEC) for characteristic the material used to conduct this study

References:

1. Xiaowu Tang, Zhenze Li, Yunmin Chen, Zhouqing Wang, Removal of Zn(II) from aqueous solution with natural Chinese loess: Behaviors and affecting factors, Desalination, Volume 249, Issue 1, 30 November 2009, Pages 49-57, ISSN 0011-9164, http://dx.doi.org/10.1016/j.desal.2008.10.023. (http://www.sciencedirect.com/science/article/pii/S0011916409007437)

2. Tonni Agustiono Kurniawan, Gilbert Y.S. Chan, Wai-hung Lo, Sandhya Babel, Comparisons of low-cost adsorbents for treating wastewaters laden with heavy metals, Science of The Total Environment, Volume 366, Issues 2–3, 1 August 2006, Pages 409-426, ISSN 0048-9697, http://dx.doi.org/10.1016/j.scitotenv.2005.10.001. (http://www.sciencedirect.com/science/article/pii/S004896970500728X)

3. Schneegurt, Mark A. and Jain, Jinesh C. and Menicucci,, John A. and Brown, Sarah A. and Kemner, Kenneth M. and Garofalo, David F. and Quallick, Matthew R. and Neal, Clive R. and Kulpa, Charles F., Biomass Byproducts for the Remediation of Wastewaters Contaminated with Toxic Metals, Environmental Science & Technology, volume 35, number 18, pages 3786-3791, 2001, doi = {10.1021/es010766e. http://dx.doi.org/10.1021/es010766e

4. Vandana Singh, Stuti Tiwari, Ajit Kumar Sharma, Rashmi Sanghi, Removal of lead from aqueous solutions using Cassia grandis seed gum-graft-poly(methylmethacrylate), Journal of Colloid and Interface Science, Volume 316, Issue 2, 15 December 2007, Pages 224-232, ISSN 0021-9797, http://dx.doi.org/10.1016/j.jcis.2007.07.061. (http://www.sciencedirect.com/science/article/pii/S0021979707010533)

5. P. E. Marino, A. Franzblau, R. Lilis, P. J. Landrigan, Acute lead poisoning in construction workers: the failure of current protective standards. Arch Environ Health. 1989 May-Jun; 44(3): 140–145.
doi: 10.1080/00039896.1989.9935877

6. Melchor Gonzalez-Davila, J.Magdalena Santana-Casiano, Frank J Millero, The adsorption of Cd(II) and Pb(II) to chitin in seawater, Journal of Colloid and Interface Science, Volume 137, Issue 1, June 1990, Pages 102-110, ISSN 0021-9797, http://dx.doi.org/10.1016/0021-9797(90)90046-Q

7. Yoshiaki Takahashi and Hideo Imai, Adsorption of heavy metal cations in montmorillonite, Soil Science and Plant Nutrition, volume 29, number 2, pages 111-122, 1983, doi = 10.1080/00380768.1983.10432413. http://dx.doi.org/10.1080/00380768.1983.10432413.

8. Gözen Bereket, Ayşe Zehra Arog, Mustafa Zafer Özel, Removal of Pb(II), Cd(II), Cu(II), and Zn(II) from Aqueous Solutions by Adsorption on Bentonite, Journal of Colloid and Interface Science, Volume 187, Issue 2, 15 March 1997, Pages 338-343, ISSN 0021-9797, http://dx.doi.org/10.1006/jcis.1996.4537
http://www.sciencedirect.com/science/article/pii/S0021979796945373

9. Susan E. Bailey, Trudy J. Olin, R.Mark Bricka, D.Dean Adrian, A review of potentially low-cost sorbents for heavy metals, Water Research, Volume 33, Issue 11, August 1999, Pages 2469-2479, ISSN 0043-1354, http://dx.doi.org/10.1016/S0043-1354(98)00475-8.
http://www.sciencedirect.com/science/article/pii/S0043135498004758)

10. Susmita Sen Gupta, Krishna G. Bhattacharyya, Immobilization of Pb(II), Cd(II) and Ni(II) ions on kaolinite and montmorillonite surfaces from aqueous medium, Journal of Environmental Management, Volume 87, Issue 1, April 2008, Pages 46-58, ISSN 0301-4797,
http://dx.doi.org/10.1016/j.jenvman.2007.01.048.
(http://www.sciencedirect.com/science/article/pii/S0301479707001417)

11. Ruey-Shin Juang, Su-Hsia Lin, Kung-Hsuen Tsao, Mechanism of Sorption of Phenols from Aqueous Solutions onto Surfactant-Modified Montmorillonite, Journal of Colloid and Interface Science, Volume 254, Issue 2, 15 October 2002, Pages 234-241, ISSN 0021-9797,
http://dx.doi.org/10.1006/jcis.2002.8629.
(http://www.sciencedirect.com/science/article/pii/S0021979702986297)

12. F.A Banat, B Al-Bashir, S Al-Asheh, O Hayajneh, Adsorption of phenol by bentonite, Environmental Pollution, Volume 107, Issue 3, March 2000, Pages 391-398, ISSN 0269-7491,
http://dx.doi.org/10.1016/S0269-7491(99)00173-6.
(http://www.sciencedirect.com/science/article/pii/S0269749199001736)

13. K. C. Das and M. Garcia-perez and B. Bibens and N. Melear, Slow pyrolysis of poultry litter and pine woody biomass: Impact of chars and bio-oils on microbial growth, Journal of Environmental Science and Health, Part A, volume 43, number 7, pages 714-724, 2008, doi :10.1080/10934520801959864
http://dx.doi.org/10.1080/10934520801959864}

14. Lehmann Johannes, Gaunt John, Rondon Marco, Bio-char Sequestration in Terrestrial Ecosystems – A Review, Mitigation and Adaptation Strategies for Global Change. V 11, N 2, 2006, 395-419.

doi: 10.1007/s11027-005-9006-5, http://dx.doi.org/10.1007/s11027-005-9006-5

15. Van Zwieten. L, Kimber. S, Morris. S, Chan. K.Y, Downie. A, Rust. J, Joseph. S, Cowie. A, Effects of biochar from slow pyrolysis of papermill waste on agronomic performance and soil fertility, Plant and Soil, V 327, N (1-2), P 235-246, 2010, doi: 10.1007/s11104-009-0050-x. http://dx.doi.org/10.1007/s11104-009-0050-x

16. Luke Beesley, Marta Marmiroli, The immobilisation and retention of soluble arsenic, cadmium and zinc by biochar., Environ Pollut. 2011 February; 159(2): 474–480. Published online 2010 November 24. doi: 10.1016/j.envpol.2010.10.016

17. Zhengang Liu, Fu-Shen Zhang, Removal of lead from water using biochars prepared from hydrothermal liquefaction of biomass, Journal of Hazardous Materials, Volume 167, Issues 1–3, 15 August 2009, Pages 933-939, ISSN 0304-3894, http://dx.doi.org/10.1016/j.jhazmat.2009.01.085. (http://www.sciencedirect.com/science/article/pii/S0304389409001162)

18. Dinesh Mohan, Charles U. Pittman Jr., Mark Bricka, Fran Smith, Ben Yancey, Javeed Mohammad, Philip H. Steele, Maria F. Alexandre-Franco, Vicente Gómez-Serrano, Henry Gong, Sorption of arsenic, cadmium, and lead by chars produced from fast pyrolysis of wood and bark during bio-oil production, Journal of Colloid and Interface Science, Volume 310, Issue 1, 1 June 2007, Pages 57-73, ISSN 0021-9797, http://dx.doi.org/10.1016/j.jcis.2007.01.020. (http://www.sciencedirect.com/science/article/pii/S0021979707000409)

19. Uchimiya Minori and Lima Isabel. M, and Thomas Klasson. K, and Chang SeChin and Wartelle Lynda H, and Rodgers James E, Immobilization of Heavy Metal Ions (CuII, CdII, NiII, and PbII) by Broiler Litter-Derived Biochars in Water and Soil, Journal of Agricultural and Food Chemistry, volume 58, number 9, pages 5538-5544, 2010, doi:10.1021/jf9044217,
URL = http://dx.doi.org/10.1021/jf9044217
eprint = http://dx.doi.org/10.1021/jf9044217

20. Xinde Cao, Lena Ma, Bin Gao, Willie Harris, Dairy-manure derived biochar effectively sorbs lead and atrazine., Environ Sci Technol. 2009 May 1; 43(9): 3285–3291.

21. Minori Uchimiya, SeChin Chang, K. Thomas Klasson, Screening biochars for heavy metal retention in soil: Role of oxygen functional groups, Journal of Hazardous Materials, Volume 190, Issues 1–3, 15 June 2011, Pages 432-441, ISSN 0304-3894, http://dx.doi.org/10.1016/j.jhazmat.2011.03.063. (http://www.sciencedirect.com/science/article/pii/S0304389411003669)

22. Myers, R.H., Montgomery, D.C., 2002. Response Surface 1 Methodology– Process and Product Optimization Using Designed Experiments, 2nd ed. John Wiley & Sons, New York, NY.

23. M. Mourabet, A. El Rhilassi, H. El Boujaady, M. Bennani-Ziatni, A. Taitai, Use of response surface methodology for optimization of fluoride adsorption in an aqueous solution by Brushite, Arabian Journal of Chemistry, Available online 6 January 2014, ISSN 1878-5352, http://dx.doi.org/10.1016/j.arabjc.2013.12.028. (http://www.sciencedirect.com/science/article/pii/S1878535214000021)

24. Douglas C. Montgomery, Design and Analysis of Experiments, 5th Edition Published by Wiley (2000-06-30)

25. G. M. Clarke and R. E. Kempson, Arnold, Introduction to the design and analysis of experiments. London, 1997. No. of pages. vii# 334. Price: @19.99. ISBN 0-340-64555-5

26. Guo, Aik Chong Lua, Textural and chemical properties of adsorbent prepared from palm shell by phosphoric acid activation, Materials Chemistry and Physics, Volume 80, Issue 1, 29 April 2003, Pages 114-119, ISSN 0254-0584, http://dx.doi.org/10.1016/S0254-0584(02)00383-8. (http://www.sciencedirect.com/science/article/pii/S0254058402003838)

27. I.A.W. Tan, A.L. Ahmad, B.H. Hameed, Preparation of activated carbon from coconut husk: Optimization study on removal of 2,4,6-trichlorophenol using response surface methodology, Journal of Hazardous Materials, Volume 153, Issues 1–2, 1 May 2008, Pages 709-717, ISSN 0304-3894, http://dx.doi.org/10.1016/j.jhazmat.2007.09.014. (http://www.sciencedirect.com/science/article/pii/S0304389407013015)

28. P. Roy, N.K. Mondal, K. Das, Modeling of the adsorptive removal of arsenic: A statistical approach, Journal of Environmental Chemical Engineering, Volume 2, Issue 1, March 2014, Pages 585-597, ISSN 2213-3437, http://dx.doi.org/10.1016/j.jece.2013.10.014. (http://www.sciencedirect.com/science/article/pii/S2213343713002066)

VITAE

Name Ahmed Hassan Alamin Ebrahim

Student ID 5510130016

Educational Attainment

Degree	Name of Institution	Year of Graduation
Bachelor of Chemical Technology	Al-Neelain University	2003
Master of Chemical Engineering	University of Gezira	2006

Scholarship Awards during Enrolment

1. DOE Research assistant scholarship, Chemical Engineering department, Engineering faculty, Prince of Songkla University, 2012-2015.

Work – Position and Address (If Possible)

1. Chemical Engineer, from May, 2005 to 26th October, 2007 at Khartoum State Water Corporation, Khartoum-Sudan.
2. Chemical, safety and Environmental, water quality Engineer, from 26th September, 2007 to 15th November, 2009 at DAMS IMPLEMINTATION UNIT, Merowe Dam, Job res Project- Sudan.
3. Chemical, Safety and Environmental Engineer from 15th November, 2009 to 30th April, 2012 at DAMS IMPLEMINTATION UNIT, ROSIERS DAM HAYTHING PROJECT- Job res Project- Sudan
4. Chemical Engineer, Head of Oil and lubricant Research lab, from 1 May 2012 up to February 2013 at CENTRAL LABORATORY FOR ENIVIRONMENTAL AND SOIL RESEARCH - Sudanese Company for Distribution of electricity
5. Teacher Assistant for master and under graduate students of chemical engineering faculty in Prince of Songkla University from November 2012 until Now.

List of Publication and Proceeding

1. A. Hassan and L. Kaewsichan, ‘‘Removal of Pb(II) from Aqueous Solutions Using Mixtures of Bamboo Biochar and Calcium Sulphate, and Hydroxyapatite and Calcium Sulphate’’, *EnvironmentAsia*, 9(1) (2016) 45-52.

2. A. H. Alamin, L. Kaewsichan, ‘‘Adsorption of Zn(II) and Cd(II) ions from aqueous solutions by Bamboo biochar cooperation with Hydroxyapatite and Calcium Sulphate ’’**,** *International Journal of ChemTech Research*, Vol.7, No.5, pp 2159-2170, 2014-2015.

3. A. H. Alamin, L. Kaewsichan, ‘‘Adsorption of Pb(II) Ions from Aqueous Solution in Fixed Bed Column by Mixture of Clay plus Bamboo Biochar’’, This manuscript had been accepted to publish in *Walailak Journal of Science and Technology*.

4. A. H. Alamin, L. Kaewsichan, ‘‘Equilibrium and kinetic studies of sorption of 2,4-dichlorophenol onto 2 mixtures: bamboo biochar plus calcium sulphate (BC) and hydroxyapatite plus bamboo biochar plus calcium sulphate (HBC), in a fluidized bed circulation column’’, This manuscript had been Accepted to publish in *Polish Journal of Chemical Technology*.

5. A. Hassan and L. Kaewsichan, ‘‘Removal of Pb(II) from Aqueous Solutions Using Mixtures of Bamboo Biochar and Calcium Sulphate, and Hydroxyapatite and Calcium Sulphate’’, “Towards International Collaboration for an Environmentally Sustainable World”, Thai Society of Higher Education Institutes on Environment June 2015. Bangkok, Thailand.

6. I have 2 more paper under review in the international journal